



T.C.

SELÇUK ÜNİVERSİTESİ

FEN BİLİMLERİ ENSTİTÜSÜ

YERRADARI VE TRAVERTEN OCAĞI UYGULAMASI

Muhammed Abbas Qasimi

YÜKSEK LİSANS TEZİ

Maden Mühendisliği Anabilim Dalını

Aralık-2014
KONYA
Her Hakkı Saklıdır

ÖZET

YÜKSEK LİSANS TEZİ

YERRADARI VE TRAVERTEN OCAĞINA UYGULAMASI

Muhammed Abbas QASİMİ

Selçuk Üniversitesi Fen Bilimleri Enstitüsü
Maden Mühendisliği Anabilim Dalı

Danışman: Prof.Dr. Mehmet Kemal GÖKAY

2014, 97 Sayfa

Jüri
Danışmanın Prof.Dr. Mehmet Kemal Gökay
Prof.Dr. Veysel Zedef
Doç.Dr Hakan Karabörk

Yerradarı (GPR) hasarsız jeofiziksel yeraltı araştırma yöntemi olarak, sıg derinlikleri incelemek için kullanılmaktadır. Kaya tabakalarının uzantıları ve kalınlıkları düşünüldüğünde bunların sığ derinliklerde GPR ile ortaya çıkarılması mümkün olmaktadır. Yerradarlarında kullanılan biostatik antenler yardımıyla yeryüzünden yeraltına doğru yöneltilen radar dalgalarının gönderilme ve geridönüş zaman aralıkları, gönderilen dalgaların dalga boylarının hassas bir şekilde ölçülebiliyor olması yerradarı uygulamalarını yaygınlaştırmıştır. Elektronik devreler konusundaki bu gelişmelere bağlı olarak yerradarında kullanılan elektromanyetik dalgalarda testler sırasında oluşan farklılıkların incelenerek değerlendirilmesi sonucu, yeraltında bulunan kaya tabakalarının şekilleri, boyutları, varsa fay ve kıvrımlar görsel olarak belirlenebilir duruma gelmiştir.

Bu araştırmanın arazi uygulamaları sırasında bir traverten ocağında yerradarı (GPR) uygulamaları yapılmış ve elde edilen veriler analiz edilmiştir. Konya'da Selçuk Üniversitesi kampüsü yakınlarındaki Ardıçlı köyünde bulunan bir traverten ocağı şevinde GSSI SIR-3000 model yerradarı ile test edilmiştir. Yapılan bu ölçümlerden elde edilen GPR verileri, bilgisayara aktarıldıktan sonra yeraltının 2-boyutlu kesit grafikleri Radan-7 yazılımı kullanılarak grafiksel sonuçlar haline getirilmiştir. Yeraltının 2-boyutlu (derinlik-yüzey uzunluğu) grafikleri, GPR ölçümünün yapıldığı ölçüm hatları boyunca, traverten kaya kütlesi içindeki kırıkların, tabakaların ve ezik zonların yerlerini belirlemekte kullanılmıştır. GPR grafiklerinde gözlenen kil tabakası ile traverten ocağının şev aynasında görülen kil tabaksının uyumlu olduğu gözlenmiştir. Ayrıca bu traverten ocağında gözlenen kırıkların üç boyutlu modellemesi, ve bunların 5-10 metre derinliğe kadar ilerlediği bu grafiklerden elde edilen diğer sonuçlar olarak ortaya konulmuştur.

Anahtar Kelimeler: Traverten ocağı, yerradarı, yerradarının travertene uygulanması, yerradarı uygulamaları.

ABSTRACT

MSc THESIS

GROUND PENETRATION RADAR AND ITS APPLICATION IN A TRAVERTINE MINE

Muhammed Abbas QASIMI

THE GRADUATE SCHOOL OF NATURAL AND APPLIED SCIENCE OF SELÇUK UNIVERSITY
THE DEGREE OF MASTER OF SCIENCE / DOCTOR OF PHILOSOPHY IN MECHANICAL ENGINEERING

Advisor: Prof.Dr. Mehmet Kemal GÖKAY

2014, 97 Pages

Jury
Advisor Prof.Dr. Mehmet Kemal Gökay
Prof.Dr. Veysel Zedef
Doç.Dr Hakan Karabörk

Ground penetrating radar (GPR) is a non-destructive geophysical exploration method that can be used in shallow subsurface exploration. Using GPR, it is possible to make high precision measurements of thickness of deposit layer and its distribution in research area. In cases when GPR measurements are performed by biostatic antenna system, time intervals after which reflected signals are received usually are measured relatively to arrival of direct signal. As a result of precise time interval among the returned GPR signals, underground rock formations, faults and other features are visualized according to signal differences.

In this research study, application and the resultant graphics of GPR on travertine mine were analyzed. GSSI SIR-3000 ground penetration radar system was used for geophysical survey of the selected travertine mine near Ardıclı (Konya) village. After collecting GPR data from field test performed on the targeted travertine rock mass, two dimensional GPR graphics were obtained by using Radan-7 software. The resultant graphics presents the section views of the underground where the GPR measurements were taken. Since the travertine in the selected mine have minor and major fractures observed on its slope, GPR test measurement line locations were pre-determine according to visualize these fracture continuity in the travertine rock mass. It is determined that some of the fractures presented signals which seemed to penetrate 5-10 meters deep from the existing slope face.

Keywords: Ground penetration radar (GPR), GPR applications, GPR application for travertine mine, Travertine mine.

ACKNOWLEDGEMENTS

First of all, I would like to express my sincere gratitude to my supervisor, Prof. Dr. Mehmet Kemal Gökay for his valuable guidance during my MSc research study. I am also grateful to "Commission of Turkish and Relative States (Yurtdışı Türk ve Akraba Topluluğu Başkanlığı, YTB)" for their funding to my MSc study, without this support I cannot perform my research in Konya-Turkey. I also would like to express my appreciation to lecturers in Mining Engineering Department of Selcuk University for their helps and their kind behaviors and great hospitality. In this point I also thank the Ministry of Mines Office of Afghanistan for their positive attitude and helps. I also send my honest regards to my family, my father, my mother and my wife for their kind attitudes.

Muhammed Abbas QASIMI
KONYA-2014

TABLE OF CONTENTS

ÖZET.....i
ABSTRACT.....ii
AKNOWLEDGE.....iii
TABLE OF FIGURE DESGN.....v
SYMBOL USED.....ix
1. INTRODUCTION.....1
1.1 Ground Penetrating Radar (GPR).....2
1.2 Travertine and its properties 5
1.3 Regional geology structure.....6
1.4 GPR as an exploration tool.....8
1.5 GPR Basics of theory.....9
1.6 Historical use of GPR technology.....13
1.7 Types of GPR Systems.....14
1.8 GPR Component.....15
1.9 GPR System Available.....16
1.10 GPR Antenna System.....17
1.10.1. GPR antenna characteristics.....19
1.10.2. GPR Antenna applications.....20
2. GROUND PENETRATION RADAR METHODOLOGY.....24
2.1 GPR Application Site.....26
2.2 Common Middle Point.....27
2.3 GPR Surveying Methods.....28
2.4 Significance of GPR.....30
2.5 Instrument types and configuration.....31
3. GROUND PENRETRION RADAR MEASUREMENT PRINCIPLE.....33
3.1 Electromagnetic Wave Propagation.....36
3.2 GPR fundamentals and material properties.....39
3.3 Reflection single-fold.....42
3.4 Multi-fold surveys.....43
3.5 Expected resolution and depth of investigation.....44
3.6 Variables Affecting GPR Resolution and Energy Penetration.....47
3.8 Investigating Faults Rock with GPR.....50
3.9 Application of GPR Data in Geographical Information System (GIS).....52
3.10 Data Collection Method for GPR using GIS.....53
4. MATERIALS & METHODS (FILD MEASUREMENT) 56
4.1 Preparing the Test Site Before GPR Measurement.....56
4.2 GPR Equipment Used During The Field Tests.....58
5. RESEARCH RESULTS (DATA ANALYZING) 60
a) Line-1 (L-1, NE-SW): 62
b) Line-2 (L-2, SW-NE): 67
c)Line-3 (L-3, SW-NE): 73
d) Line-4 (L-4, SW-NE): 78
e)Line-5 (L-5, NE-SW):.....83
5.1. THREE DIMENSIONAL (3D) FRACTURES EXTENSION IN THE SEARCHED TRAVETINE MINE.....88
6. CONCLUSIONS.....91

TABLE OF FIGURE CONTENTS

Figure1.1 Schematic of Basic Ground penetrating Radar System (Olhoeft, 2000; Beres & Haeni, 1991).....3

Figure 1.2 GPR can be deployed in a number of ways the two principal approaches are depicted in figure (a) illustrates the reflected signal detection concept while (b) demonstrates the signal transmission or Tran's illumination concept. (Annan & Davis, 1978) ……..4

Figure 1.3 outline geological map (modified from MTA, 2002) showing the outcrop of the Paleozoic Konya complex, (Göncüoğlu et al, 1997; ……..7

Figure1.4 Location and geological map of the study area (Özcan et al., 1988, Eren1993a, 1993b, 1996a and Kurt, 1994)……..8

Figure 1.5 A diagram of how the electromagnetic wave is transmitted and reflected by a GPR unit (Davis & Annan, (1989)……9

Figure 1.6 Ground penetrating radar; moving the transmitter (left) and receiver (right) in a continuous method (Bristow and Jol, 2003).....11

Figure 1.7 Reflection profile produced by a GPR system (Bristow and Jol, 2003).....12

Figure 1.8 Type GPR Models (Daniels DJ, 2004). …….....15

Figure 1.9 Typical GPR system block diagram, (Zoubir, et al., 2002).....18

Figure 1.10 GCB- 200, medium depth stratigraphy, dry soil (Bekic, 1964)……..21

Figure 1.11 GCB-100, deep stratigraphy dry soil (Bekic, 1964)……21

Figure 1.12 GCB- 100, deep utility detection, average soil (Bekic, 1964)…….22

Figure 1.13 GBC- 700, utility detection, average soil (Bekic 1964) …….....22

Figure 2.1 Ground penetrating radar survey of an archaeological site in Jordan. (Conyers And Goodman, 1997).....25

Figure 2.2 Common Middle Point (CMP) profile of Russell Spit in Western Nevada, (Daniels 2004) ……28

Figure 2.3 shown method of surveying GPR system (Bekic, 1964)……....29

Figure 2.4 shows moving type of photos the GPR systems (Bekic, 1964).....30

Figure 3.1 Ground penetrating radar measurement principle (Robinson, 2003)…….34

Figure 3.2 Travel paths of different GPR wave types in a two-layer soil with different relative permittivity's (Robinson, 2003)…….....34

Figure 3.3 GPR trace. Note, the a wavelet always consists of a number of " wiggles" which are displayed in the radar gram as a series of lines (e.g. red-blue-red) (Robinson, 2003).....35

Figure 3.4 (a) Origin of a radar gram. Amplitudes which excess a pre-defined positive or negative threshold are displayed in color. In this example negative amplitudes are shown in blue while positive amplitudes are displayed in re; modified after (Reynolds, 1997) (b) Example radar gram (Robinson, 2003).....35

Figure 3.5 GPR waves are characterized by the velocity of propagation and degree of attenuation. Velocity generally increases with frequency as depicted in (a). Attenuation also increases with frequency (b) and its alternate form, skin depth ($\delta=1/\alpha$) decreases with frequency (c). For successful GPR measurements a plateau event exist where these properties become frequency independent. İn some high loss materials, the plateau may ever exist a depicted in (c). (Davis and Annan, 198).....40

Figure 3.6 Typical exploration depths achievable in common materials where GPR is a useful technique (Annan and Davis, 1989).....41

Figure 3.7 GPR wavelets are generally as shown in (a) which is characteristic of small dipole antennas. The corresponding frequency spectrum is shown in (b). Pulse duration and bandwidth are inversely related. (Annan and Davis, 1989) ….....42

Figure 3.8 Multi-fold and CMP soundings surveys (Annan and Davis, 1989) 43

Figure 3.9 Multifold data are normally acquired or sorted in CMP (common mid-point) (Annan and Davis, 1989) ……44

Figure 3.10 the 25-MHz antenna capable of transmitting radar en erg to more than 20 m is difficult to transport to the field and within grids. It is capable of resolving only very large objects of many meters in dimension Conyers and Cameron, 1998) ……...45

Figure 3.11 the 900-MHz antenna high frequency and small and can easily fit in a suitcase Conyers and Cameron, 1998) …….....46

Figure 3.12 GPR reflection profile (top). Letters K,L,R,S,T show offsets in stratigraphy signaling possible faulting (bottom). (Cai et al., 1996) …….....51

Figure 3.13 the whole workflow of managing GPR data in GIS (Paterson, D.G., 2000)……53

Figure 3.14 collecting GPR data at the *CATS test site*. Antennas can be attached to survey wheels, which can be programmed to collect a given number of reflection traces every programmed distance along a transect (Conyers and Goodman, 1997) ……...54

Figure 4.1. GSSI's SIR-3000 ground penetration radar control unit, (GSSI, 2011)…...58

Figure 5.1 Analysed travertine mine bench view. Actually this single benched travertine mine has face cut by dimond capsulated stell-rope. The face demonstrates

fracture intersections and their 3D bedding planes. Red lines separate weathered and main travertine zones. Yellow lines on to other hand show claystone bedding, thickness 0.75-1.5 meters, underlying the top travertine bedding …….....61

Figure 5.2. Travertine mine face and measuring lines followed during field measurement.....62

Figure 5.3a. GPR test graphic, (Line-1, distance between 0-4 m)……..…… ..63
Figure 5.3b. GPR test graphic, (Line-1, distance between 4-10 m)…….. ..63
Figure 5.3c. GPR test graphic, (Line-1, distance between 10-16 m)……..63
Figure 5.3c. GPR test graphic, (Line-1, distance between 10-16 m)…… ..64
Figure 5.3e. GPR test graphic, (Line-1, distance between 23-31 m)…… ..64
Figure 5.3f. GPR test graphic, (Line-1, distance between 31-38 m) …….. ..64
Figure 5.3g. GPR test graphic, (Line-1, distance between 39-47 m)…….…… ..65
Figure 5.3h. GPR test graphic, (Line-1, distance between 47-53 m)…… …….. ..65
Figure 5.3i. GPR test graphic, (Line-1, distance between 53-62 m)…… ……..….. ..65
Figure 5.3j. GPR test graphic, (Line-1, distance between 63-71 m)… ……..……. ..66
Figure 5.3k. GPR test graphic, (Line-1, distance between 71-79 m)……66
Figure 5.3l. GPR test graphic, (Line-1, distance between 80-89 m)……..... ..66
Figure 5.3m. GPR test graphic, (Line-1, distance between 90-98 m)……..... ..67
Figure 5.3n. GPR test graphic, (Line-1, distance between 98-101 m)……. ..67
Figure 5.4a. GPR test graphic, (Line-2, distance between 0-4 m)……. ..68
Figure 5.4b. GPR test graphic, (Line-2, distance between 4-9 m)…… ..68
Figure 5.4c. GPR test graphic, (Line-2, distance between 9-14 m)…… ..68
Figure 5.4d. GPR test graphic, (Line-2, distance between 14-21 m)……. ..69
Figure 5.4e. GPR test graphic, (Line-2, distance between 22--28 m)……. ..69
Figure 5.4f. GPR test graphic, (Line-2, distance between 29-36 m)…….. ..69
Figure 5.4g. GPR test graphic, (Line-2, distance between 36-44 m)……. ..70
Figure 5.4h. GPR test graphic, (Line-2, distance between 44-50 m)…….…… ..70
Figure 5.4i. GPR test graphic, (Line-2, distance between 51-59 m)……. ..70
Figure 5.4j. GPR test graphic, (Line-2, distance between 59-66 m)……... ..71
Figure 5.4k. GPR test graphic, (Line-2, distance between 67-75 m)……. ..71
Figure 5.4l. GPR test graphic, (Line-2, distance between 75-83 m)…….. ..71
Figure 5.4m. GPR test graphic, (Line-2, distance between 83-90 m)…… ..72
Figure 5.4n. GPR test graphic, (Line-2, distance between 91-98 m)……. ..72
Figure 5.4o. GPR test graphic, (Line-2, distance between 98-105 m)…….. ..72
Figure 5.5a. GPR test graphic, (Line-3, distance between 0-5m)…….. ..73
Figure 5.5b. GPR test graphic, (Line-3, distance between 5-11m)…… ..73
Figure 5.5c. GPR test graphic, (Line-3, distance between 11-17 m)……74
Figure 5.5d. GPR test graphic, (Line-3, distance between 17-24 m)…… ..74
Figure 5.5e. GPR test graphic, (Line-3, distance between 24-31 m)…….. ..74
Figure 5.5f. GPR test graphic, (Line-3, distance between 31-37 m)……. ..75
Figure 5.5g. GPR test graphic, (Line-3,distance between 37-44 m)……. ..75
Figure 5.5h. GPR test graphic, (Line-3, distance between 44-50 m)..... ..75
Figure 5.5i. GPR test graphic, (Line-3, distance between 50-56 m)……. ..76
Figure 5.5j. GPR test graphic, (Line-3, distance between 56- 63 m)…… ..76
Figure 5.5k. GPR test graphic, (Line-3, distance between 63-70 m)…….. ..76
Figure 5.5l. GPR test graphic, (Line-3, distance between, 70-77m)…….. ..77
Figure 5.5m. GPR test graphic, (Line-3, distance between 77-83 m)……. ..77
Figure 5.5n. GPR test graphic, (Line-3, distance between, 83-90 m)…… ..77

Figure 5.5o. GPR test graphic, (Line-3, distance between, 90-93 m)…….. ..78
Figure 5.6a. GPR test graphic, (Line-4, distance between 0-2 m) …… ..79
Figure 5.6b. GPR test graphic, (Line-4, distance between 2-8 m)…… ..79
Figure 5.6c. GPR test graphic, (Line-4, distance between 8-14 m)…… ..79
Figure 5.6d. GPR test graphic, (Line-4, distance between 14-23 m)…… ..80
Figure 5.6e. GPR test graphic, (Line-4. distance between 23-31 m)…… ..80
Figure 5.6f. GPR test graphic, (Line-4. distance between 31-38 m)…….. ..80
Figure 5.6j. GPR test graphic, (Line -4, distance between 37-45 m)…… ..81
Figure 5.6k. GPR test graphic, (Line 4-, distance between 45-54 m)…… ..81
Figure 5.6l. GPR test graphic, (Line -4, distance between 54-62 m)…… ..81
Figure 5.6m. GPR test graphic, (Line -4, distance between 62-70m)…… ..82
Figure 5.6n. GPR test graphic, (Line -4, distance between 70-78 m)…….. ..82
Figure 5.6o. GPR test graphic, (Line-4, distance between 78-87m)…… ..82
Figure 5.6p. GPR test graphic, (Line 4-, distance between 87- 93 m)…….. ..83
Figure 5.7a. GPR test graphic, (Line -5, distance between 0-1m)…… ..83
Figure 5.7b. GPR test graphic, (Line -5, distances between 1-7 m)……..84
Figure 5.7c. GPR test graphic, (Line -5, distance between 7-14 m)……..84
Figure 5.7d. GPR test graphic, (Line -5, distance between 14- 22 m)…….. ..84
Figure 5.7e. GPR test graphic, (Line -5, distance between 22-29 m)…… ..85
Figure 5.7f. GPR test graphic, (Line -5, distance between 29-36 m)…… ..85
Figure 5.7g. GPR test graphic, (Line -5, distance between 36-44 m)…….. ..85
Figure 5.7h. GPR test graphic, (Line -5, distance between 44-51 m)…… ..86
Figure 5.7i. GPR test graphic, (Line -5, distance between (51-58 m)……..86
Figure 5.7j. GPR test graphic, , (Line -5, distance between 58- 65 m)…….. ..86
Figure 5.7k. GPR test graphic, (Line -5, distance between 65-70 m)…… ..87
Figure 5.7l. GPR test graphic, (Line -5, distance between 70-78 m)…… ..87
Figure 5.7m. GPR test graphic, (Line -5, distance between 78-86 m)…….. ..87
Figure 5.7n. GPR test graphic, (Line -5, distance between 86-93 m)…… ..88

Figure 5.8. Three dimensional model of measured travertine rock mass at the mine. The fracture orientations are presented here according to the GPR graphics obtained from the field tests along the presented measuring lines. Red recordings represent the distance from the line starting point. Blocks front face represents the depth and illustrates the depth continuity of the determined fractures……..90

SYMBOLS USED

EM	Electromagnetic
CMP	Common Mid-Point
DE	Dielectric
SNR	Signal-to-noise-ratio
CW	Continuous- wave
FM	Frequency Modulated
RF	Reflection Energy
CEC	Cation Exchange Capacity
UHF	Ultra High Frequency
VHF	Very High Frequency
б	Conductivity,
E	Dielectric permittivity,
μ	Magnetic permeability,
ω	Radian frequency

1. INTRODUCTION

Ground penetrating radar (GPR) is one of the newer geophysical methods. By exploiting the wave propagation characteristics of electromagnetic fields, GPR provides a very high resolution sub-surface mapping method. In many respects GPR is the electromagnetic counterpart of seismic reflection.

In the exploration context, GPR has limited exploration depths, so it is not necessarily a tool for all applications. GPR is most effective in electrically resistive environments where very detailed information is desired. Applications in the mining exploration context include mapping of veins and fracture zones, delineating crown pillar thickness, mapping overburden thickness, locating old mine workings, and definition of placer potential.

GPR in its present form started to emerge from the polar ice radio echo sounding in the late 1960s. Since that time, the method has seen a constant and continuous growth both in applications, number of practitioners and in instrument sophistication. Early utilization of the method for engineering and soils applications as well as mining are given by Morey (1974), Cook (1973), Annan and Davis (1976), Coon et al. (1981) and Ulriksen (1982). An extensive overview of the method is given by Davis and Annan (1989). The proceedings of GPR conferences held biannually during the last decade also provide an excellent source of GPR reference material.

GPR can be deployed in number of manners; the primary modes are either in a reflection configuration or in a transillumination mode. “The most common approach to carrying out GPR surveys has been to work in the reflection measurements can be a single source and receiver combination or more sophisticated multi-transmit/receive observation such as those used in multi-fold seismic reflection. More recently developments have led to a growing use of the transillumination mode,” (Annan and Davis 1978; Owen 1981; Davis and Annan 1986; Olhoeft 1988; Olsson et.al., 1990; and Annan et al.,1997).

In this study, physical and theoretical basis of GPR, current instrumentation performance levels, survey procedures, as well as data processing, interpretation and display are searched and presented. Geophysical Survey Systems Inc. (GSSI) is the world’s leading manufacturer of ground penetrating radar (GPR) equipment. This

company’s cutting-edge products designed to address a wide range of challenging application, therefore GSSI’s GPR were selected for Selcuk University GPR measurement study group to obtain unsurpassed data quality and field-proven reliability. This thesis contains GSSI-SIR-3000 (GPR) model’s field measurements which are the newest GPR product results in the world. This rugged, high-performance radar system provides unrivaled scan rates with low noise.

As GSSI (2009) presented in its web page, “GSSI introduced the first commercial ground penetrating radar system in 1974. For nearly 40 years, GSSI has led with a series of “firsts” including the first digital storage GPR system, the first commercially available GPR data post-processing software package and the first GPR system designed specifically to produce high resolution images in scanned concrete. Today, GSSI offers the industry's broadest range of ground penetrating radar solutions - covering a range of applications from archaeology, mining, geology and environmental, utility detection, concrete inspection and bridge and road condition assessment”. The presented here includes the field works performed by GSSI SIR-3000 (GPR) model in Ardıclı travertine mine. The data obtained from this field study were then analyzed and discussed for travertine rock mass for its intact, fractured and clay contains parts.

1.1. Ground Penetrating Radar (GPR)

Ground penetrating radar (GPR) is a geophysical method that uses radar pulses to image the subsurface. This nondestructive method uses electromagnetic radiation in the microwave bad (UHF/VHF frequencies) of the radio spectrum and detects the reflected signals from subsurface structures. GPR can be used in a variety of media, including rock, soil, ice, fresh water, pavements and structures. It can detect objects, changes in material, voids and cracks in different mediums.

Daniels (2004) stated about GPR that; “GPR uses high-frequency (usually polarized) radio waves and transmits into the ground. When GPR waves hit a buried object or a boundary with different dielectric constants at the measurement sites, receiving antenna records variations in the reflected return signal. The principles involved are similar to reflection seismology, except that electromagnetic energy is used

instead of acoustic energy, in this method reflections appear at boundaries with different dielectric constants instead of acoustic impedances."

The depth range of GPR is limited by the electrical conductivity of the ground, the transmitted center frequency and the radiated power. As conductivity increases, the penetration depth decreases. This is because the electromagnetic energy is more quickly dissipated into heat, causing a loss in signal strength at depth. Higher frequencies do not penetrate as far as lower frequencies, but give better resolution. Optimal depth penetration is achieved in ice where the depth of penetration can achieve several hundred meters. Good penetration is also achieved in dry sandy soil or massive dry material such as granite, limestone, and concrete where the depth of penetration could be up 15-metre (49 ft.). In moist and/or clay-laden soil and soils with high electrical conductivity, penetration is sometimes only a few centimeters, (Daniels, 2004).

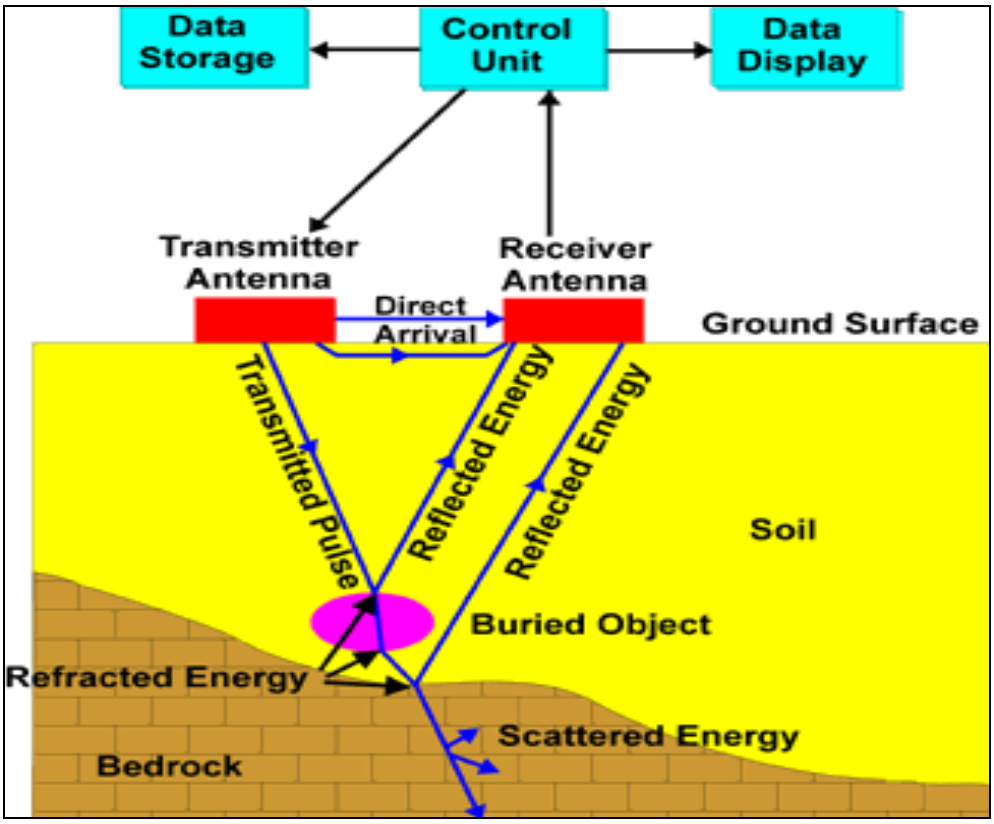


Figure 1.1. Schematic view of basic ground penetrating radar working system (Olhoeft, 2000; Beres & Haeni, 1991).

Ground penetrating radar (GPR) is a rapidly growing field that has seen tremendous progress in the development of theory, technique, technology, and range of

applications over the past 15-20 years. GPR has also become a valuable method utilized by a variety of scientists, researchers, consultants, and university students from many disciplines. The diversity of GPR applications includes a variety of areas such as the study of groundwater contamination, geotechnical engineering, sedimentology, glaciology, and archaeology. Ground penetrating radar (GPR) also known as ground probing radar, impulse radar or subsurface interface radar, is a geophysical method used for high resolution imaging of shallow subsurface features. It is similar to air-directed radar in that it transmits a burst of electromagnetic energy and then waits for reflections from targets to be received before repeating the process continuously. However, it differs significantly from that better known form by transmitting the energy instantaneously over a wide frequency range, utilizing a very short transmission pulse and a broadband antenna design. The usual operating frequency varies between about 25 MHz and 1000 MHz (covering the VHF/UHF bands), (Annan and Cosway, 1991).

The energy is transmitted into the ground using antennas that are in direct contact with the surface, and as this energy propagates to greater depths, a series of reflections are directed back to the surface where they are detected by the receiving antenna. The method is only suitable for shallow investigation (up to tens of meters in the best conditions) because the ground absorbs the energy at a rapid rate, and as it propagates to greater depths. Eventually there is insufficient energy to generate a reflection from a deep target that can be redirected back to the surface and detected by the receiver, (Annan and Cosway, 1991).

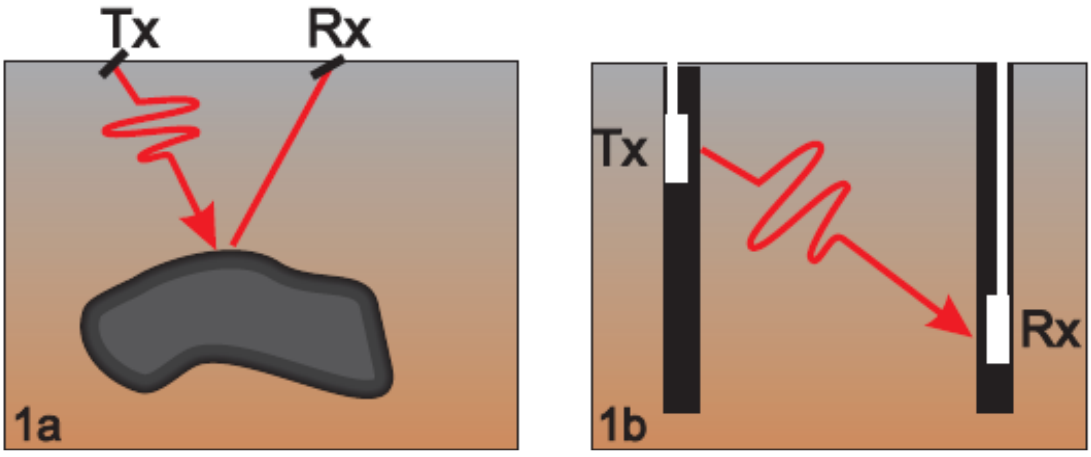


Figure 1.2 GPR can be deployed in different manner; two main principal approaches are presented above. a) Illustrates the reflected signal detection concept, b) demonstrates the signal transmission or Trans-Illumination concept, (Annan & Davis, 1978).

In this report (Davis and Annan 1989), it was stated also that "Although the GPR method has been widely applied to a range of applications in Australia, there are only a limited number of application where it can be regarded as having been successful, compared to the extent in which it is used in say Europe and the USA. The main reason for this is the occurrence of soils that are generally more conductive than those in other countries. Despite this fact, there are at least four groups in Australia who have designed and built world class systems for specialized applications, and the number of practitioners has risen greatly in the twenty years since it was first introduced here".

GPR is an easy to deploy geophysical technique that produces high resolution images of the shallow subsurface in a manner analogous to reflection seismic. It is usually used as a surface technique although borehole radar is used in specialist applications (only surface GPR is considering). Like many geophysical techniques, GPR can provide very useful data if applied in the appropriate context and this is discussed in the section below. Hence, any subsurface investigation that requires shallow, high-resolution imaging may benefit from the inclusion of GPR.

1.2. Travertine And Its Properties

Travertine forms from geothermal springs and is often linked to calcium carbonate precipitation systems. Macrophytes, bryophytes, algae, cyanobacteria, and other organisms often colonise the surface of travertine and are preserved, giving travertine its distinctive porosity. Some springs have temperatures high enough to exclude macrophyets and bryophytes from the deposits. As a consequence, deposits are in general, less porous than tufa. Thermophilic microbes are important in these environment and stromatolitic fabrics are common. When it is apparent that deposits are devoid of any biological component, they are often referred to as calcareous structure. Travertine formation results from crystal growth in a supersaturated solution. Understanding the growth process is challenging, since the chemical conditions at the crystal surface cannot be ascertained by direct analysis, (Nancollas, 1979).

Travertine stone is one of the most widely used stones in today's building industry. Travertine is utilized in both floor and wall tile applications; countertops,

patios, building exteriors and outdoor pathways. Commonly mined in Italy and Turkey, travertine stone continues to be a popular import for construction products all over the world. This thesis study contains field measurements obtained by GPR at a not in use travertine mine near Selcuk University main campus. The mine is located 5 km from the campus, 25 km away from Konya city center.

1.3. Regional Geological Structure

The Konya Complex forms part of the Afyon-Bolkardağ zone, as shown on Figure 1.3. (Göncüoğlu et al,. 1997; Okay and Tüysüz, 2003) presented, they work that; "Geological formation named *Konya Complex* has complicated internal structural relationships of the Silurian-Carboniferous rocks exposed west of the city of Konya, which cannot be treated simply as a conventional stratigraphic unit. As discussed below, the Konya Complex has been described as including olistostromes with olistoliths, but is here reinterpreted as a mélange terrane overall. An olistostrome is traditionally defined as a sedimentary unit in which detached blocks (olistoliths) are emplaced within a sedimentary matrix by mas-flow processes. Mélange is considered as a non-genetic term for a pervasively mixed unit comprising exotic blocks of one or more lithologies with or without a sedimentary matrix. In this sense, mélange can form by sedimentary or tectonic processes, and thus includes olistostromes".

The field geological researches were performed by (Özcan et al., (1988), Eren (1993a, 1993b) and Kurt (1994). They described the geological evidences for their study area which includes Sızma, Ardıclı village and surroundings. They stated that; in the area given in Figure 1.4; "there are two metamorphic units, which are autochthonous and allochthonous. The Miocen-Quaternary aged cover rocks overlie these units by angular unconformity (Figure 1.4). The autochthonous unit includes the Upper Permian-Cretaceous Gokceryurt Group divided into three formations which are gradational to one another. These are, in ascending order, the Upper Permian Derbent formation composed of metacarbonate, phyllite and graphite schists. The Upper Permian-Upper Triassic Aladag formation consisting of alternation of metaconglomerate, metasandstone, phyllite and metadolomite and the Upper Triasic-Cretaceous Lorasdag Formation comprising a thick sequence of metacarbonate rocks. In the southwest of the

study area, the allochthonous Ladik metamorphites, which in Silurian-Mesozoic in age, tectonically overlie the Gokçeyurt Group".

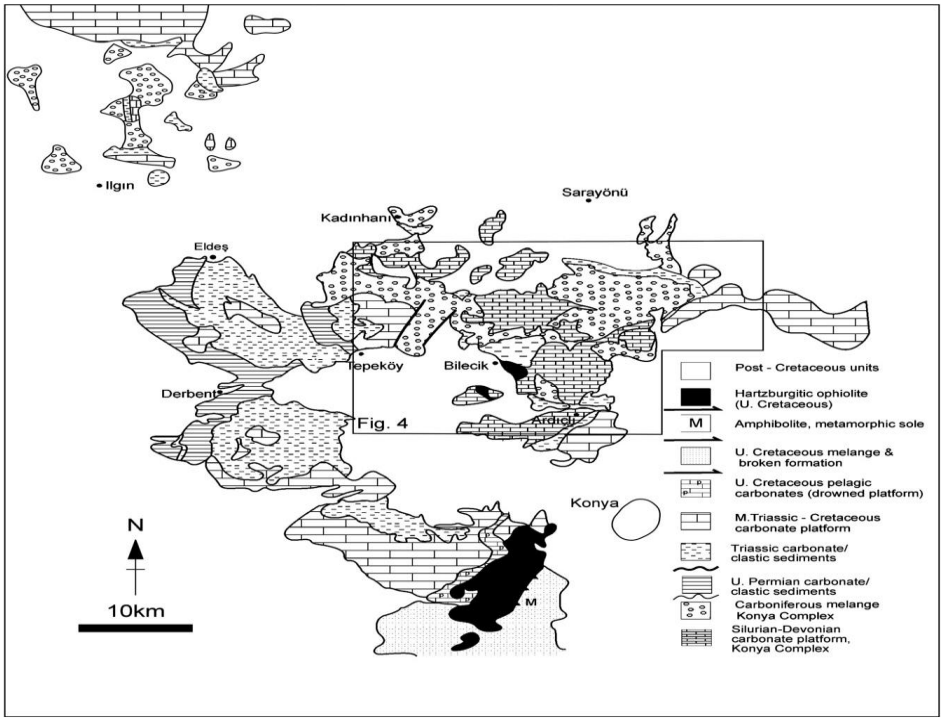


Figure 1.3 Outline geological map (modified from MTA, 2002) showing the outcrop of the Paleozoic Konya complex (Göncüoğlu et.al, 1997).

They also added that, "the Ladik metamorphites can be divided into Silurian-Lower Permian aged Sızma group and Upper Permian Mesozoic aged Ardıçlı group. Sızma group included, in ascending order, Silurian-Lower carboniferous reefal complex of the Bozdag formation The Bozdag formation passes into the Devonian-Lower Permian aged Bagrıkurt formation consisting of metaconglomerate, metasandstone, phyllite, graphitic schist, calcerous-schist, metachert, metatuff and metaconglomerate. Metamagmatitic rocks, which are composed of hornblende metagabbro, metdolerite, metabasalticandesite, metabsites, Kmetatrachyandesite, cut the Sızma group rocks in different geometrical direction. The Upper Permian to Mesozoic aged Ardıclı Group uncomfortably overlying the Sızma Group is made up of Bahcecik Ertugrul and Kızıloren formations. These units laterally and vertically interfinger to each other. The youngest unint of the study area, the Upper Miocene-Pliocene aged alluvial fan deposits, lacustrine carbonate, pyroclastic sediment and volcanic rockscover the older rocks with angular unconformity (Figure 1.4)."

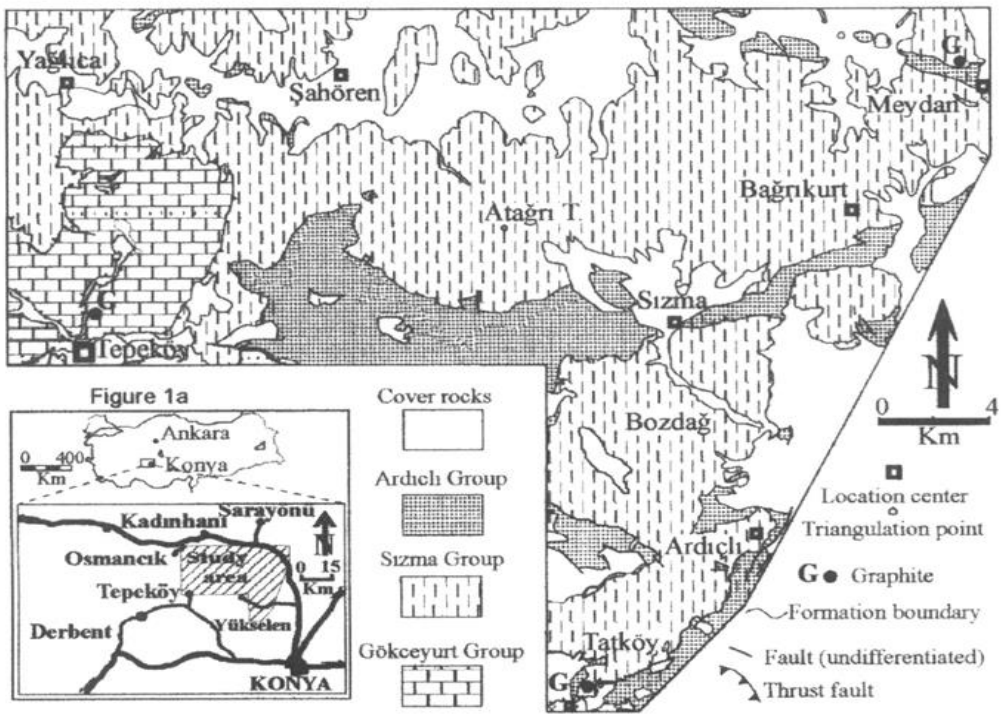


Figure 1.4. Location and geological map of Ardıclı-Sızma-Sahoren region (Özcan et al., 1988, Eren1993a, 1993b, 1996a and Kurt, 1994).

1.4. GPR As An Exploration Tool

Geophysical methods can be very useful in exploring for oil, minerals. They can be used also for locating buried shallow objects. Most methods in use today were developed five or six decades ago and have not been improved upon greatly since their inception. Each method has its strengths and often severe limitations that are imposed by nature. The advantage of geophysical survey techniques is that they do not disturb the site, can usually be performed quickly, and they are very cost effective compared to excavation costs. When they can be used these methods can be very helpful in evaluating the site geologically and for delineating areas of interest and eliminating barren ground. Among the more recent tools developed for probing beneath the surface of the earth is ground-penetrating radar. (Annan, A.P., 1973).

GPR's utilize a very short burst of radio-frequency energy radiated into the ground to detect discontinuities in the ground. These discontinuities can be cavities, voids, transitions between soil and rock, filled areas or buried objects. The performance of these radars is limited by attenuation of the signals in moist soils, especially soils

having high clay content. GPR's are similar to normal atmospheric and space radars in that an echo is reflected back to the observer from a remote target. Rather than bouncing a signal from an aircraft of space vehicle, GPR's look for a boundary between rock and air (a cave or cavity) or between one type of soil and another (for example undisturbed soil-to back-filled soil). The strength of the echo is dependent on the absorption of the signal, the size and shape of the target, and the degree of discontinuity at the reflecting boundary. (Annan A.P, 1973).

1.5. Basic Theory of GPR

As Meyers et al., (1996) stated that; "GPR uses electromagnetic (EM) radio waves. EM waves are essentially the same as the radio waves that a car antenna receives from a broadcasting radio station. The EM waves are radiated from a transmitter that pulses a signal into the ground. From there the waves are diffracted, refracted, and most importantly reflected. The reflected signals are sent back to the surface where they are measured by a receiver unit, amplified, and digitized by the computer unit that is used to record the measurements (Figure 1.5)."

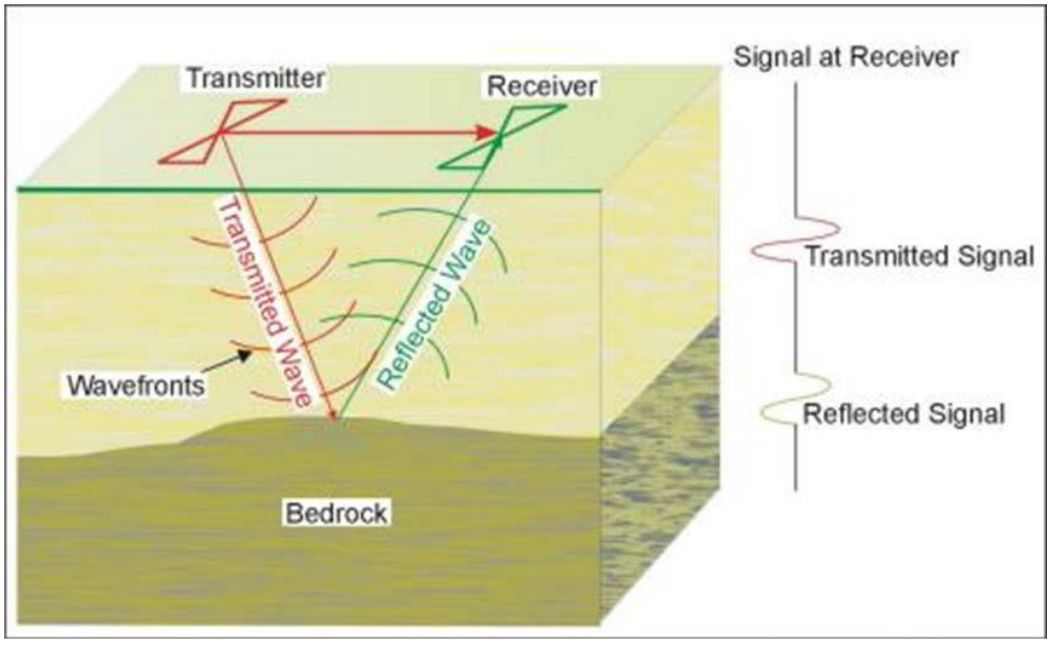


Figure 1.5. A diagram of how the electromagnetic wave is transmitted and reflected by a GPR unit (Davis and Annan, 1989).

Davis and Annan, (1989) stated that, "reflection of the wave is due to the subsurface materials having different dielectric properties. They also reported that; "When the types of properties of one material are different than that of another above it, a reflected wave will be produced. Each material has its own conductivity level, which produces a certain velocity for the traveling EM waves. Using the reflection and the two way elapsed time of the EM pulse's travel, a cross-sectional reflection profile is creating. The profile is often able to be viewed in real time from a computer where the collection of the reflected EM data is taking place. The real time viewing of results allows for possible changes to any parameters that may be adversely affecting the results, including location and equipment settings. Upon further visual interpretation of the results on paper or on a computer screen, a reflection showing continuity throughout the profile may be evidence of a feature of interest. The reflection profile is only part of the puzzle to understanding subsurface phenomena. A further understanding of the geomorphological background of the study area is necessary to complete it. Data collection, while following the same principles, can be achieved in different fashions. The transmitter and receiver are moved along a specified transect in either a stepped or continuous fashion. A step mode of data collection involves both the transmitter and receiver being moved separately at a fixed distance from one another. Continuous data collection is when the transmitter and receiver are fixed to each other at a given distance and slowly dragged across the targeted area (Figure 1.6)".

Step mode is the preferred method for GPR systems because of the higher level of accuracy. This higher level of accuracy is achieved due to the nature of each antenna meeting solidly with the ground and a pause while the pulse is being sent and received. Continuous collection can lead to 'smearing' of the data because the antennae are moving as the data is collected, (Bristow and Jolt, 2003).

There are many factors other than stepped or continuous collection that must be considered before using GPR at a study site. First, one must establish the objectives of the study; what, if any, feature is one attempting to find or subsurface information is one trying to be obtained. The desired results will tell a researcher where to look, or the desired depth of study. Bristow and Jolt (2003) stated that, "The preferred depth of the information is crucial to decide. This is necessary to be arranged, what kind of antennae should be used along with the correct transmitter/receiver voltage".



Figure 1.6. Ground penetrating radar; moving the transmitter (left) and receiver (right) in a continuous method (Bristow and Jolt, 2003).

Smith and Jolt (1995) stated that, "In order to achieve the proper sampling depth, or being able to image at a depth useful for a particular study, multiple factors come into play. First parameter is the physical composition, or what sort of stuff the ground is made of certain materials are conductive to a better or worse setting for GPR sampling. Dry sands and gravels provide a good opportunity for data collection, while saturated clay in one of the worst scenarios. The saturated clay is highly electrically conductive and causing the GPR signal to attenuate (lose energy) whereas the sand and gravel has a high resistivity that will allow profile imaging for tens of meters"

Similarly, Bristow and Jolt (2003) stated that; "the next factor in determining the depth of GPR waves is frequency of the antennae used. In general, the lower the frequency is the deeper it will penetrate. There is a "give and take" involved with frequency selection though. While the lower frequency (around 10 to 50 MHz) can travel further, it also provides less resolution than a higher frequency (400 to 1000 MHz). A compromise between depth and resolution must be found for a good result that best shows the nature of what being imaged. Step size also plays an important role in the horizontal resolution of the GPR profile. The maximum effective step size is determined dividing the wavelength by 4 (any smaller will make no difference). Time

involved imaging an area is a factor that must also be considered. A smaller step size, when using a stepped mode of data collection, will take the user much longer to complete a transect. Larger step sizes can be used for areas having continuous horizontal layers where small variations are not as likely to occur."

Before any data has been collected in a study area, it is important to convert the incoming data to be useable. The reflection profiles taken with the GPR unit are shown on a two dimensional Cartesian plane. The x-axis on this graph shows distance along the measuring side. This graph's y-axis shows the time, it takes for the pulsed EM wave to travel to the reflected area back (shown in nanoseconds) in Figure 1.7.

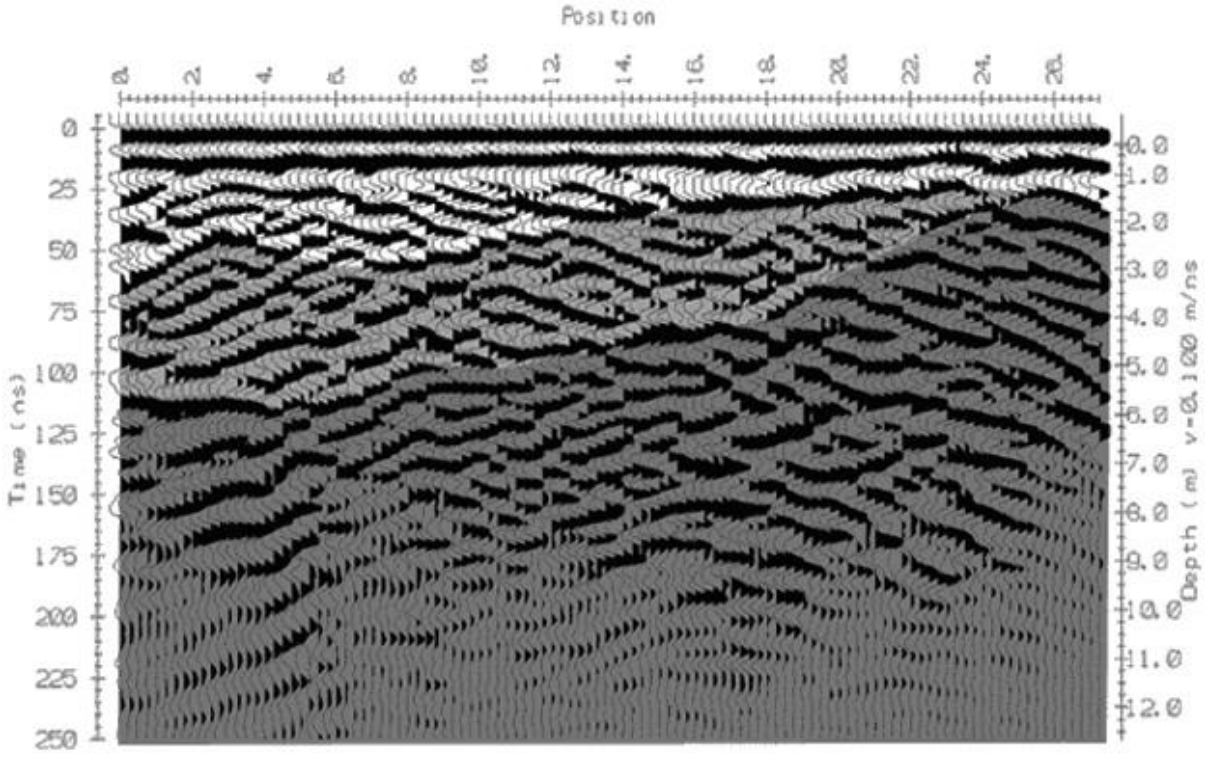


Figure 1.7. Reflection profile produced by a GPR system, (Bristow and Jolt, 2003).

As there is not much tangible use for travel time, the data must be converted in a way that helps to better understand the real world meanings of the profile. To achieve a better understanding of the profile and subsequently the subsurface, time must be converted to depth. For time to be converted to depth, the propagation velocity of EM energy through the profiled sediment has to be determined. "A common way to find sediment's velocity is to use common midpoint (CMP) soundings. CMP surveys are done by setting up a transect in the area of study that is on a horizontal surface. The

transmitter and receiver start as close together as possible and are moved in opposing directions in successive intervals, the smaller the interval the more precise. The antennae are moved in opposite directions for as far as the user sees fit or until the cables will not allow any further separation. Resulting reflection profile will allow for the calculation of velocity where the slope of the dipping lines is inversely proportional to the velocity" (Bristow and Jolt, 2003). The velocity is then applied to the time interval to determine depth. The depth will be nonlinear due to changes in the velocity the material being imaged.

1.6. Historical Use of GPR Technology

The foundation for radar systems in general was laid by Hülsmeyer "when he obtained the worldwide first patent in radar technology on April 30th, 1904. Six years later Leimbach and Löwy applied for a patent to use radar technology to locate buried objects. The system they offered used surface antennas together with continuous-wave radar. In 1926, a pulse radar system was introduced by Hülsenbeck. In this radar technique, radar invention particularly improved to get better depth resolution and it is still widely used nowadays (Hülsmeyer, 1904, Löwy, 1910).

One of the first worldwide ground penetrating radar surveys was performed in Austria in 1929 by Stern. He measured the depth of a glacier. Thereafter ground penetration radar technology had not been used up to World War II. Before the war some patents were filed in the field of subsurface radar. This changed after the Second World War. Different scientific teams began to work on radar systems for viewing into the ground in the early 1970's. At the beginning, these radars were developed for military applications such as locating tunnels in the demilitarized zone between North and South Korea. Soon thereafter public utility and construction companies were interested in such radars as a practical tool to map pipes and utility lines under city streets (Morey, 1974). Other scientific investigations were started to use ground penetrating radar technology to explore underground water table levels and salt deposits.

According to Wollny and Sass (2001) the first affordable GPR systems were sold in 1985 and first comprehensive reference books was written in the 1990s.

Nowadays there are various companies producing GPR systems while others provide measurements services. Moreover, universities worldwide conduct research in the field of ground penetrating radar systems. Most GPR systems are designed for surface applications where the transmitter and receiver are located above ground. Nevertheless there are applications where the GPR system has to fit into a narrow borehole which can be more than a kilometer long. These measurement tasks are conducted with a borehole radar as a special GPR tool.

1.7. Types of GPR Systems

Ground penetrating radar systems are a versatile technology which has found an application in nearly all areas of life and new uses for them continue to appear every day. However, the basic design for ground-penetrating radars includes several main components: computer, antenna, data digitizer, radar electronics equipment and display unit. Changing or upgrading the computer, display or data transfer units does not limit the basic functionality of the GPR system in any way. Antenna and the data digitizer are both integral elements of the system, but it is essentially the radar that is the core of every GPR. Although ground penetrating radar systems are highly adaptable and suitable for almost any kind of application, the distinction of different types of GPR is rarely based on the type of research it is used for. The division is based on the method through which the data is collected and it is possible to differentiate two approaches: the time domain and the frequency domain. Impulse radars are designed to operate in the time domain, whereas continuous-wave radars are designed to operate in the frequency domain. In theory, given the same set of circumstances, impulse and continuous-wave radars with identical specifications will produce the same results. However, their performance in the real world is what sets them apart, and each one of them has its own unique set of advantages and disadvantages, (Daniels, 2004).

Impulse and continuous-wave radars also differ in their availability. Ground penetrating radar systems which use impulse radar technique dominate the commercial market and are available for anyone to purchase. Continuous-wave radars, although being constantly developed over the years, have been limited to use in research facilities, universities and government laboratories. Custom ground penetrating radar



Figure 1.8. Main parts of basic GPR system, (Daniels, 2004).

systems featuring advanced techniques and solutions have been integrated into the GPR, such as ultra-wideband, synthetic-aperture, noise and arbitrary waveforms radars. Impulse radars facilitate time domain pulse and it is transmitted by the control unit and amplified by the antenna, and reflected wave is received as a function of time. The waveforms generated by the computer show the amplitude of energy reflected from the underground objects versus time. Most of the ground-penetrating radar systems which are built around the impulse technique send a pulse to an antenna, which in turn produces an electromagnetic wave. The center frequency of the electromagnetic wave is determined by the properties of the antenna, and the corresponding bandwidth is determined by the pulse width (Daniels, 2004).

1.8. GPR Components

The process of using ground penetrating radar is amusingly simple even though it is intimidating at first glance. There are four main components that make up a working GPR system. The first component is an antenna that transmits the high energy radar frequency used to penetrate the ground. This antenna is placed at or near ground level over the site that is being analyzed. Radar waves are created by focusing high voltage toward the center of a bow-around the copper plate as the current travels from

the plate in regulated pulses. An electromagnetic field is created around the copper plate, as the current travels from the plate center to the plate edges and back again. The radar waves are then transmitted into the ground at a pre-determined frequency to be reflected back to antenna. The second component of the GPR system is a receiving antenna. The receiving antenna is placed at an appropriate distance away from the transmitting antenna determined by the frequency used. If the two antennae are too close together severe distortion can occur in the received data due to interference caused by the resonation of the copper plate. The receiving antenna records the reflected radar waves and it transfers the data via fiber-optic cables to the third component, a console. The control unit then digitizes the information and displays it on the fourth component, a computer or a printout (Daniels, 2004).

1.9. GPR Systems Available

The first impulse-based ground-penetrating radars intended for commercial use were built in the mid-1970s, and right away, they were able to demonstrate their exceptional capabilities, which placed them at the very top as one of the most valuable geophysical tools. Over the years, with the development of new technology, the equipment surrounding the radar, such as display units and the units which recorded the information acquired by the system, has evolved significantly, but the application of the impulse technique has remained largely the same (Annan, 1973).

Annan pointed that; “The Radars that are constructed to operate in the frequency domain and which transmit the signal continuously are called continuous-wave (CW) radars. In case the carrier is frequency-modulated (FM), the radar is called FM-CW. Continuous-wave ground penetration radar performs a frequency “sweep” over a fixed bandwidth, beginning with a start frequency and ending with a stop frequency. The reflected wave is received and interpreted as a function of frequency indicating the amplitude of energy scattered from underground objects. The next step is to mix, or heterodyne the received signal with a segment of the transmitted signal filtered and digitized during the frequency sweep. The digitized waveform acquired from the complete sweep is then transformed into the time domain. The final result is called a synthesized pulse”.

Ground penetrating radar systems which employ synthesized pulse methods have been integrated into commercially available network analyzers and commercial synthesized source and spectrum analyzer. However, the sweep rate was slow due to limitations of the equipment used in testing and problems regarding the data storage. The implementation of continuous-wave ground penetrating radar systems has been slow because of the state of technology at that particular time. With the development of low-cost parts, test equipment previously used was abandoned and more advances components, such as frequency sources and faster digital samplers, appeared nowadays. Regardless of the method, ground penetrating radar systems are an essential tool which can be used for a wide range of purposes. Its application is only limited by the imagination of the person using it, and with the development of new solutions and hardware, (Annan A.P, 1973).

1.10. GPR Antenna Systems

Ground penetration radars have transmitting antennas which are operate in the Megahertz range and the waves that propagate tend to have wavelengths on the order of 1.0m or less. Horizontal and vertical resolution are dependent upon the wavelength, such that the smaller the wavelength, the better the resolution. Although higher frequency sources will yield smaller wavelengths (better resolution), the higher frequency signals will not penetrate as deep as lower frequencies. Thus, a careful choice must be made regarding the GPR antennas to use in a survey based on expected target and the project goals. Once a source antenna is chosen for a particular survey, GPR data can be collected rapidly (Harry, 2009).

Zoubir, et al., (2002) reported also that; “There are two distinct types of GPR: time-domain and frequency-domain. Time-domain or impulse GPR transmits discrete pulses of nanosecond duration and digitizes the returns at GHz sample rates. The time domain radars are relatively simple, cheap and robust. The weak points of the time-domain approach are a low signal-to-noise ratio and typically low accuracy of the measured data. The frequency domain GPR system transmits single frequency either uniquely, as a series of frequency steps. The amplitude and phase of the return signal is measured and the resulting data can be converted to the time domain. The frequency

domain has a higher signal-to-noise ratio due to a higher and more uniform spectral density of the radiated signal. It allows to use a much larger frequency bandwidth than the time-domain approach. On the other hand, the frequency-domain approach requires more bulky and more expensive equipment and a larger measurement time". Basic GPR system primarily consists of a data collection unit, transmitting antenna and receiving antenna as shown in Figure 1.9. If the same antenna functions as a transmitter and receiver, the system is called mono-static, otherwise it is called bi-static system. The separation of the two antennas is often fixed and the survey method using this system is referred to as common offset method (Cardimona, 2002).

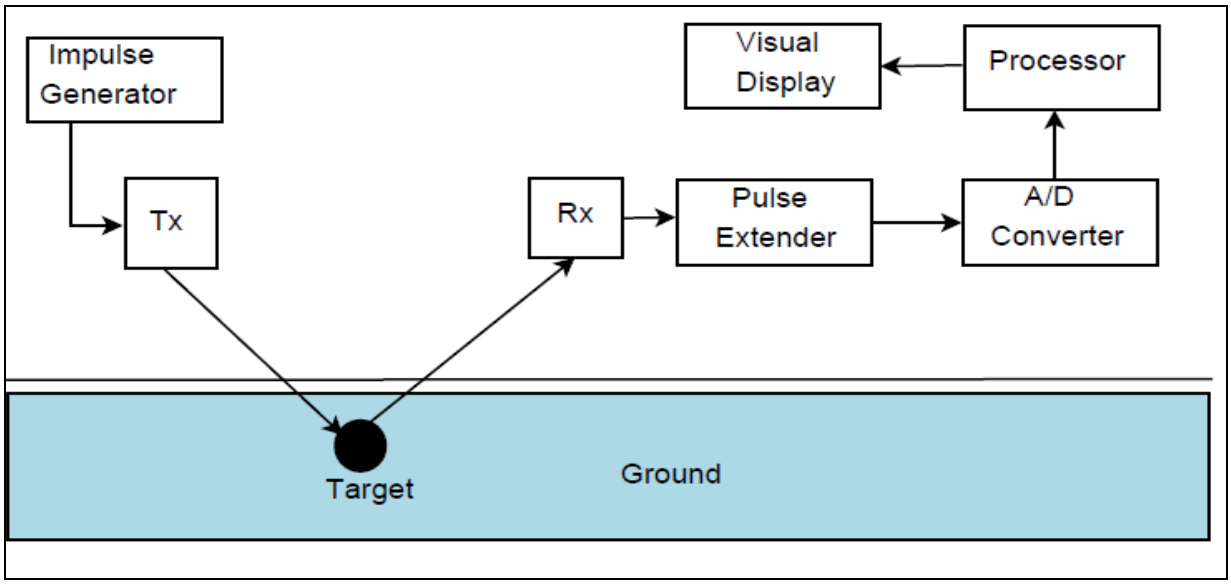


Figure 1.9. Typical GPR system, block, diagram, (Zoubir, et al., 2002).

GPR systems are either ground-coupled or air-coupled. Ground-coupled antennas are placed directly on the ground surface and then dragged over it. Air-coupled antennas on the other hand are often mounted on a specially designed cart or vehicle that drives it over the ground. Since the signal from the ground-coupled antenna does not travel through air, the majority of the energy from the antenna is transmitted into the target. Therefore ground-coupled antenna produces more visible subsurface features than the air-coupled system, (Gerald and Buchegger 2006).

1.10.1. GPR antenna characteristics

Ground penetrating radar antennas create and detect key EM fields. The transmit antenna must translate the excitation voltage into a predictable temporal and spatial distributed field. The receiving antenna must detect the temporal variation of a vector component of the EM field and translate it into a recordable signal. The following are general desired GPR antenna characteristics (Engheta et al, 1982).

i) The exact source and detection location must be definable. The transmitter and receiver responses (transfer functions converting electric field to from voltage current) must be time and space invariant.

ii) The vector character of the field linking the source voltage and received voltage must be quantifiable.

iii) The bandwidth of antennas must match the system application needs.

Current travel time across the antenna dimension must be comparable to the temporal rate of change of the exciting voltage or field. In frequency domain terminology, the antenna dimension must be similar to the wavelength of the signals. For efficient operation, finite-size antennas must be used. They have the following characteristics:

i) Field creation and detection occurs over a spatially (and temporally) distributed region, (in other words, source and detection points are imprecise),

ii) Field transit time (or wavelength) in GPR application depends on the host environment and is not invariant. (In other words, antenna response cannot be perfectly invariant),

Therefore, it can be concluded that; *"spatially distributed antenna"* means less-precise vector characterization of the response since isolation of response to a single vector component becomes geometrically difficult. On the other hand "*finite-dimension antennas*" have a preference to emit energy at frequencies that resonate on the structure.

Bandwidth is best maximized by damping an antenna which makes it less sensitive to its surroundings and less efficient. Antennas that have been proven most effective for GPR are short electric dipoles types. Resistively loaded small dipoles yield a fair degree of faithfulness to desired predictable and invariant behavior while retaining some efficiency, Smith (1984). The directional characteristics of a short electric dipole antenna are controlled by the ground. Although the analysis of this problem is a complex problem and the basic characteristics of the problem were explained by Annan (1973), Annan et al. (1975), Engheta et al. (1982) and Smith (1984).

1.10.2. GPR Antenna applications

Stratigraphy: stratigraphy is a survey process to determine ground conditions more precisely (Figure 1.10 and 1.11); for example; rock layers, disturbance in the rock and soil masses, homogeneity of rock-soil mass, water table levels in underground etc. (Bekic, 1964).

Depth: If the depth of interest is deep, that means it vary from 5-30 meters. Shallow objects in underground are disregarded. The amount of traces is lowered as much as possible due to the characteristics of the target, layers usually don't change abruptly in a few centimeters. Antenna recommended for this survey is GCB-100.

If the depth of interest is medium depth, that means it vary from 3–10 meters and the majority of shallow objects are disregarded. The amount of traces amount is lower than for shallow applications, but slightly higher than for deep surveys. This is a result of smaller targets like voids and water leakages. Antennas recommended for the survey are GCB-200, GCB-300 and GCB-400.

If the depth of interest is shallow depth, that means it vary from 0-2.5 meters and the amount of traces is the highest for these applications. In this case, the researcher will be interested not only in the rock layers, but probably in possible cracks as well. Antennas recommended for the survey are GCB-400, GCB-700 and GCB-1000 (Bekic, 1964).

Utility detection: Utility detection is a survey process during GPR to determine the position of man-made objects more precisely pipes, tunnels, trenches etc. In underground.

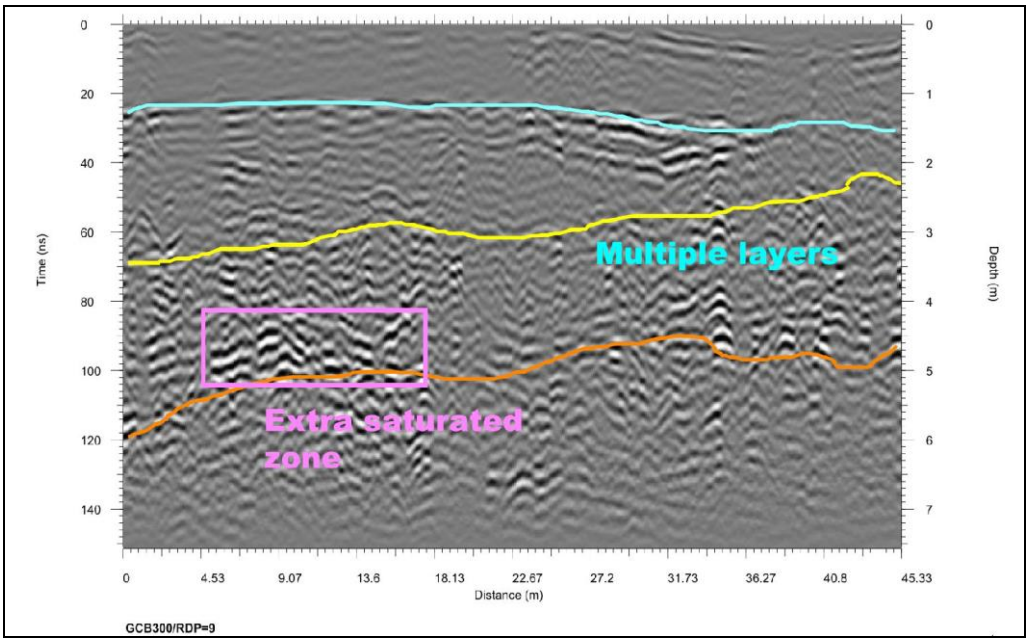


Figure 1.10. Ground section obtained by GPR (with GCB-300 antenna) for medium depth stratigraphy for dry soil (Bekic, 1964).

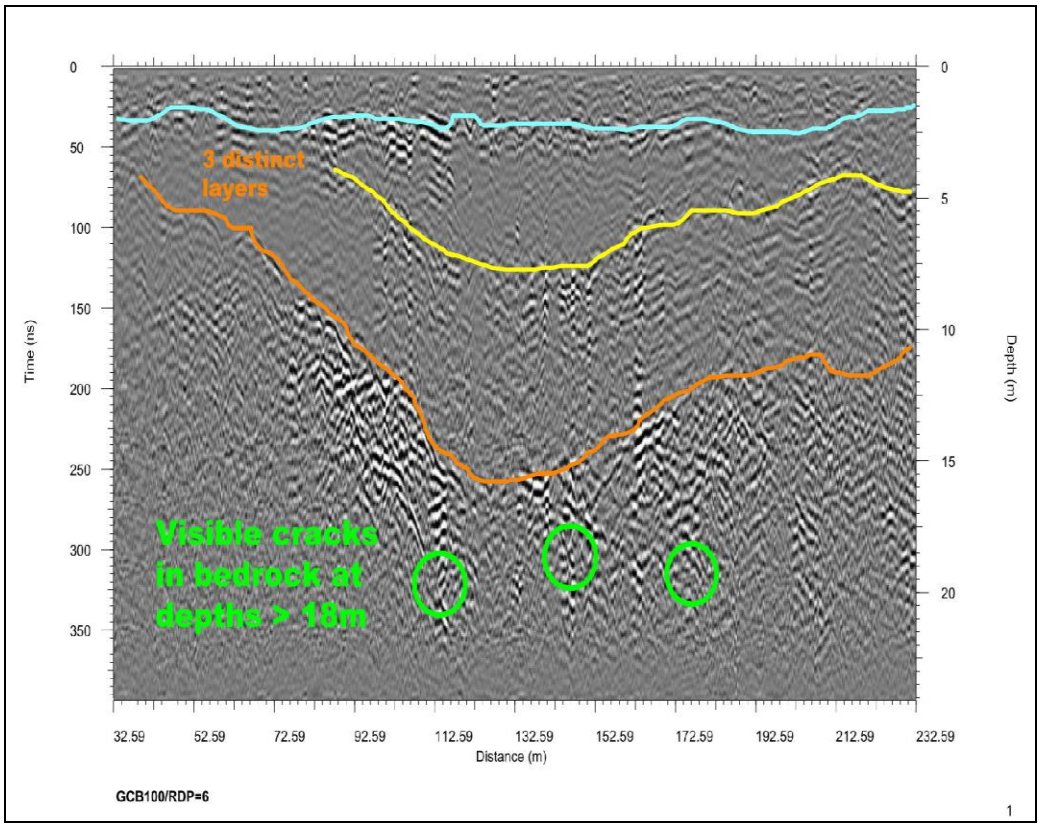


Figure 1.11. Ground section obtained by GPR (with GCB-100 antenna) for deep stratigraphy for dry soil (Bekic, 1964).

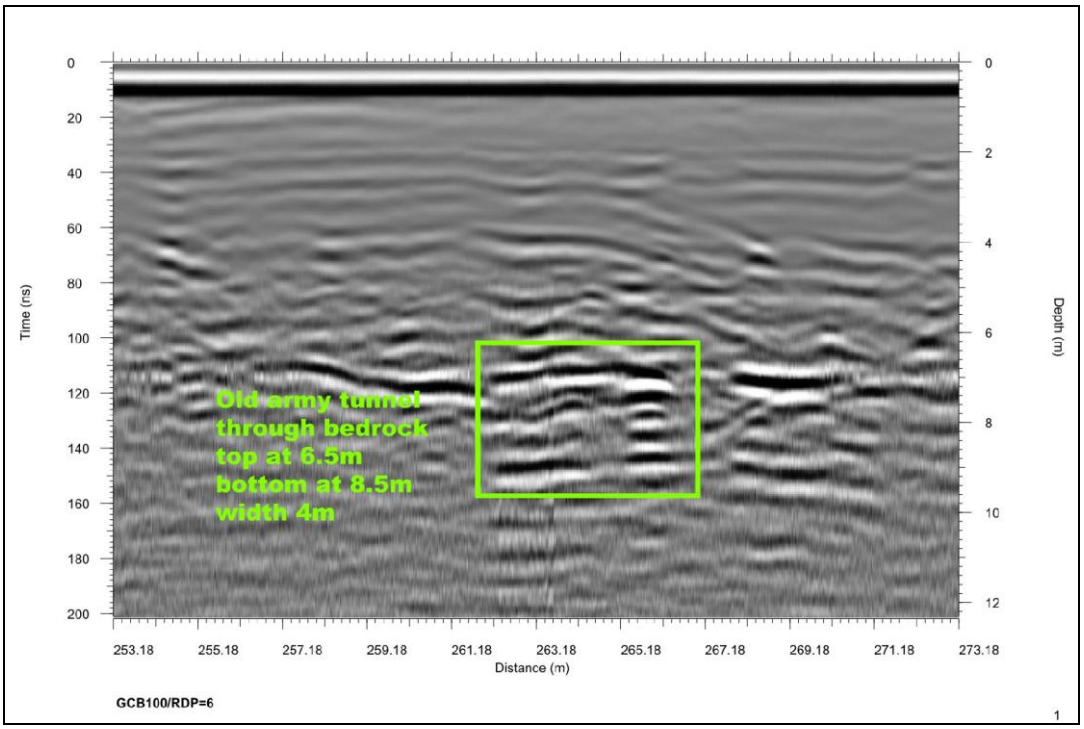


Figure 1.12. Utility detection by GPR in average soil by using GBC-100 antenna, (Bekic,1964).

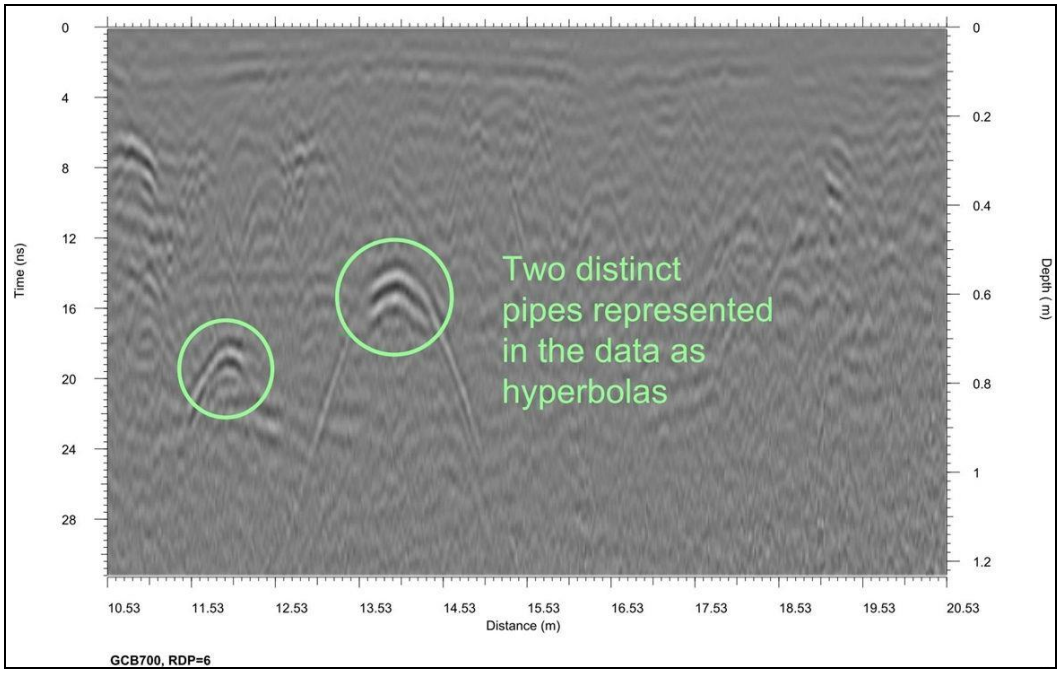


Figure 1.13. Utility detection by GPR in average soil by using GBC-700 antenna. (Bekic, 1964).

Frequencies: Under normal conditions, the most dominant factor in the collection of good data while using GPR is choosing the right frequency. There is a wide range of antenna frequencies to choose from, and since the site itself is the determining factor of which one to use, the choice can get complicated very quickly. There are two very important factors that must be considered when choosing a frequency.

The first factor is the depth of the study in question. Different frequencies penetrate to different depths with different results. Characteristically, lower frequencies (<100 MHz) penetrate to depths of 30 meters or more. But return with a rather low-resolution representation of a profile. Higher frequencies (>300 MHz), return a relatively high-resolution representation, but only penetrate to depths of 5 meters or less. This shows that depth is a very important factor to consider.

The second factor that must be considered is the material present at the location. Certain sediments or materials cause problems when using GPR. For example, radar energy is weakened much more rapidly by clays than by other sediments such as sand or silt. Magnetic properties of materials can also interfere with the GPR equipment and cause distortion in the data. The frequency chosen when using GPR will have a serious impact on the data collected, so all factors must be considered the first time so as to avoid repetitive work, (Annan and Davis, 1976).

2. GROUND PENETRATION RADAR METHODOLOGY

The GPR method provides a high-resolution image of subsurface features in the form of a cross section view that is essentially a map of the variation in ground electrical properties. These can be correlated with physical changes such the soil, bedrock interface, the boundary between different soil types, the water table, underground structures such as pipes, cables and tunnels as well as voids and cavities. Features in the GPR section will correlate with geological cross sections if for instance stratigraphic boundaries representing different rock types correspond to significant variations in the electrical properties, but not necessarily to other physical properties such as density, grain size or chemical composition, (Annan and Davis, 1977).

The short pulses of radar energy are radiated into the ground from a transmitting antenna placed either on the ground surface or in close proximity. Energy reflected back to the surface from subsurface targets is detected by the receiving antenna, also located in close proximity to the surface. The antennas physical size or dimension limits the frequency (or wavelength) of the transmitted pulse. A high frequency waveform (short wavelength) will provide a more detailed or higher resolution image than a low frequency waveform, but the higher frequencies are attenuated or absorbed at a greater rate so the penetration depth is not as great as lower frequencies, for any specific application, the appropriate choice of antenna frequency involves a compromise between resolution (or size of objects/features to be detected) and the depth of interest (Morey, 1974).

The transmission is characterized as a single burst of energy after which the receiver then ‘listens’ and records any reflected energy such that the recording time (from the point of transmission) represents the depth to the source of the reflection. That is, a reflection from a deeper target will appear later in time in the GPR section since the energy has travelled further than for the shallower targets. At any instance, the receiver is only on for a finite period of time (of the order of several hundred nanoseconds) after which another pulse is transmitted to repeat the process. The GPR section is actually a time section, however with knowledge of the propagation velocity, time is converted to depth, (Morey, 1974).

The two most important soil and rock electrical properties are the dielectric constant and conductivity. Both are greatly influenced by water (soil moisture content). Therefore water has a significant influence on GPR performance overall. Soil conductivity limits the maximum depth of energy penetration (or target detection depth) since it influences the rate at which the energy is absorbed. A more conductive soil (one that is wetter and or has a higher clay content) will absorb the energy at a far greater rate than a low conductivity soil such as dry sand (Figure 2.1). The penetration depth in dry clay soils will typically be in the range of one or two meters and a wet clay will reduce penetration to less than one meter, whereas dry sand soil will allow penetration to more than 10 meters. Rock types with low conductivity (high resistivity) include limestone, coal, granite and other crystalline rock, whereas rock types that are more conductive include basalt, shale and mudstones or any weathered terrain with reasonably high porosity.

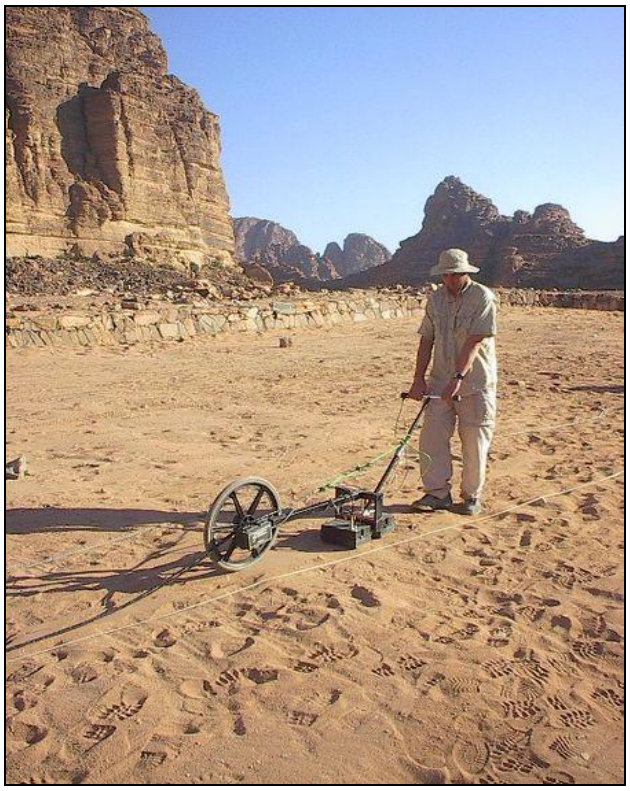


Figure 2.1. Ground penetrating radar survey of an archaeological site in Jordan, (Lawrence and Goodman, 1997).

The Radio frequency (RF) energy propagates through the ground at about one-third the speed of light or 10cm.ns^{-1}. Griffin and Pippett (2002) stated that “the velocity

of propagation will vary for different earth materials, but will generally be within the range 8–12 cm.ns^{-1} and is determined by the relative dielectric constant (expressed as a quantity relative to the value of air). All materials of interest will vary between the range 1 (for air) and 81 (water). Geologic materials will generally fall within the range 5–15".

A reflection will occur in response to changes in the dielectric constant, and this may not necessarily correlate with properties such as density, which most people intuitively understand from their experience with seismic methods. However, the dielectric constant or electrical permittivity is analogous to the acoustic impedance in seismic, in a mathematical sense. That is, as well as determining velocity, the change or contrast in the dielectric constant with different earth materials will cause a reflection whose strength (or amplitude) is dependent on the magnitude of that contrast. To summarize the importance of water in understanding GPR performance, a higher moisture content in the soil will reduce the possible depth of penetration, but may provide for a stronger reflection, since the presence of water will increase the dielectric constant significantly, (Ulriksen, 1982).

2.1. GPR Application Sites

Application of radar techniques for ground visualization opens new dimension for engineers in their design works. Main applications of GPR can be listed as follows; Rock related sites, environmental problems, glaciological researches, engineering and construction applications, archaeology and its excavation sites, forensic sciences etc. In these group of applications two of them are more related with the study performed during this thesis study. One of them is rock related and the other is engineering & construction applications. Ground penetration radar applications to understand rock mass related subjects can be listed as follows;

a) Detection natural cavities and fissures,
b) Subsidence mapping,
c) Mapping of superficial deposits,
d) Soil stratigraphy mapping,
e) Geological structure mapping,

f) Mapping of faults, dyes, coal seams,
g) Lake and river bed sediment mapping,
h) Mineral exploration and resource evaluation.

GPR applications in engineering and construction purposes can also be listed as follows;

a) Road pavement analysis,
b) Void detection,
c) Location of reinforcement (rebar's) in concrete,
d) Location of public utilities (pipes, cables, etc),
e) Testing integrity of building materials concrete testing (Yelf, 2007).

2.2. Common Middle Point

The common middle point (referred to hereon as CMP) is a method used to determine the velocity at which the radar waves are penetrating the subsurface stratigraphy. The CMP method involves shooting radar at pre-determined increments outward from a common middle point until a side profile such as the below figure is produced. The method is dependent on the simple physics equation,

Distance (meters) = Velocity (meters/ns) x Time (ns).

The average velocity is found by determining the average slope of the profile created. This slope is calculated by dividing the distance (m) traveled from the midpoint, by the deepest time (ns) achieved during the test. This number is equal to the slope of the line on the profile, as well as the average velocity of the radar waves in meters/nanosecond, (Daniels, 2004).

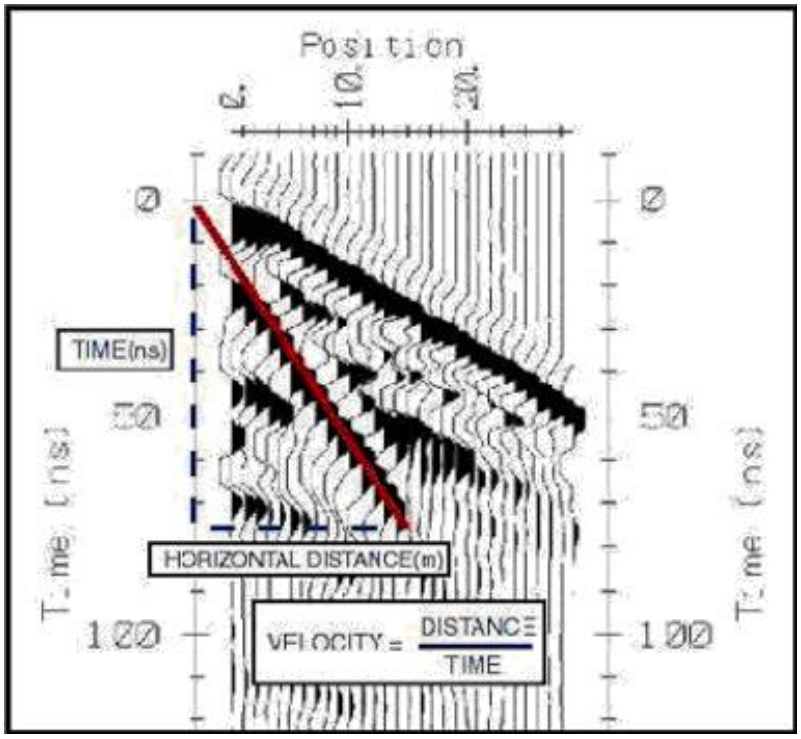


Figure 2.2. Common Middle Point (CMP) profile of Russell Spit in Western Nevada, (Daniels, 2004).

2.3. GPR Surveying Methods

Annan and Davis (1976) reported that; "The GPR technique is similar in principle to sonar methods. The radar transmitter produces a short pulse of high frequency (25–1000 MHz) electromagnetic energy. Variations in electrical impedance are largely due to variations in the relative permittivity or dielectric constant of the ground. The reflection coefficient for a normal incident signal is

$$R = \frac{\sqrt{K1} - \sqrt{K2}}{\sqrt{K1} + \sqrt{K2}}$$

Where;

K_1 : the dielectric constant of medium 1,

K_2 : the dielectric constant of medium 2.

The power reflected is $|R|^2$. Water has a dielectric constant of 80 (compared, for example to 5 for materials), so water table in underground is a strong reflector."

The mode of GPR surveying deployed here was common-offset, single-fold reflection profiling. In such a reflection survey a system with fixed antenna geometry is moved along a survey line to map reflections versus position. The radar section is built up from successive traces that are either recorded with the radar stationary at each point or moved continuously in a walking mode. All radar traces are accumulated by stacking traces in order to improve the signal to noise ration. In walking make, a slight smearing of the data will occur, but it is minimal due to the very high propagation velocities of electromagnetic waves. There are seven parameters to define for a common-offset, single-folded GPR reflection survey. These are the frequency, the time window, the time sampling interval, the station spacing, the antennae spacing, the line location and spacing and the antennae orientation. These are selected from a consideration of (Annan and Davis,1976).

a) What is the target depth?
b) What is the target geometry?
c) What are the target electrical properties?
d) What is the host material?
e) What is the survey environment like?

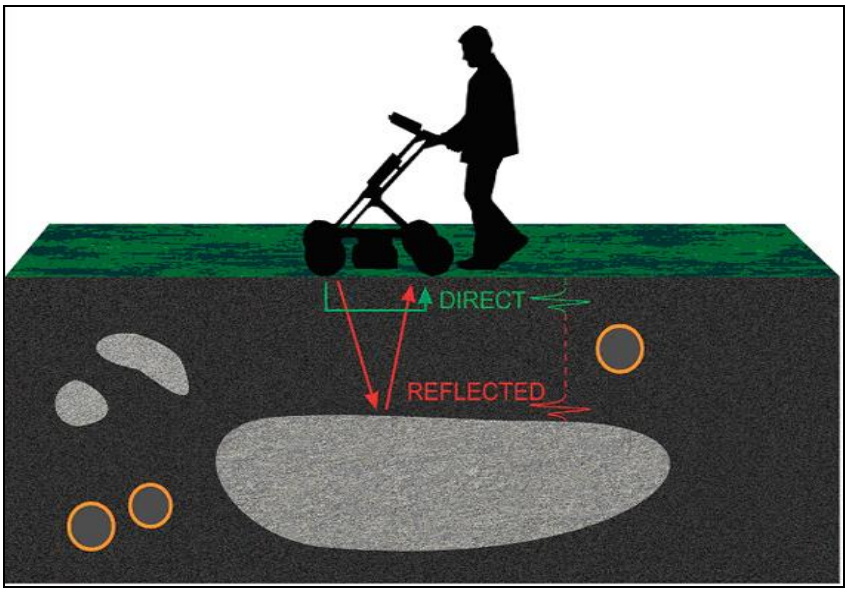


Figure 2.3. GPR surveying method illustrated by (Bekic, 1964).



Figure 2.4. GPR system on carrying cart, (Bekic, 1964).

Ground penetrating radar (GPR) is a non-invasive method of material analysis based on transmitting an ultra-wide band EM signal into the materials. A part of the EM wave is reflected when it reaches a boundary between two materials with different electrical properties. The reflected signal gets recorded at the source of the EM wave and is displayed for the operator and frequently recorded for late analysis. One of the first commercial GPR systems were developed in the early 1970's mainly for mining applications. During the last 40 years they have evolved greatly, starting as analogue instruments and entering the digital era sometime during the 1990's. Although most of the nowadays GPR systems are light-weighted. Sometimes they are mounted on a cart (Figure 2.3 and 2.4). This allows the user to move easily on the field while collecting the GPR data, (Bekic, 1964**).**

2.4. Significance of GPR

Due to the nature of GPR being a low cost convenient method of research, it is a tool that can improve the quantity, quality and relative ease of research as compared to other more invasive methods of research such as trenching or extensive digging. For instance, an area that may have once required the digging of many small pits or extensive coring to determine the depth of bedrock underneath the surface can now be accomplished by simply and quickly applying GPR while the data can be interpreted later. In this instance GPR not only would save a large amount of time, but it would most likely also save a large amount of money. Funding is a highly important aspect of research and can potentially make or break a given project. Saving money in one area allows for that money to be applied elsewhere. The resulting money saved can be applied to more research, ultimately getting more research done for the same amount of money required in the use of traditional methods. GPR systems are also fully mobile allowing them to be taken into remote areas which are hard to access with other exploration equipments (Figure 2.4). Using GPR as a standalone method may not be a feasible option or be quite as precise as needed for some types of research requiring very detailed information. But in many instances GPR can be used as a complement to other methods to significantly improve the chances for efficient, effective research, (Cai, et al., 1996).

Cai et al. (1996) wrote that; “When using GPR for fault investigation it can be coupled with traditional trenching methods. A trench is expensive, time consuming, and it disturbs the area. If a trench is put in a position that is later found to be undesirable it can have adverse effects on the study that are far reaching if there are not sufficient funds for additional trenches. GPR surveys throughout an area can be very useful in narrowing down a suitable location for the trench. This will either save money over digging a new trench, or providing valuable information that would have been unobtainable using a trench in a less suitable location when another could not be funded. GPR data can also be used to extend the information gained from an open trench laterally, and in many instances can travel to much greater depth, to create a more comprehensive model of the faulted area”.

2.5. Instrument Types And Configuration

The following is a list of commercially available GPR systems with a brief summary of the key similarities and differences and how this relates to certain limitations.

i) Geophysical Survey Systems Inc. of Burlington New Hampshire, USA. GPR system includes the SIR2000, SIR10 system. These systems have a range of in-house and third party antennas ranging in frequency from 40 to 15000 MHz and all being shielded antennas.

ii) Mala Geosciences Inc. of Mala, Sweden. This company has the RAMAC/GPR system. The RAMAC system has a full range of antennas from 25 to 1000 MHz including borehole probes, either 100 or 250MHz. the RAMAC system console controls both the unshielded and shielded antennas and the borehole probe with a PC Notebook computer as the acquisition, display and storage device. The Mala's ranges of antennas include 25, 50, 100 and 200 MHz unshielded and 100, 250, 500, 800 and 1000 MHz shielded.

iii) Sensor and Software Inc. of Toronto, Canada. This company has the pulse EKKO100 and pulse EKKO 1000 systems and the Nogun systems. The pulse EKKO 100 system is designed for low frequency systems using unshielded antenna and the pulse EKKO 1000 system is for the higher frequency applications using shielded antennas from 200 MHz to 900 MHz. The Nogun systems are a single frequency unit with either 250 or 500 MHz. Both pulse EKKO and the Nogun systems use a PC Notebook computer as the acquisition, display and storage device (Annan and Cosway, 1991).

3. GROUND PENETRATION RADAR MEASUREMENT PRINCIPLE

Standard ground penetrating radar systems consist of a transmitting and a receiving antenna. High-frequency (range: 50 MHz) electromagnetic pulses are emitted into the ground by the transmitting antenna. The radar wavelet propagates through the soil or rock while the velocity of the wavelet depends on the dielectric properties of the ground. At interfaces, e.g., boundaries of different soil and rock layers or distinct objects, where the dielectric properties of the different media change erratically, the electromagnetic wave is partially reflected. The travel time and amplitude of the wavelet is recorded by the receiving antenna. The travel time of the wavelet which is recorded by the receiving antenna depends on the path along which the wavelet propagates and the dielectric properties of the materials. Figure 3.1 and 3.2 show travel path of various wave types through the soil. The first wavelet which is detected by the receiving antennas the so-called air wave which propagates through the air between both antennas with the vacuum speed of light. The second wavelet which reaches the receiver is the so-called ground wave. It propagates also directly between the transmitter and the receiver along the air-soil interface and can be applied to infer the near-surface soil moisture content. Air- and ground wave are also known as “direct waves” which always occur, independent of soil structure, (Gerhards, 2008).

In layered soil we can detect further, reflected and refracted wavelets. Reflections occur at interfaces between soil layers with different dielectric properties. If $\varepsilon'_1 > \varepsilon'_2$, a further type of wave, so-called refracted wave, is originated and propagates parallel to the boundary of the second layer (Figure 3.2), (Robinson, 2003).

The signals of the various emitted wavelets reach the receiving antenna at different times. Plotting the recorded amplitudes as a function of time results in a so-called “trace” Figure 3.3 shows a trace which consists of air wave, ground wave and reflected wave. In a standard GPR measurement, the antennas are pulled along the survey track while traces are triggered at a fixed interval by a measurement wheel which is connected to the back of the antenna. This results in a series of traces which are finally displayed by the measurement software as a function of position and time (Figure 3.4) in a so-called radargram (Robinson et.al, 2003).

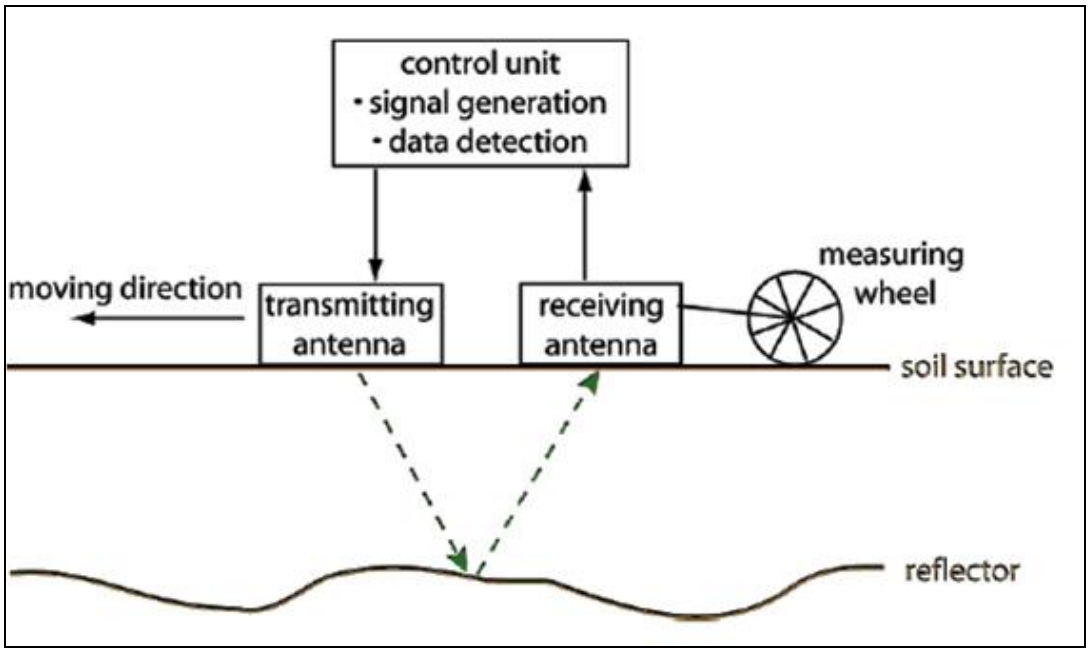


Figure 3.1. Ground penetrating radar measurement principle, (Robinson, 2003).

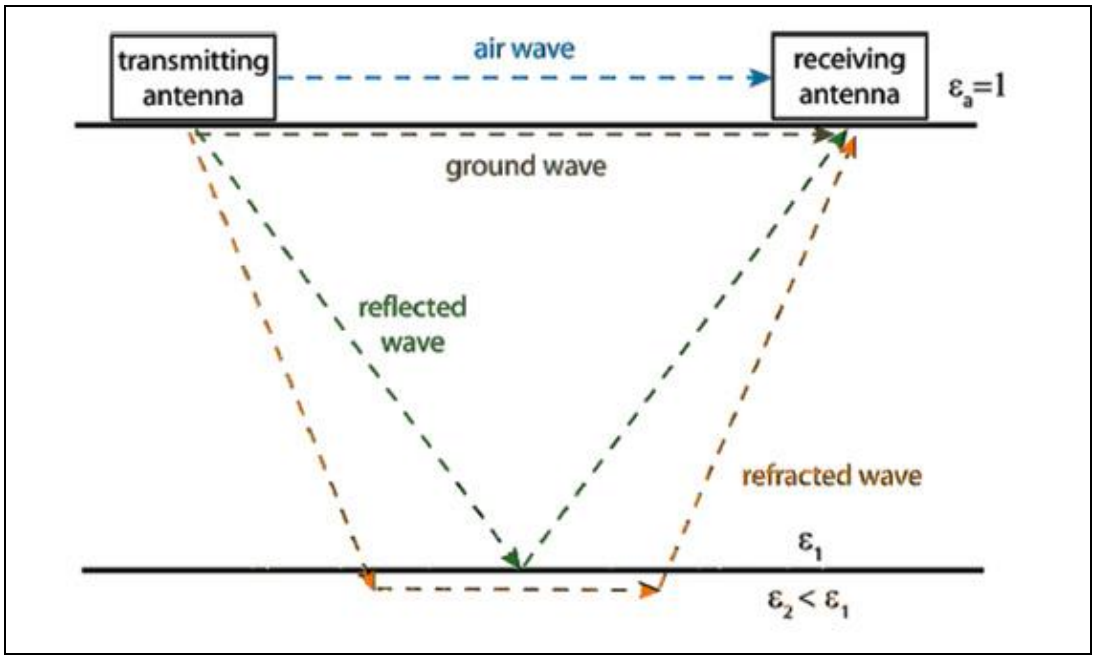


Figure 3.2. Travel paths of different GPR wave types in a two-layer soil with different relative permittivities, (Robinson, 2003).

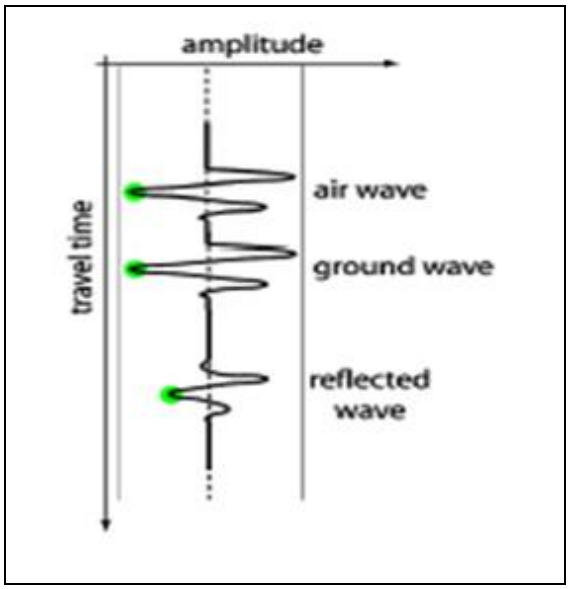


Figure 3.3. GPR traces, a wavelet always consists of a number of "wiggles" which are displayed in the radargram as a series of lines (e.g. red-blue-red) (Robinson, 2003).

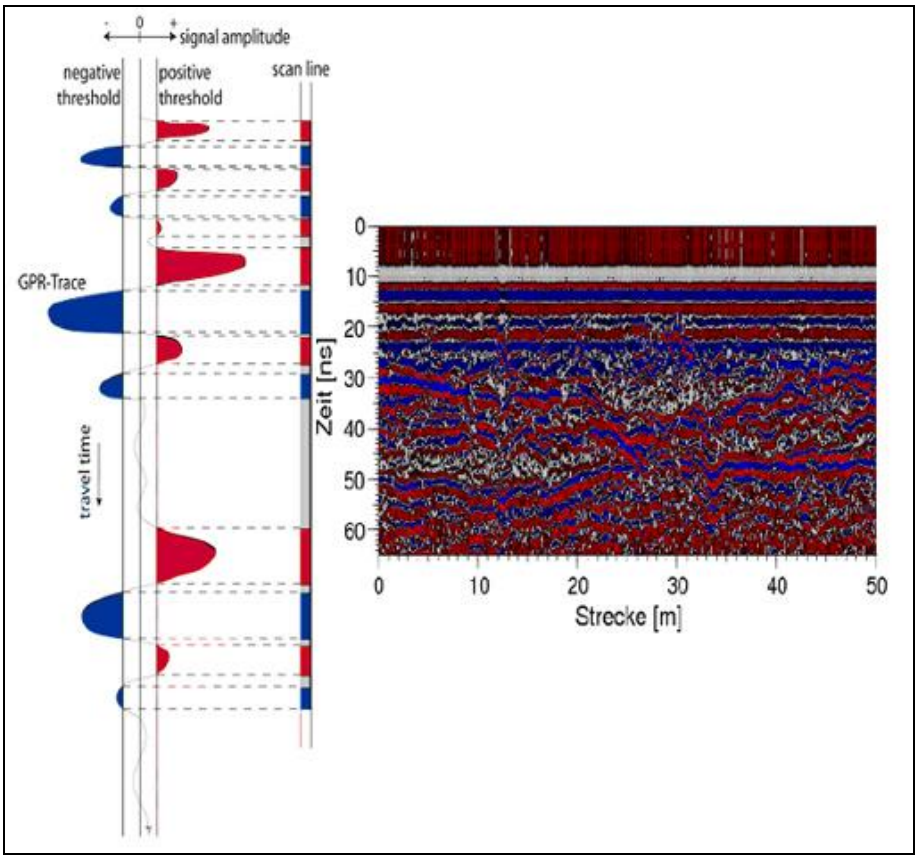


Figure 3.4. Origin of a radargram. Amplitudes which excess a pre-defined positive or negative threshold are displayed in color. In this example negative amplitudes are shown in blue while positive amplitudes are displayed in red, (modified after Reynolds, 1997), Robinson, 2003).

3.1. Electromagnetic Wave Propagation

Geophysical methods based on wave phenomenon (such as GPR, remote sensing, and seismic surveys) generally provide more realistic images and have better resolution than other methods such as those based on diffusion or potential fields. One reason for this is that the distance to reflectors can be easily measured using the two-way travel time of the waves. Another reason is that wavelets propagating through a lossless non-dispersive medium are stationary and the spatial resolution in the direction of wave propagation does not decrease with distance from the reflector. This contrasts with all potential fields methods such as; gravity, magnetic, and DC resistivity surveys. With these methods, it can be more difficult to determine the range to the anomalous body and the spatial image resolution decreases with distance to the anomalous body. Wave based methods are not without limitations however. The spatial resolution of wave based methods is limited, and the size of detectable anomalies is a function of the wavelength of the investigation waves. The resolution of the GPR method is generally higher than that of the seismic method because the waves used in GPR surveys have shorter wavelengths than those used in seismic surveys (Arcone, et al., 2003).

When a GPR is operated in a conductive or lossy environment, the preceding comments are less accurate. In general, the fields close to the antennas are better described by diffusive energy transport rather than wave propagation. Thus, the spatial resolution of images produced very near the antennas is less than that of the images further away. For the case of conductive or dispersive ground, fully propagating fields never develop at any distance from the antennas because the energy transport is a combination of diffusion and propagation. In this case, the entire survey space is filled with either energy being transported diffusively or with waves that have a diffusive component. Even so, the standard propagating wave analysis techniques can be used for dispersive ground if modified appropriately. The point is that high resolution GPR imaging in lossy ground poses unique challenges that require better techniques than the current state of the art due to the presence of diffusive energy transport. Therefore, one of the goals of this dissertation is to present means for improved imaging and signal processing in conductive or lossy ground conditions. The primary tool for these improvements is a means to estimate the shape of the subsurface waveforms (Robertsson and Holliger, 1998).

The propagation of waves in a homogenous medium can be described with knowledge of the electrical properties of the medium. The propagation and attenuation versus distance of a monochromatic wave (or a spectral component of a wave field) is specified in a given medium by the wave number "k" (Ward and Hohmann, 1987);

$$\boldsymbol{k = \sqrt{-YZ} = \beta - i\alpha,} \qquad \textit{(3.1)}$$

Where; Y : the admittivity of the medium,
Z : the impedivity of the medium,
B : the phase constant,
A : the attenuation constant,
I : the square root of negative.

Ward and Hohmann (1987) stated that, "fourier decomposition can be used to express any wave field in terms of its spectral components. The admittivity and impedivity are in turn properties of the electrical properties of the material according to;

$$Y = \sigma + i\omega\varepsilon \qquad (3.2)$$

$$Z = i\omega\mu \qquad (3.3)$$

Where; Ϭ : conductivity,
E : dielectric permittivity,
μ : magnetic permeability,
ω : radian frequency.

The dielectric permittivity and the magnetic permeability are functions of frequency and are in general complex numbers. Here however, the magnetic permeability's assumed to be that of free space, and all materials are assumed to be linear and isotropic. The propagation constant is composed of a real and an imaginary part. The real part describes the change in phase of the wave versus distance, and the imaginary part describes the attenuation versus distance. The ratio of the imaginary and real parts is called the loss tangent, and is proportional to the ratio of the energy lost per cycle (dissipation only) to the amount of energy stored (or propagated). With the permeability being that of free space the electric loss tangent is given by;

$$\tan \delta_e = \frac{\sigma + \omega \varepsilon''}{\omega \varepsilon'} \tag{3.4}$$

Where; tan δ $_e$ is the electric loss tangent, ἐ and ἕ are the real and imaginary dielectric permittivity respectively. An analogous magnetic loss tangent can be written, however here, it is assumed that no magnetic losses occur".

Olhoeft (1984) wrote that, "estimated the depth of penetration (in meters) for most commercial GPR systems to be about 0.5 divided by the loss tangent. Equipment improvements in the last 20 years push this depth to about 0.75 divided by the loss tangent. Generally, conductivity values greater than about 30 mS/m cause too much loss for effective GPR surveys".

When waves travel through a medium, the amplitude of the wave is anttenuated by dissipative losses and scattering losses. Generally, dissipative loss and scattering are functions of wave polarization for anisotropic media. In this dissertation however, the attenuation properties of all media are assumed isotropic and independent of polarization. Dissipative losses occur in mediums with non-zero conductivities and with dielectric losses. In addition to zero frequency conductivity, several dominant processes contribute to the lossy dielectric effects observed in low frequency (10 to 500 MHz) GPR surveys there are other loss mechanisms which produce smaller effects. They are bound water polarization, the Maxwell-Wagner effect, colloidal polarization, and double layer polarization (Ishida et al., 2000).

These dielectric loss mechanisms can be modeled using a simple relaxation model. This model describes the frequency dependent changes in dielectric properties using relaxation oscillators where charge is displaced. Relaxation oscillators have a characteristic recovery time, which affects the frequency response. A good discussion of these phenomena is given by Olhoeft (1985), Wtorek (2003) and Sihvola (1999).

Scattering losses occur at all frequencies due to scatters of all sizes, and are frequency dependent. Rayleigh scattering occurs when the scatters are smaller than about a tenth of a wavelength, Mie scattering occurs for larger scatters, and optical scattering occurs when the scattered is larger than a few wavelengths. Ulaby et al., (1982), Balanis (1989) and Mishchenko et al., (2002) discuss the scattering of electromagnetic waves in detail. Although multiple scatters locate within the same

Fresnel zone may cause amplitude loss, they cannot be independently resolved by far-field observations due to the diffraction limit. Under some circumstances, it may be possible to resolve small heterogeneities beyond the diffraction limit in the near-field region if short wavelength evanescent waves can be measured (Kelso et al,. 2001; Durig et al,. 1986). Scatters too small to be imaged may cause loss, and the composite lossy effect of the small scatters can be accounted for in the frequency dependent material properties. However, the effects of scattering are often treated separately so that the material properties reflect only conductivity and dielectric relaxation effects. The frequency dependence of scattering losses varies widely, but often follows a power law (ω^n where n varies from -1 to 4, Balanis, 1989), (Kelso et al,. 2001; Durig et al,. 1986).

3.2. GPR Fundamentals And Material Properties

The foundation of GPR lies in electromagnetic theory. The history of this field spans more than two centuries and is the subject of numerous researches. The goal in this chapter is to provide the basic building blocks needed to work quantitively with GPR without reiterating reams of theoretical development. GPR represents a subset of the full electromagnetic field. GPR signals are electromagnetic waves; Maxwell's equations which mathematically describe electromagnetic physics plus constitutive relationships which quantify material properties are the foundations for quantitatively describing GPR signals (Annan and Davis, 1989).

Waves can propagate a sufficient distance through earth materials to useful. Annan and Davis (1989) wrote that, "GPR frequencies are predominantly in the 1 to 10000 MHz range. In general, electrical conductivity dictates depth of exploration. In sea water, for example, radio signal will only penetrate a few millimeters whereas in highly resistive granite formations signals can be transmitted through tens and even hundreds of meters of rock and still be detected". A good overview is given below and some of the main points are reviewed as Annan and Davis (1989) were described before.

Figure 3.5 shows the electromagnetic wave propagation properties versus frequency for typical geologic material. When velocity and attenuation show a plateau (which occurs typically in the 1 to 1000 MHz frequency range), then GPR becomes a

viable method. This plateau occurs when displacement currents dominate conduction currents in the medium. In the plateau region, velocity and attenuation become essentially frequency independent and electromagnetic pulses can be transmitted with minimal dispersion although suffering significant attenuation. This plateau is sometimes referred to as the GPR window. Since attenuation is exponential with distance, there is always a finite depth of exploration (Annan and Davis, 1989).

The frequency at which the GPR wave property plateau occurs increases as the direct current (DC) electrical conductivity rises. Often the plateau disappears all together as the low frequency conductivity merges with loss effects at higher frequencies which are most often induced by the presence of water. In general, clay minerals and electrically conductive pore water limit penetration while changes in water content dominate velocity and reflectivity.

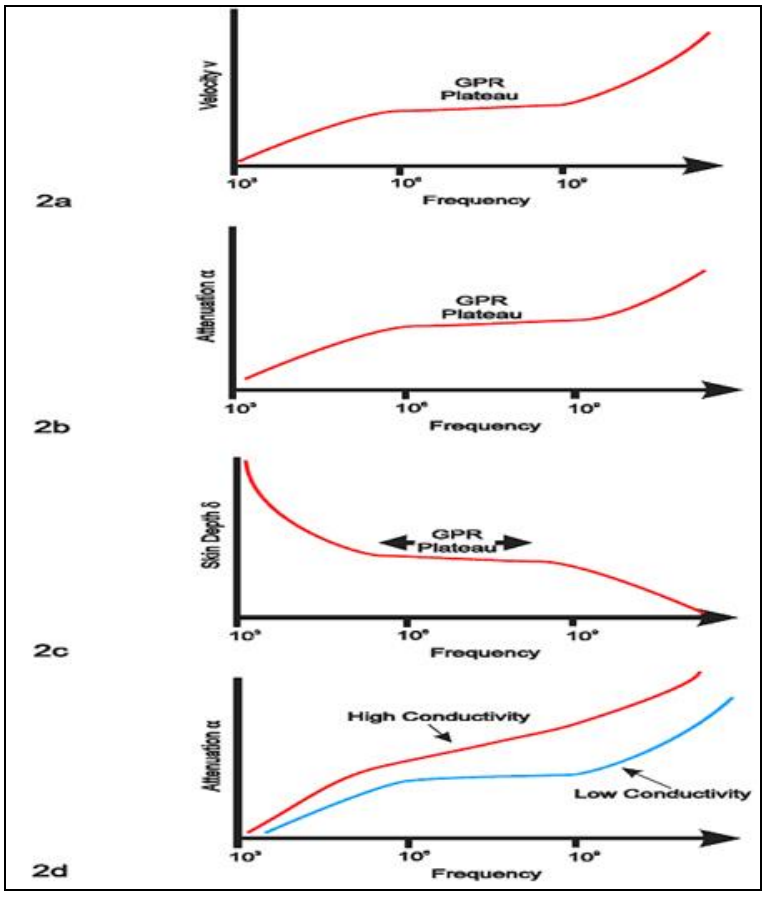


Figure 3.5. GPR waves are characterized by the velocity of propagation and degree of attenuation. a) Velocities generally increase with frequency as depicted in. b) Attenuation also increases with frequency. c) its alternate form, skin depth ($\delta=1/\alpha$) decreases with frequency. d) For successful GPR measurements a plateau event exist where these properties become frequency independent. In some high loss materials, the plateau may ever exist a depicted in, (Annan and Davis, 1989).

The subject of electrical properties of geologic materials is extremely wide ranging. An extensive discussion of the subject is given by Olhoeft (1987). Most important for GPR users is the exploration depth. A simplified chart of exploration depth for common materials is presented in Figure 3.6 (Annan and Davis, 1989).

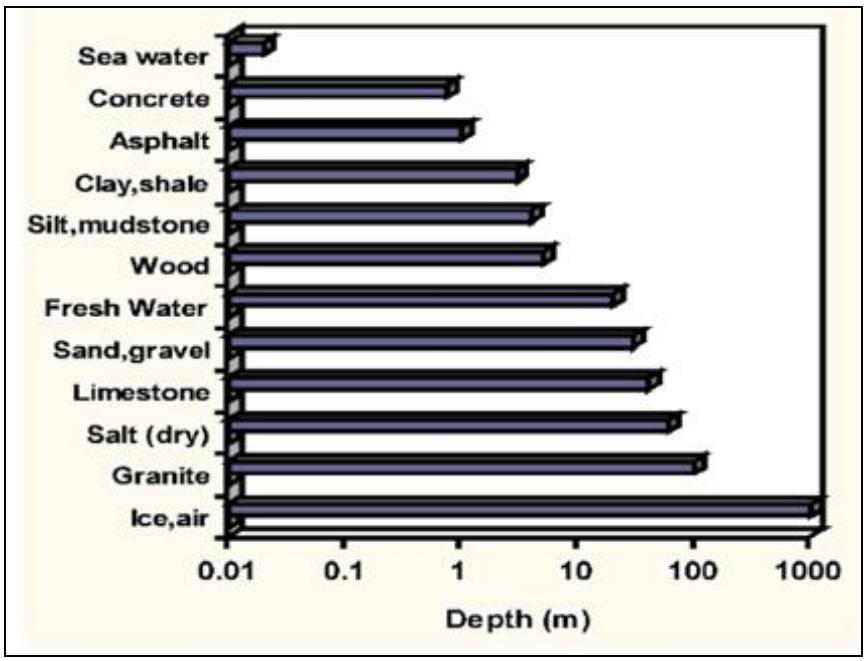


Figure 3.6. Typical exploration depths achievable by GPR in common materials, (Annan and Davis, 1989)

Reflection GPR maps subsurface features by detecting electromagnetic waves which are reflected. By measuring at a number of positions, the location and the depth to subsurface objects can be inferred. Reflections are caused by changes in electrical character between the reflector and the surrounding host material. Event very minor changes in material composition or in water content give rise to changes in electromagnetic impedance which in turn cause radar reflections (Figure 3.7). Mineralized zones which form metallic conductors will reflect all incident signal. As a result, contacts between rock types, fracture zones, shear zones and mineralized areas as well as voids and cavities give rise to good detectable radar response and are most often the targets in GPR investigations (Olhoeft, 1987).

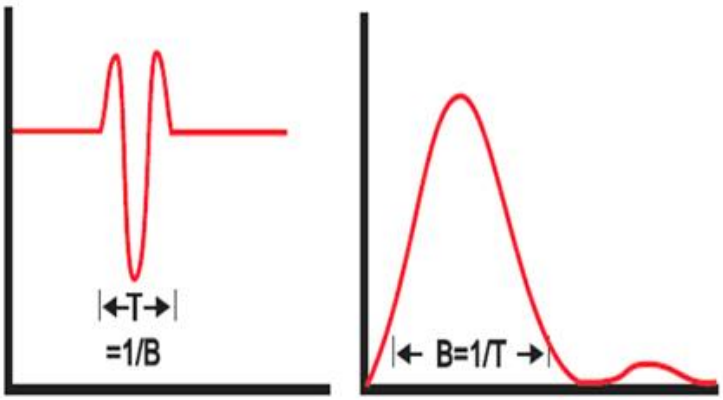
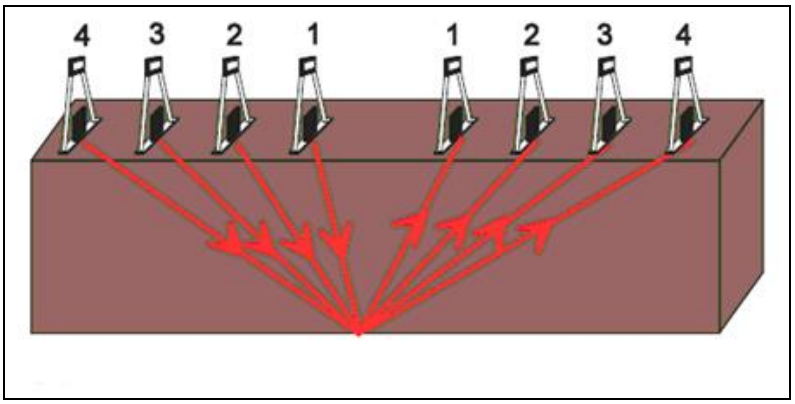


Figure 3.7. GPR wavelets are generally as shown in (a) which is characteristic of small dipole antennas. The corresponding frequency spectrum is shown in (b). Pulse duration and bandwidth are inversely related, (Annan and Davis, 1989).

3.3. Reflection of Single-Fold Mode

The most common mode of GPR data acquisition is referred to as "reflection mode single fold" coverage. A single transmitter and receiver are transported over the ground surface in a fixed configuration and data acquired versus position. A typical radar record is a reflection section such as shown in Figure 3.8 which display position horizontally and travel time vertically with the amplitude of the echoes coming back out of the ground being displayed as a gray scale amplitude plot. Note that examples presented here are intentionally formatted in a variety of manners to indicate the various display methods now used, (Annan and Davis, 1989)

Annan and Cosway (1992) discussion was "conducting a survey requires considerable planning. First, one must define the operating frequency range. Second, the geometry of the measurement system such as the spacing between the antennas and the antenna orientation must be decided. Next, the spatial and temporal sampling intervals must be defined. In addition, most real surveys must cover a 3 dimensional area so line separation or (line density) must be defined as well as line orientation must be established".



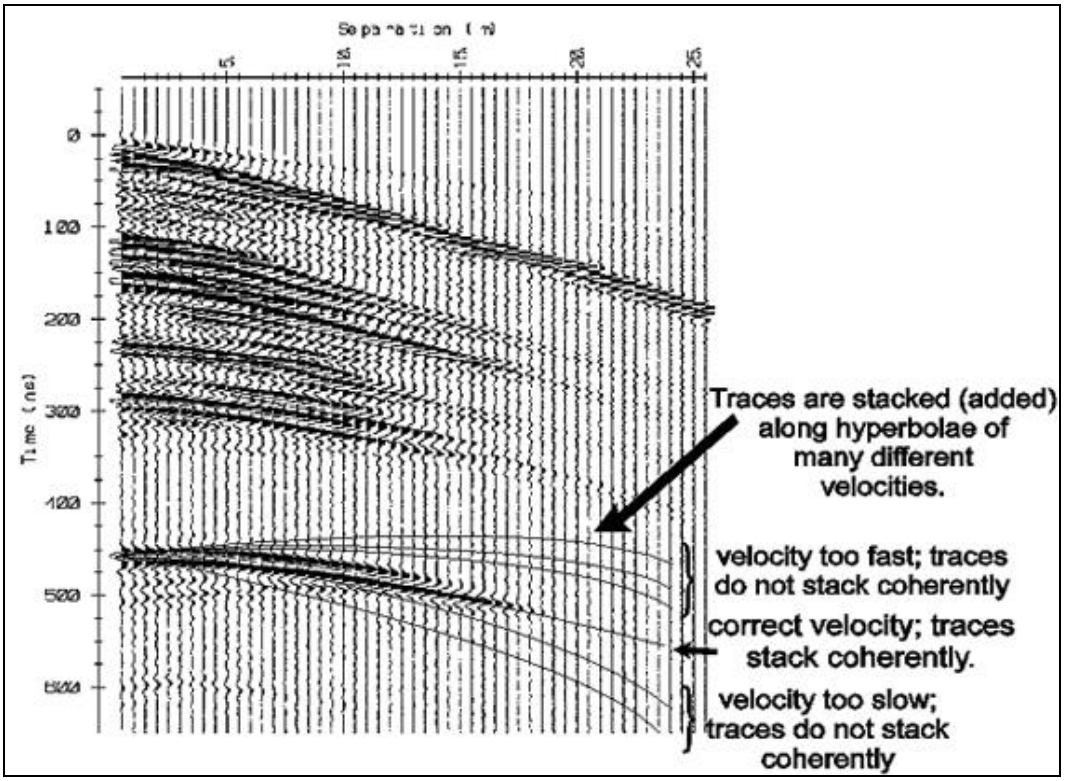


Figure 3.8. Multi-fold and CMP soundings surveys, (Annan and Davis, 1989).

3.4. Multi-Fold Surveys

In the last five years, it has become practical to acquire multi-fold data. In a multi-fold survey a multiplicity of measurements are made at different spatial separations between the transmitter and the receiver over common point (Figure 3.9). These data are processed just as in multi-fold seismic to extract velocity versus depth and also to stack the traces together to improve signal to noise Design and execution of

Velocity (m/ns)

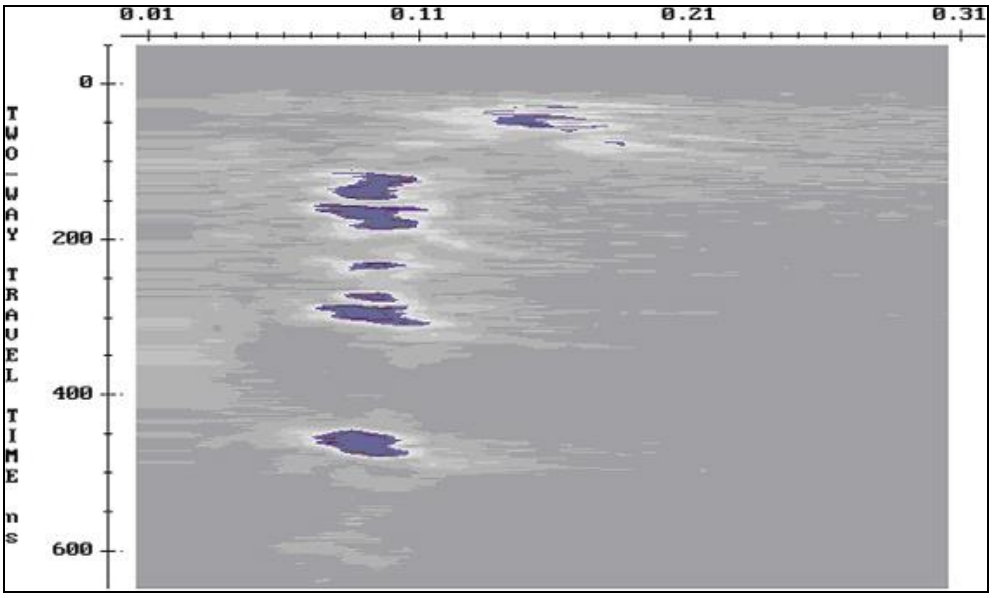


Figure 3.9. Multifold data are normally acquired or sorted in CMP (common mid-point), (Annan and Davis, 1989).

multi-fold surveys are based on the fundamentals of simpler single-fold measurements. In general, most of the parameters have to be defined in the same way. As indicated, the benefit of such a survey is in the extraction of velocity versus depth which helps to transform the original data image into a true depth cross-section (Fisher et al., 1992).

3.5. Expected Resolution And Depth of Investigation

The resolvable thickness of a geological layer depends on the radar wavelength. (Peart and Raines, 1994) stated that, "if the maximum resolution is taken as 0.25 of a radar wavelength, then for a GPR system operation at 50 MHz, in a medium maximum spatial resolution will be between 0.35 – 0.56 m. Vertical definition is mainly affected by attenuation and scattering of the signal. It should be noted that thin layers, i.e. very much less than one wavelength, can generate strong reflections if they are associated with a high reflection coefficient, although the thickness of the layer will not be resolvable. The attenuation of the radar signal in the ground is largely controlled by the conductivity of the materials through which the signal passes".

The depth to which radar energy can penetrate and the amount of definition that can be expected in the subsurface is partially controlled by the frequency of the radar energy transmitted. The frequency controls both the wavelength of the propagating wave and the amount of spreading and attenuation of the energy in the ground (Annan and Davis, 1989).

Conyers and Cameron (1998) said also that, "one of the most important variables in GPR surveys is the selection of an antenna with the correct operating frequency for the desired depth and resolution of target features. "Commercial GPR antennas range from about 10 to 1200 MHz center frequency. Proper antenna frequency selection can in most cases make the difference between success and failure in a GPR survey and must be planned for in advance. In general, the necessary depth of investigation, the lower the antenna frequency that should be used, lower frequency antennas (below 100 MHz) are large, heavy, and difficult to transport to and within the field (Figure 3.10). They must be either towed behind a vehicle on a trailer or sled or carried manually". In contrast, a 900 MHz GPR antenna or other higher frequency antennas (Figure 3.11) are quite small and can easily fit into a suitcase.



Figure 3.10. This 25-MHz antenna is capable of transmitting radar wave more than 20 meter depth. It is relatively difficult to transport to the field. It is capable of resolving only very large objects of many meters in dimension, (Conyers and Cameron, 1998).



Figure 3.11. The 900 MHz GPR antenna, (Conyers and Cameron, 1998).

Subsurface feature resolution varies with radar energy frequency. Low-frequency antennas (10- 120MHz) generate energy with wavelengths of many meters that can penetrate up to 50 m in certain condition but are capable of resolving only very large subsurface features. In contrast, the maximum depth of penetration of a 900 MHz antenna is about 1 m or less in typical soils, but its generated reflections can resolve features down to a few centimeters. A tradeoff therefore exists between depth of penetration and subsurface resolution. These factors are highly variable, depending on many site-specific factors such as overburden composition and porosity and the amount of moisture retained in the soil. In practices, it is often better to accept lower spatial resolution in favor of range where there are many thin layers or scattering targets that are not of primary interest (Conyers and Cameron, 1998). As a summary wave frequencies which GPR are used can be divided in to two main groups;

a) Low frequency GPR: They have deep penetration capacity with low resolution properties.

b) High frequency GPR: They have shallow penetration capacity with very high resolution properties.

3.6. Variables Affecting GPR Resolution And Energy Penetration

The success of GPR surveys in field works is to a great extent dependent on soil and sediment mineralogy, clay content, ground moisture, depth, surface topography and vegetation. It is not a geophysical method that can be immediately applied to all geographic or archaeological settings, although with thoughtful modifications in acquisition and data processing methodology, GPR can be adapted to a great variety of site conditions. The maximum effective depth of penetration of GPR waves is a function of two main factors:

1) The frequency of the waves that are propagated into the ground,

2) The physical characteristics of the material through which they pass.

The physical properties that affect the radar waves as they travel through a medium are electrical conductivity and the magnetic permeability. Soils, sediment or rocks that are dielectric will permit the passage of a great deal of electromagnetic energy without dissipating it. The more electrically conductive a material, the less dielectric it is, and energy will attenuate at a much shallower depth. In a highly conductive medium the electrical component of the propagating electromagnetic wave is being conducted away in the ground, and when this happen the wave as a whole dissipates. This occurs because for propagation to occur the electrical and magnetic waves must constantly "feed" on each other during transmission, (Bedal, 2000).

Highly electrically conductive media include those that contain salt water and some that have certain types of electrically conductive clay, especially if that clay is wet. Any soil or sediment that contains soluble salts or there are electrolytes in the ground water will create a medium with a high electrical conductivity. Often desert soils, even if they appear to be extremely dry and therefore should readily allow radar transmission, contain hydrous salts in their interstices, which conduct electricity. In these types of soils radar energy will become attenuated at a shallow depth. Other minerals in the ground, especially those that can dissolve in water, will create free ions, which allow for greater electrical conductivity. Sulfates, carbonate minerals, iron, salts of all sorts and any charged elemental species of mineral will create a highly conductive

ground and readily attenuate radar energy at shallow depths. Under the very unfavorable conditions of wet (with slightly saline water), a calcareous sediment or soils that contain certain clay-rich minerals, the maximum depth of GPR penetration in the ground can be much less than a meter, no matter what frequency of antenna is used (Conyers and Goodman, 1997).

Magnetic permeability also affects radar penetration in a medium. It is a measure of the ability of a medium to become magnetized when an electromagnetic field is imposed upon it. Most soils and sediments are only slightly magnetic and therefore usually have a low magnetic permeability. The higher the magnetic permeability, the more electromagnetic energy will be attenuated during its transmission, and when this occurs the magnetic portion of the EM wave is destroyed, just as with increased electrical conductivity the electrical component is lost. Media that contain magnetite minerals, iron oxide cement or iron-rich soils can all have a high magnetic permeability and therefore transmit radar energy poorly. Radar energy will not penetrate metal. A metal object will reflect all of the radar energy that strikes it and will "shadow" anything directly underneath. Buried metal objects are quite easy to see in GPR reflection profiles because they usually create multiple reflections stacked on top of one another below the metal object (Conyers and Goodman, 1997).

One of the most important variables in GPR surveys is the selection of antennas with the correct operating frequency for the depth necessary and the resolution of the features of interest. General purpose GPR systems use dipole antennas that typically have a two octave band width, meaning that the frequencies vary between one half and two times the dominant frequency. For example a 300 MHz center frequency antenna generates radar energy with wavelengths ranging from about 150 to 600 MHz. Some of the important factors that must be considered in choosing an antenna frequency (Conyers and Lucius, 1996) are:

1) Electrical properties of the ground at the site,
2) Depth of radar energy transmission necessary to study the material features of interest,
3) Size and dimensions of the archaeological features that must be resolved,
4) Site access, and
5) Presence of possible external electrical interference within the frequency spectrum of the antenna contemplated for use.

The penetration depth of GPR is determined by antenna frequency and the electrical conductivity of the earthen materials being profiled (Daniels, 2004). Daniels also (2004) stated that, "soils having high electrical conductivity rapidly attenuate radar energy, restrict penetration depths, and severely limit the effectiveness of GPR. The electrical conductivity of soils increases with increasing water, clay and soluble salt contents."

Electrical conductivity is directly related to the amount, distribution, chemical composition, and phase (liquid, solid, or gas) of the soil water (McNeill, 1980). Daniels pointed (2004) that; "at a given frequency, the attenuation of electromagnetic energy increases with increasing moisture contents. The lack of adequate data on soil moisture and the high spatial and temporal variations in the degree of soil wetness within most soil map units precluded the use of moisture content in the preparation of GPR soil suitability maps. As a consequence, properties selected to prepare these maps principally reflect variations in the clay and soluble salt contents of soils. These properties include clay content and mineralogy, electrical conductivity, sodium absorption ratio, and calcium carbonate and calcium sulfate contents."

Clays have greater surface areas and can hold more water than the silt and sand fractions at moderate and higher water tensions. Because of their high adsorptive capacity for water and exchangeable cations, clays produce high attenuation losses (Daniels, 2004). As Saarenketo (1998) wrote that; "as a consequence, the penetration depth of GPR is inversely related to clay content. While soils with more than 35 percent clay are restrictive, soils with less than 10 percent clay are generally favorable to deep penetration with GPR. Soils contain various proportions of different clay minerals (e.g., members of kaolin, mica, chlorite, vermiculite, smectite groups). The size, surface area, cation-exchange capacity (CEC), and water holding capacity of clay minerals vary greatly. Variations in electrical conductivity are attributed to differences in the CEC associated with different clay minerals". Electrical conductivity increases with increasing CEC (Saarenketo, 1998). Soils with clay fractions dominated by high cation exchange capacity clays (e.g., smectitic and vermiculitic soil mineralogy classes) are more attenuating to GPR than soils with an equivalent percentage of low cation exchange capacity clays (e.g., kaolinitic, gibbsitic, and halloysitic soil mineralogy classes). Soils classified as kaolinitic, gibbsitic, and halloysitic characteristically have

low cation-exchange capacity and low base saturation. As a general rule, for soils with comparable clay and moisture contents, greater depths of penetration can be achieved in highly weathered soils of tropical and subtropical regions that have kandic or oxic horizons than in soils of temperate regions that have argillic horizons. Compared with argillic horizons, kandic and oxic horizons have greater concentrations of low activity clays (Soil Survey Staff, 1999).

Electrical conductivity is directly related to the concentration of dissolved salts in the soil solution, as well as the type of exchangeable cations and the degree of dissociation of the salts on soil particles (Soil Survey Staff, 1993). The concentration of salts in the soil solution is dependent upon the degree of water-filled porosity, the soil texture, and the minerals found in soils. In semi-arid and arid regions, soluble salts and exchangeable sodium accumulate in the upper part of some soil profiles. These salts produce high attenuation losses that restrict penetration depths (Doolittle and Collins, 1995). Because of their high electrical conductivity, saline (saturated extract electrical conductivity around 4 mmhos cm^{-1}) and sodic (sodium absorption ratio around 13) soils are considered unsuited to GPR. Calcareous and gypsiferous soils are characterized by layers with secondary accumulations of calcium carbonate and calcium sulfate, respectively. These soils mainly occur in base-rich, alkaline environments in semi-arid and arid regions. High concentrations of calcium carbonate and/or calcium sulfate imply less intense leaching, prevalence of other soluble salts, greater quantities of inherited minerals from parent rock, and accumulations of specific mineral products of weathering (Jackson, 1959). Grant and Schultz (1994) observed a reduction in the depth of GPR signal penetration in soils that have high concentrations of calcium carbonate.

3.7. Investigating Rock Faults With GPR

Studying the locations and characteristics of active fault zones is highly important to the further the studies of future seismological activity of a region to determine the potential for earthquakes. GPR as a methodology has been found to be a useful tool in rock mass exploration as well. An application of GPR that has not seen as much widespread attention as maybe some others are faulted areas. Faults can be a difficult area to study due to the nature of a fault itself. Most of the activity in terms of

fault processes happens beneath the surface and this is where GPR can be used to make the process of fault research much easier. The type of information that can be gained with the use of GPR on a fault depends on the question that is trying to be answered. The most common way to use GPR on a fault is to use the equipment to locate the fault. In some areas finding a fault is very simple, with scarp faces or fractures in the earth's surface being quite obvious to the trained eye. In other instances locating a fault may be more difficult, requiring the use of a map or aerial photographs to interpret its presence. Even if a fault is active, deformation processes visible on the surface could be tens to hundreds of years old or older. During that time geomorphic processes can be actively eroding or burying expressions of active faulting on the landscape (Mc Claymont et al., 2008). They pointed that "a GPR transect run perpendicular across a suspected fault line gives the opportunity of narrowing the search area or may even provide strong enough evidence to directly locate the fault. Further exploration of a faulted area could produce evidence for new unknown subsidiary faults caused by or related to the original fault in question".

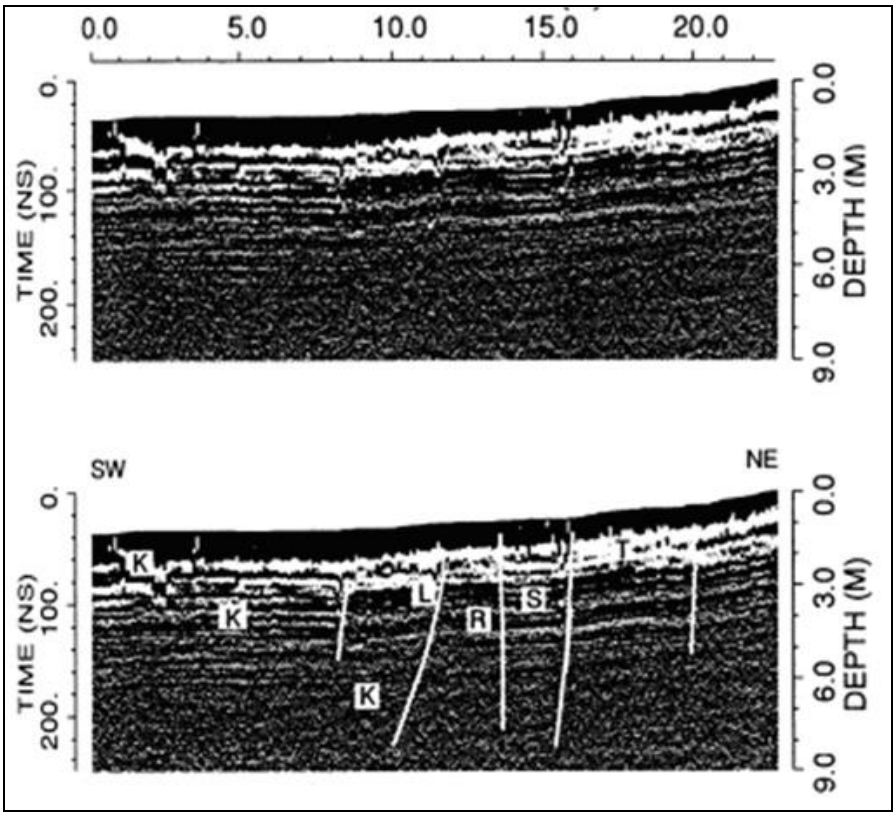


Figure 3.12. When the field measurement performed by GPR, a raw reflection profile (top graphics) can be handled. Evaluations of this raw graphic give results like shown at bottom. The letters K,L,R,S,T show offsets in stratigraphy signaling possible faulting (Cai et al., 1996).

Once a fault is located, GPR can provide additional information as well. When a fault is being imaged by a GPR system it is usually not the direct reflections from the fault plane itself that show its position. Rather the position of fault strands can be located from offsets in stratigraphy, (Figure 3.12), which can be difficult to locate (Cai et al,. 1996).

A sharp, relatively vertical change in the continuity of stratigraphic layering can indicate the lateral displacement of a strike-slip fault. Instead of the same materials continuing uninterrupted, the fault will cause a displacement that leads to the layering becoming discontinuous from one point to the next and in the right set of conditions, with enough displacement and vertical change in layering, can be imaged with GPR (Christie et al., 2008) stated that, "many times heavily faulted areas will show evidence of multiple fractures across the same GPR transect. Scarp facies can be buried over time by sediments filling it in so that the ground looks relatively flat. GPR evidence of these facies are indicators of normal faults where one side has slipped downward relative to the other crating the scarp facie. With proper calculation of the velocity of the material being shot with GPR it is possible to calculate the vertical displacement that has affected a faulted area."

3.8. Applications of GPR Data in Geological Information System (GIS)

GPR may be viewed as a kind of source of spatial data; so aided by the capability of GIS in management and analysis of spatial data, GPR data can be used more effectively and efficiently. In what follows, some feasible ways of utilize GPR data in GIS.

The format of GPR data is different from vector-graphs and images. It save the physical characteristics of electromagnetic waves (amplitude, frequency etc.), and ordinary GIS software can't process it. So the management of GPR data can be managed in geo-database in two ways. One way is to save them like satellite imageries, but the amount of data to save is very large. Another way is to extract some information from the GPR data. In this way, the GPR data need preprocessing and extracting spatial information and statistical or geo-statistical information derived from these data in GPR software. The spatial information consists of the coordinate of GPR data and the spatial

position of the interface between main soil layers. The statistical or geo-statistical information describes the whole feature of the data about velocity, absolution, amplitude, and so on. Using the coordinate of the GPR data can be denoted on a topographical map, the spatial position of the interface between main soil layers can be saved as elevations on related coordinate, and each interface should be saved independently. The statistical or geo-statistical information should be saved as attribute information linked with the coordinate of the GPR data. Figure 3.13 shows the whole workflow (Freeland, 1998; Paterson, 2000; Antunes et.al, 2002).

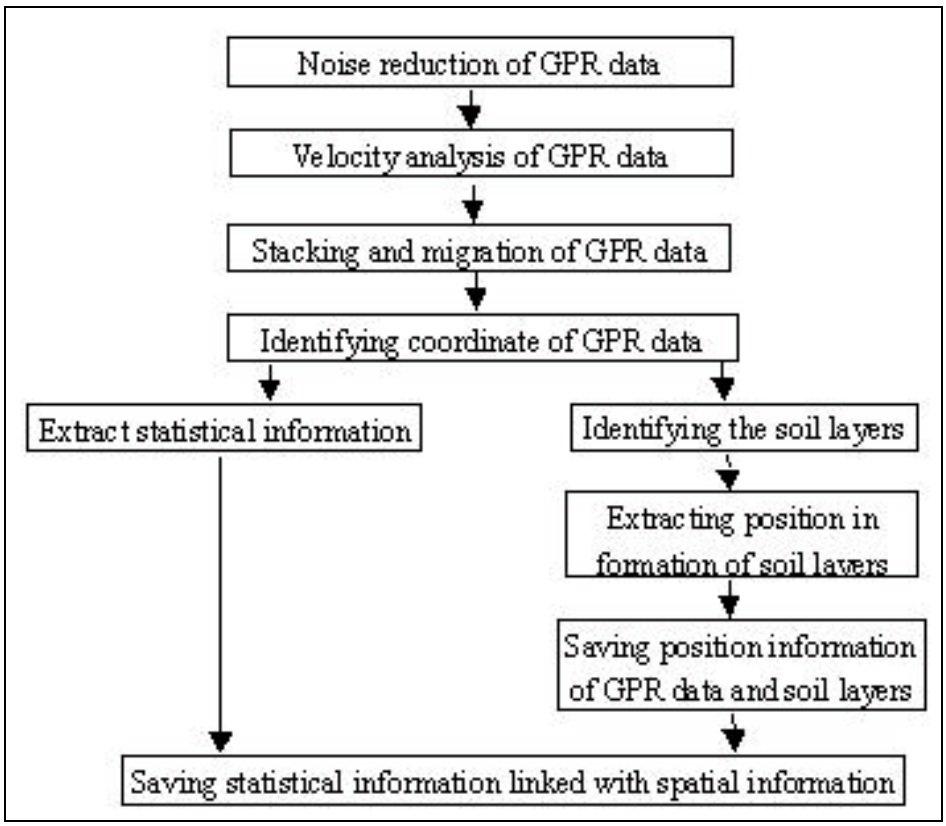


Figure 3.13. The whole workflow of managing GPR data in GIS. (Paterson, D.G., 2000).

3.9. Data Collection Methods For GPR by Using GIS

In order to collection GPR reflections, paired antennas, located within a "box," are moving along the ground in transections (Figure 3.13). One antenna generates the propagating radar waves and a second antenna records the reflection traces generate

from below. When many hundreds or even thousands of reflection traces are stacked together, as they are collection along an antenna transect, a reflection profile is produce. Reflection profiles are collected by moving antennas in transects. Within this fiberglass housing showing in Figure 3.13, there is a pair of transmitting and receiving antennas, with a 400 MHz center frequency. Energy is transferred to and from the control system by means of a cable. Most GPR systems can also be programmed to collect data with a survey wheel, or some similar device that can measure where the antennas are in distance along each transect, which can expedite data processing as all recorded reflection traces can be assigned a specific location within a grid. GPR surveys are most often done by establishing a grid over the desired area. Rectangular or rectilinear grids are preferable to other grid designs for a number of important reasons. Digital reflection



Figure 3.14. Collecting GPR data at the *CATS test site*. Antennas can be attached to survey wheels, which can be programmed to collect a given number of reflection traces every programmed distance along a transect, (Conyers and Goodman, 1997).

data from a rectangular grid can easily be exported to computer display and imaging processing programs that are pre-set for this gridding method. In this way the data can be quickly processed and interpreted without time consuming transect surveying and drafting. In addition, with a rectangular grid, important reflections in each profile can be immediately correlated to others and reflections can be "tied" to parallel or perpendicular transects throughout the grid. In all cases a sketch of the grid, with notes

on the transect length, orientation and beginning and end locations should be noted. The antenna is pulled along transects within the grid. Transects are typically spaced about 25 to 100 cm apart, depending largely on the antenna frequency being used and the amount of coverage desired. Time and financial restraints are also common factors affecting collection procedures, since smaller transect spacing will require more surveying time (Conyers and Goodman, 1997).

The most tedious, but also important, part of a survey is performed by the person pulling the antennas. This job is the most difficult during continuous data acquisition because the person pulling the sled must not only walk backward but must also make sure that the antennas are moving parallel to the designated transect line. Some people use a cart or other devices to move equipment across the ground. If data are being acquired in continuous acquisition mode, where radar pulses are being generated at a programmed number per second, the antenna puller must also pay attention to when the antennas move past designated surface markers. At each pre-surveyed location a marker button must be pushed to place marks in the reflection records. When a survey wheel is used, or antennas are moved in steps, manual marks of this sort are not necessary and antenna pulling is an easier task. Another important aspect of moving the antennas along the ground is making sure that the antennas are in the same orientation and the same distance above the ground, or directly touching it at all times. Changes in antenna orientation with respect to the ground will potentially cause variations in the recorded reflections that can be confused with “real” changes in the ground. This phenomenon is called antenna coupling loss and very important in GPR field measurements, (Conyers and Goodman, 1997).

GPR application in Turkey is a new research area and site engineering applicability of GPR was performed also by Kadioglu & Kadioglu (2006). In this research researchers studied about marble reserve thickness together with its main discontinuities. Kadioglu et.al. (2005) wrote about similar GPR applications for andesite rock mass before. Andesite rock mass in this research was measured for their rock mass extensions. An other study was the one reported by Seren & Acikgoz (2012). They also wrote about GPR field measurements performed in massive limestone reserve near Ankara-Turkey.

4. MATERIALS & METHODS (FIELD MEASUREMENTS)

Most GPR antennas are prepared to be handled easily. Common method of operation is to drag the antennas slowly across the ground surface in a straight line traverse while GPR equipments are working. During this measurement action, transmitting and receiving radar waves are continued to obtain GPR-profiles, underground wave distribution cross-section graphics. This profiles represents the accumulation of reflected waves that have been received by GPR receiver antena. The series of single waveforms are combined together to give the effect of mapping rock mass layers, cavities, weakness zones or objects in the ground. The receiving antenna and circuitry records for finite period of time, so that the derived time record or waveform has an early time period corresponding to reflections from shallow targets and later time corresponding to deeper targets with amplitude representing the strength of the reflection. For this reason the GPR sections can be thought of as a depth section or profile view of the subsurface condition below the traverse line.

In general, operation of a commercial GPR system requires two operators, one to drag the antennas along the ground, the other to control the instrument operations from a console which is often simply a laptop personal computer and another electronic module connected to the antennas by cable or optic fibre. Many commercial operators may use vehicles such as small cart or 4-wheeled motorbikes to assist with both instrument carriage and antenna mobility. Sometimes operators should carry the antennas due to very rough or sloped field conditions. Therefore GPR instrument configuration and survey design depend on the targeted survey objectives and physical factors such as the terrain and site layout especially the roughness of the ground surface. Presence of obstructions such as water courses, trees, rocks or man-made structures are also influencing the plan of the measurement paths.

4.1. Preparing The Test Site Before GPR Measurement

According to engineering decision which includes the GPR reading, the selected test site should be informed. The knowledge about the test site is sometimes are very obvious if the test site is in urban areas. Sometimes it has photographs in internet.

However if the test site is given as a field, that can be anywhere, including; rough hill sides, sand deserts, rocky dry areas, wet plains, forest areas or mixture of them. Therefore information about the test site should be collected precisely to plan the GPR measuring paths (profile lines). Since the GPR antennas should be dragged along a predetermined path or positioned simultaneously on this path, its direction and length should be decided according to test site slopes and any other obstructs. During the GPR testing the coordinates along the pre-determined paths should also be recorded. This is sometimes performed by using ground positioning system instruments such as Garmin, Magellan etc. They can handle coordinate in the form of ED50 format and 6 degree readings with reasonable measurement error. Otherwise GPR operators can use more reasonable devices such as; distance control along a travers line (measuring path) can be provided by a range of means that include odometers attached to wheels or cotton string on a spool tied of at the starting point.

To a great extent, the appropriate field procedures are determined by actual system being used and while the commercial systems have certain similarities, there are some that are better suited to particular applications than others. For example, to gain data quality improvements using the low frequency antenna it is recommended that the antenna should be manhandled to each measurement point and kept stationary for the duration of the recording time in order to obtain the best possible result. They can be used also by continuous dragging across the ground either by man or vehicle. However in this cases, the data quality will be reduced.

The survey objective has a significant impact on instrument configuration as well as field layout by determining in the first instance the appropriate antenna frequency. Other factor such as the target size determine measurement path (line) spacing and number of samples required along the traverse line in order to satisfy basic spatial sampling criteria, according to such factors as target depth, antenna frequency, reflector geometry and instrument measurement parameters (pulse characteristics and high frequency signal sampling). (Annan and Cosway, 1991).

4.2. GPR Equipment Used During The Field Tests

The Geophysical Survey Systems, Inc.'s SIR-3000 Ground Penetrating Radar (GPR) was used during this thesis research in the field. This high performance, single channel radar system provides unrivaled data quality. The SIR-3000 is small, portable and designed for single-user operation. It is compatible with all GSSI antennas, making it an affordable option for all GPR applications.

The GSSI SIR-3000 is accepted as industry's number one choice for data accuracy and versatility. Its small, lightweight control unit is designed for single-user operation (Figure 4.1). The SIR-3000 provides the essential features and flexibility that experienced GPR users require, as well as simplified, application specific user interfaces for novice GPR users. The SIR-3000 incorporates advanced signal processing and display capability for in the field 3D imaging also. Unlike other data acquisition products on the market, the SIR-3000 is interchangeable with all GSSI antennas, making it an affordable and flexible option for multi-application users (GSSI, 2011).

The main features of the equipment can be listed below. GPR equipment used in field should be versatile and robust. Due to field conditions, rain, sun, cold and hot weather conditions commonly main situation in field works. The machines should also transportable easily.

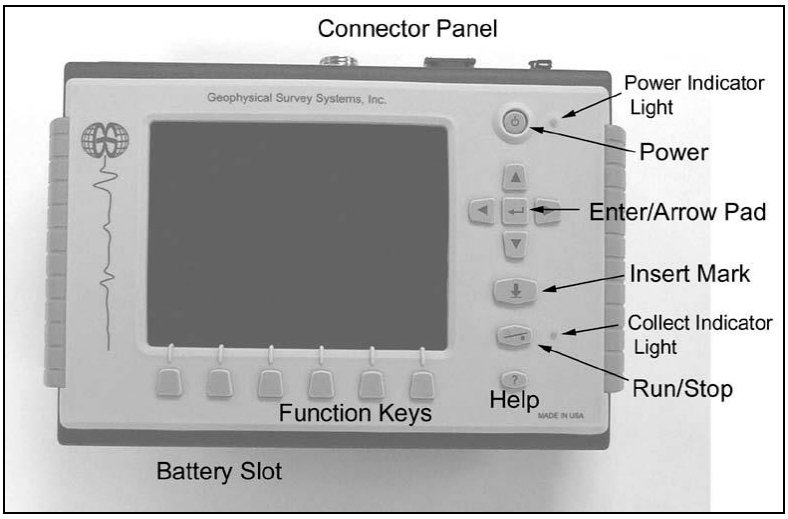


Figure 4.1. GSSI's SIR-3000 ground penetration radar control unit, (GSSI, 2011).

Heavy equipments are difficult to carry in field if the area is very rough so GPR operator should carry the equipment by hand. Therefore the following GSSI's SIR-3000 features are controlled by thinking these field application conditions, its advantages can be seen more clearly. The GPR equipment which was used in the selected travertine mine has the following features;

It has a modular design therefore;

- It is compatible with most GSSI antennas,
- It is lightweight and portable,
- It has removable, rechargeable batteries.

It has an integrated system, therefore;

- It has Windows based user interface,
- It has GPS integration,
- It has high resolution color screen that is visible over a wide range of light conditions,
- It is rugged and weather resistant.

It deliver results through;

- Removable compact flash card memory,
- Large internal data storage.

These features open the usage of GSSI's SIR-3000 in different application sites. Common application sites can be listed as; concrete inspection, utility location, geological investigation, forensics, bridge deck inspection, mining operations and many other custom applications.

The GSSI SIR-3000 is capable of attaching ground positioning system (GPS) coordinates to individual data profiles. This will allow GPR operator to place the beginning and the end of your survey lines into a larger, real-world coordinate system. This feature of the SIR-3000 provides also that;

i) Survey in straight lines,

ii) Have a GPS coordinates for measurement paths.

Attaching a GPS with its own data logger will allow the GPR operator collect GPS data points with a much finer resolution. RADAN 6 or any new version of this software will then be able to wrap data files and show coordinates of the GPR test lines' positions in standart x,y,z coordinate systems (in ED50 format for example) (GSSI, 2011).

5. RESEARCH RESULTS (DATA ANALYZING)

Ground penetrating radar is practical equipment for shallow depth exploration studies. One of the great advantage of the GPR method is the fact that the raw data is acquired in a manner that allows it to be easily viewed in real time using a computer screen. Most of the field GPR equipments have its own screens which present the output raw graphics while the testing is performed. Often very little processing is required for an initial interpretation of the data, with most of the effort directed towards data visualization. On the other hand, depending on the application and target of interest, it may be necessary to perform sophisticated data processing and many practitioners find that the techniques common to seismic reflection such as deconvolution and migration can be successfully applied.

As stated earlier, the basic form of the data is a profile or section view of subsurface features beneath a straight-line travers with the vertical dimension being two way travel time (usually expressed in nanoseconds) just like seismic sections. However, because most people are interested in converting this to a depth section, it is necessary to have some knowledge of the propagation velocity through the soil and rock in order to rescale the data appropriately. Depending on the required accuracy, this can be as simple as applying a nominal velocity based on textbook data and some knowledge of the likely soil/rock type and moisture content. Alternatively it can involve simple data processing using seismic processing techniques such as common mid-point and velocity analysis of a normal move out section. Calibration through direct measurement of the depth to certain recognizable features using either drilling or trenching is also commonly applied after the testing procedures.

Field study was realized during this thesis practical works by handling GSSI SIR-3000 GPR equipment. The field measurements were obtained at a travertine mine near Selcuk University main campus in Konya. This mine has single bench with average 10 meter height. The length of bench is about 120 meter (Figure 5.1). GPR measurements were planed to visualize the rock mass nearer this bench. Therefore the fractures seen on the bench slope were mapped carefully and their coordinate were recorded with respect to the starting point of the targeted bench.

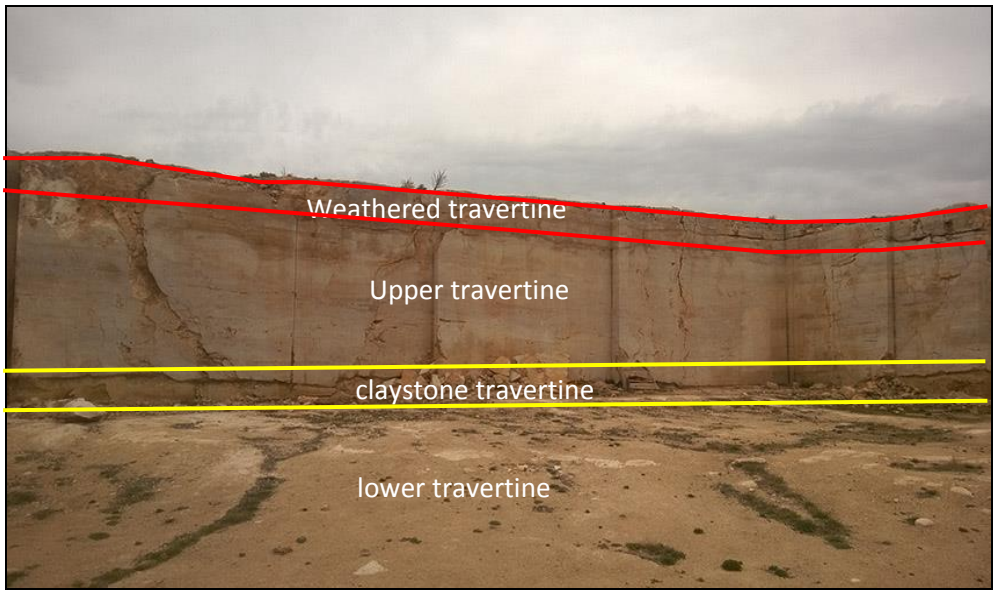


Figure 5.1. Analysed travertine mine bench view. Actually this single benched travertine mine has face cut by diamond capsulated still-rope. The face demonstrates fracture intersections and their 3D bedding planes. Red lines separate weathered and main travertine zones. Yellow lines on to other hand show claystone bedding, thickness 0.75-1.5 meters, underlying the top travertine bedding.

Then operation area was divided by five parallel straight lines which averagely 5 meters apart. Each measuring line was 105 meters long, that means by applying GPR measuring performance, total A= 25 x 105 = 2625 m^2 were studied tor underground fracture recognition. The mine opened more then 5 years ago and due to operational circumstances, its operations were stopped. The mine area has two travertine beddings separated with claystone intersection. Claystone bedding is yellow in color and consists of sandy clay as well. Travertine beddings have also clayey zones in there. Travertine beds have flowing texture in this mine as well. These features which sometimes form weakness parts in the bench were detected through GPR readings performed during this study. GPR measurement lines were elongated parallel to the face as shown in Figure 5.2. GPR measurements were arranged in a way that, each line was passed through twice for radar reading with to visualize different depth. One of them pre-set to show 7 meters depth to present discontinuities more clearly. Same rack section measured with same GPR equipment to visualize 21 meters depth to explore the deeper rock formations. This reading was actually arranged after several pre-reading procedure. After realizing the depth of lower travertine bedding is around 18-21 meters from surface, then the GPR readings set to see accordingly, 21 meters depth. The measuring lines's GPR readings are presented below after getting the related radar graphics from collecting data.

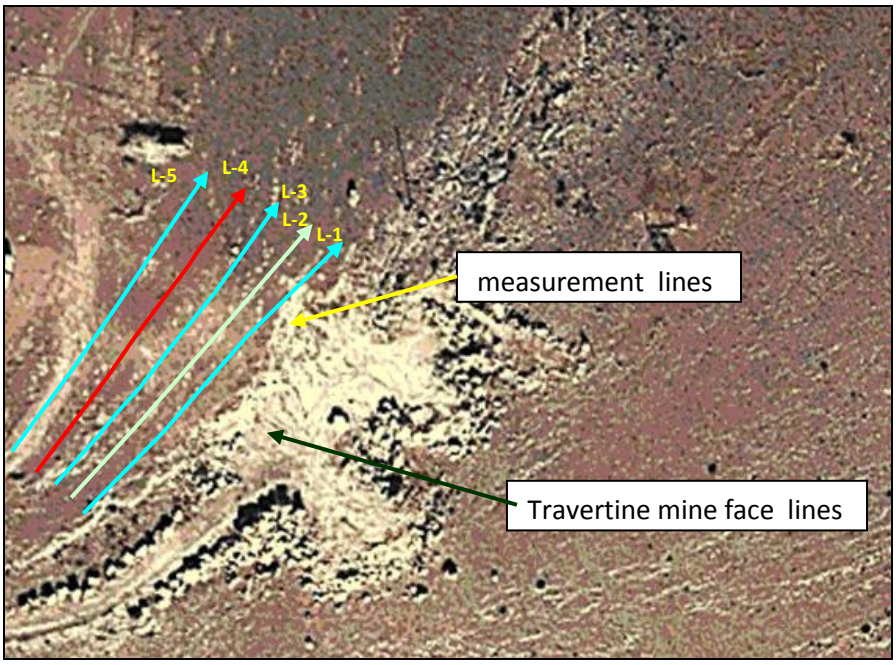


Figure 5.2. Travertine mine face and measuring lines followed during field measurement.

a) Line-1 (L-1, NE-SW): This measuring line was elongated from NE to SW direction. It is 5 meters away from the travertine bench face. Since the fractures were recorded along the face, this line reading was important if the existing discontinuities are continued under this line. GPR readings were arranged to visualize 22 meters depth. Measurement was takes approximately 10 minutes to finish. The data collected was saved to GPR equipment internal memory to ready to transfer to the computers. After realizing this data transfer, the resultant field data analysed through Radan-7 software to obtain the following graphics. These are the ones which internal weakness zones were more easily detected. During the measurement, required field notes and explanations were also recorded separately to help the analyses of the resultant radar graphics. The following graphics are the ones obtained from Line-1 SW-NE reading;

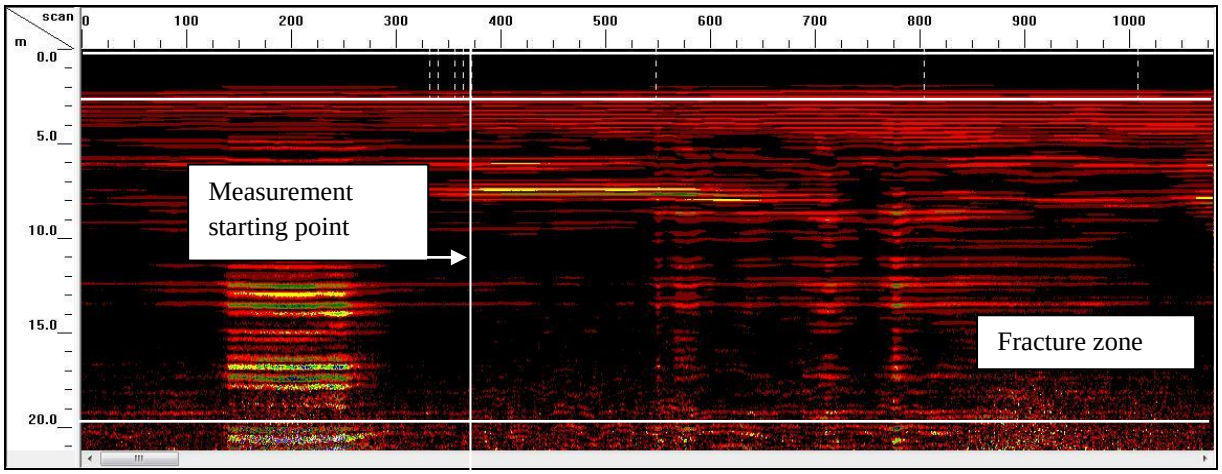


Figure 5.3a. After starting point of GPR gave ground view up to 21 meters. Black coloured part of the graphics are travertine rock mass. It can be seen that up to 2.5 meters the weathered travertine zone is obvious. Fractures in first 1-3 meters along the measuring line were also shown out. (Line-1, distance between 0-4 m).

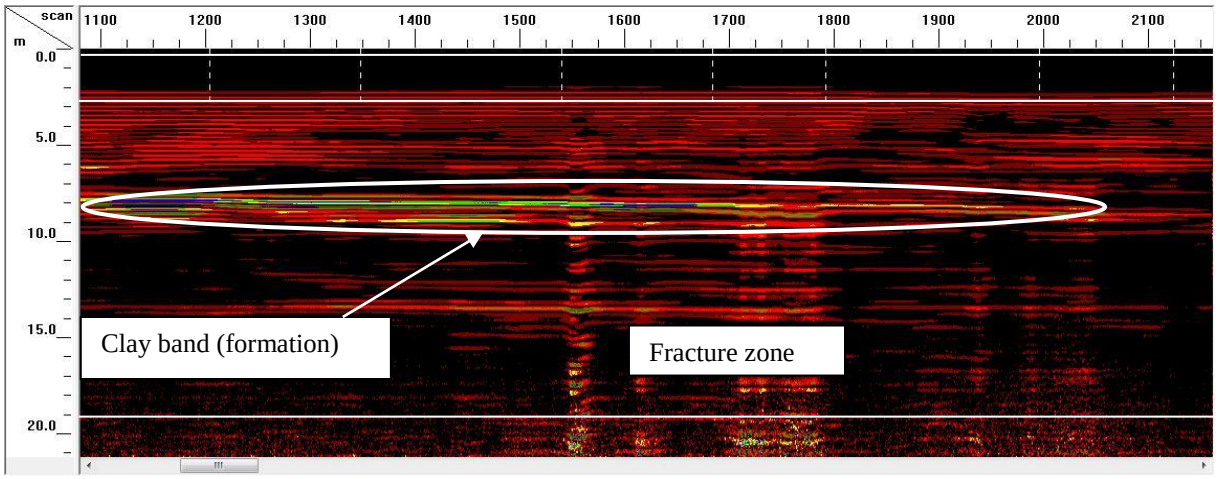


Figure 5.3b. Travertine rock mass was determined disturbed by a horizontal zone in yellow and blueish color. This zone was determined at 7.0-8.0 meters depth and named as claystone as it was observed travertine mine's bench face (Figure 5.1). Additional fractures were also shown in the graphics together with baserock mass, limestone) starting from 20-21 meters depth. From this graphics it is seen that some fractures are effective deep enough to reach more than 21 meters. (Line-1, distance between 4-10 m).

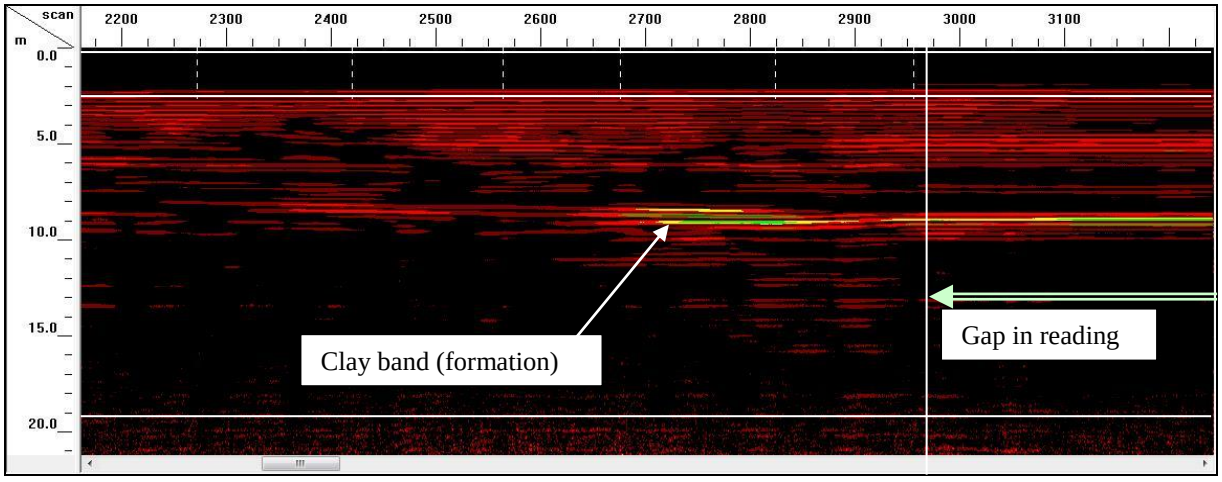


Figure 5.3c. Travertine rock mass was determined here with obvious clayband layers, together with baserock level, (Line-1, distance between 10-16 m).

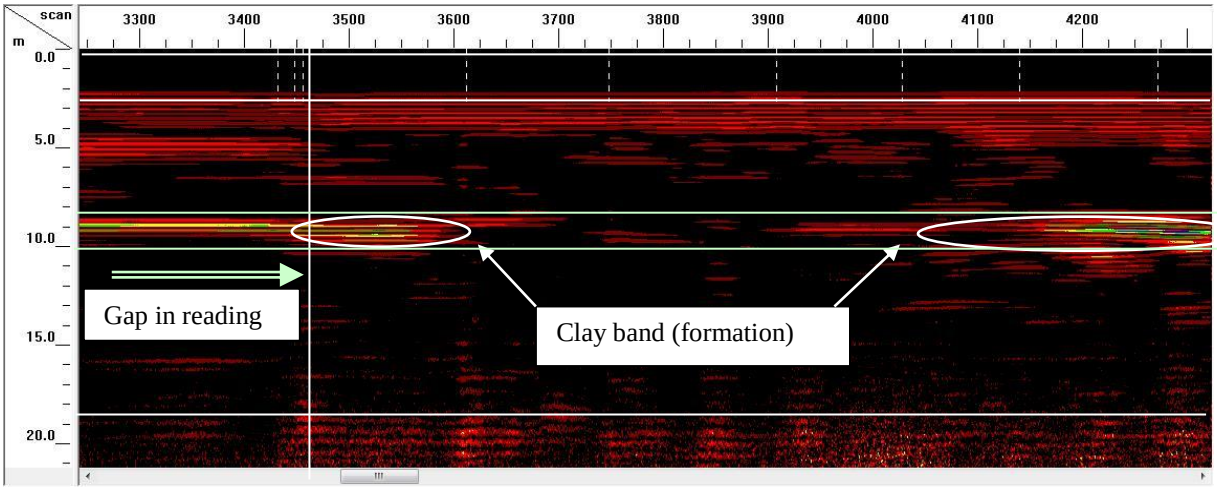


Figure 5.3d. Travertine rock mass between 2.0-8.0 meters were shown in the radar screen as here, that means it has heterogeneous character and flow marks in it. In this figure clayband were determined more clearly, (Line-1, distance between 16-22 m).

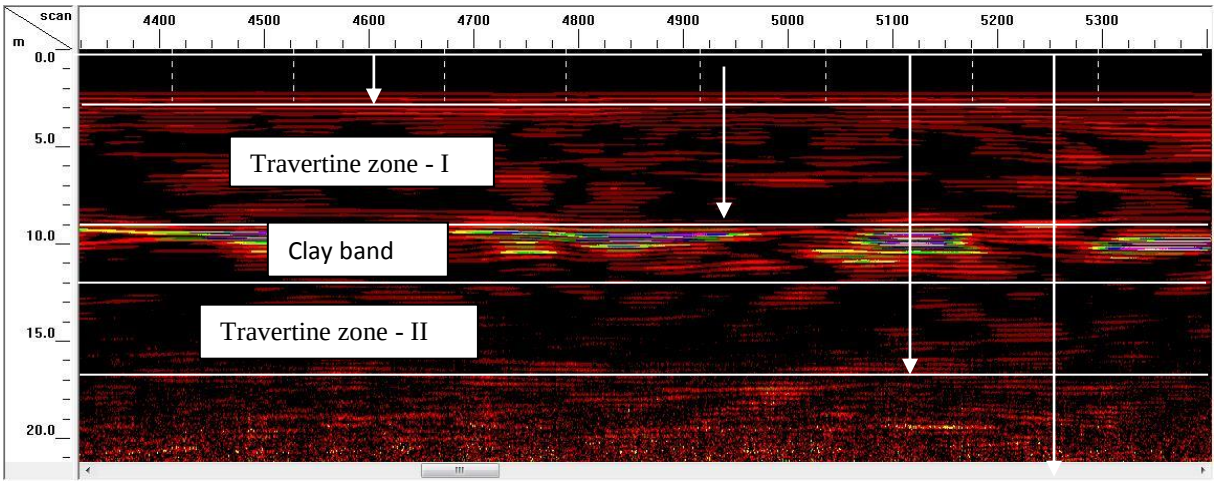


Figure 5.3e. In this radar view travertine rock mass can be named and the claystone layer (1.5-2.0 meters thick) in between them were shown clealy, (Line-1, distance between 23-31 m).

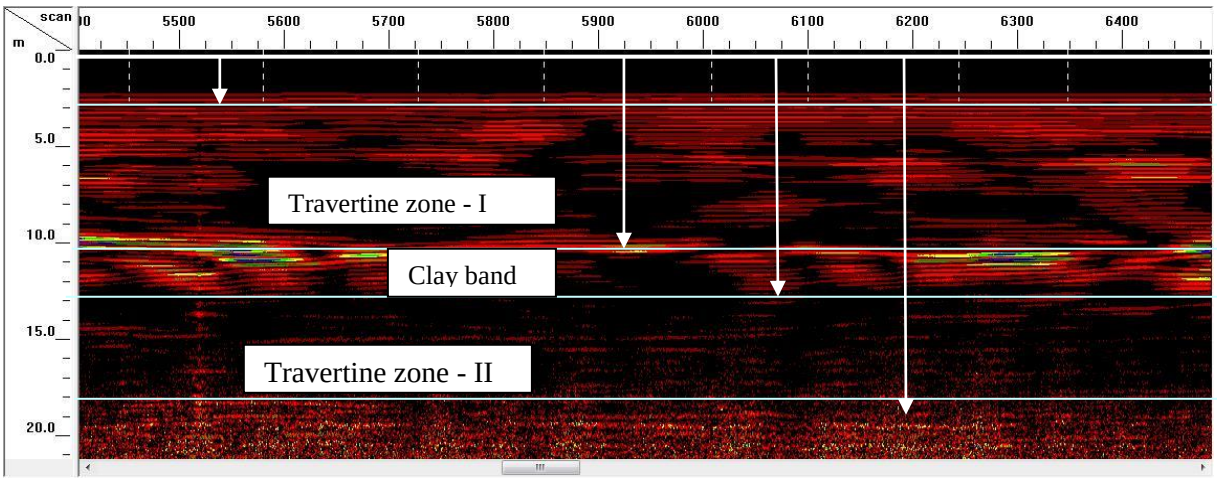


Figure 5.3f. Travertine rock mass radar screen, (Line-1, distance between 31-39 m).

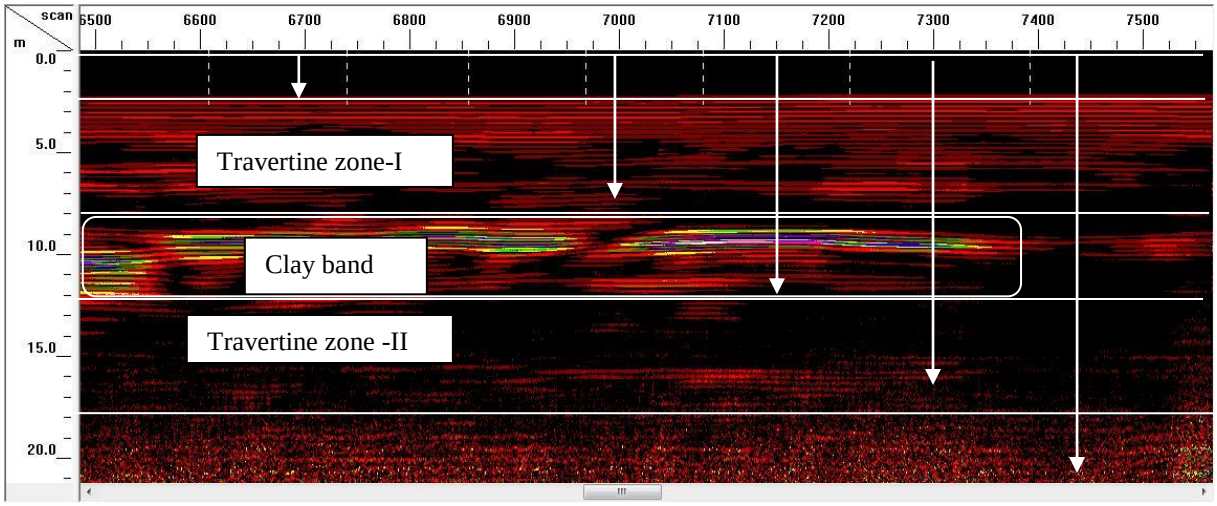


Figure 5.3g. Travertine rock mass bedding differences together with claystone layers, (Line-1, distance between 39-47 m).

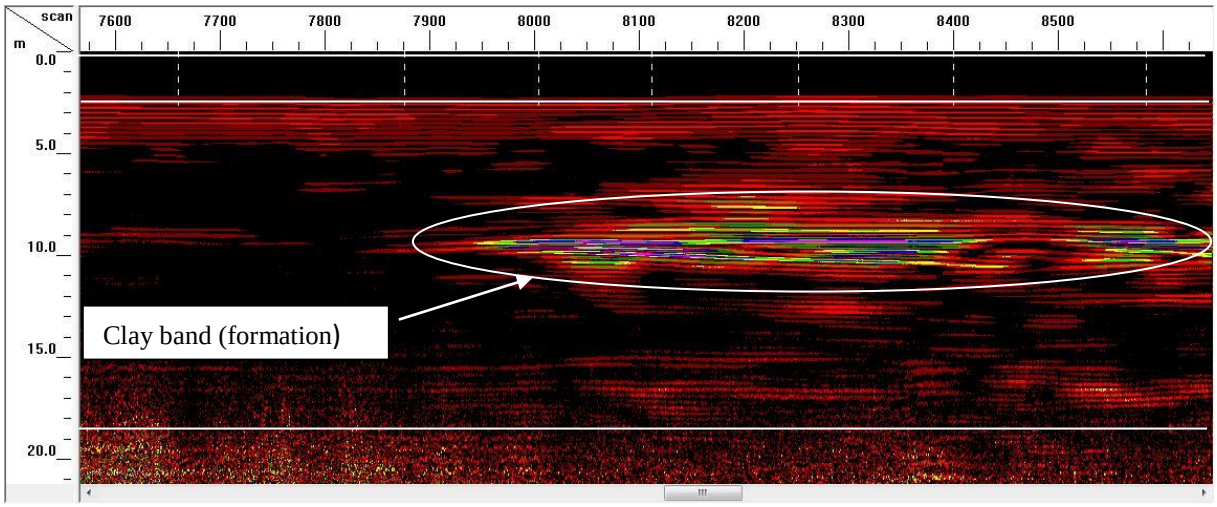


Figure 5.3h. The disturbed zone was determined by radar (GPR) reading located 49–55 meters with respect to Line-1 starting point. The zone effective at 50-52 meters and the disturbed (weakness) thickness at this area was seemed as 5-6 meters. (Line-1, distance between 47-53 m).

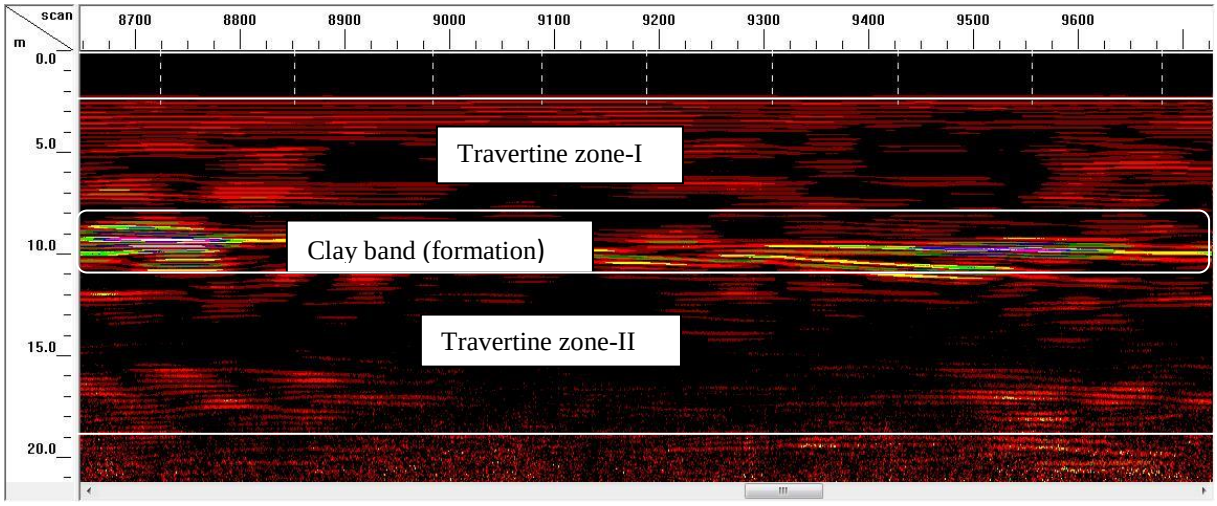


Figure 5.3i. Travertine rock mass bedding differences together with claystone layers, (Line-1, distance between 53-62 m).

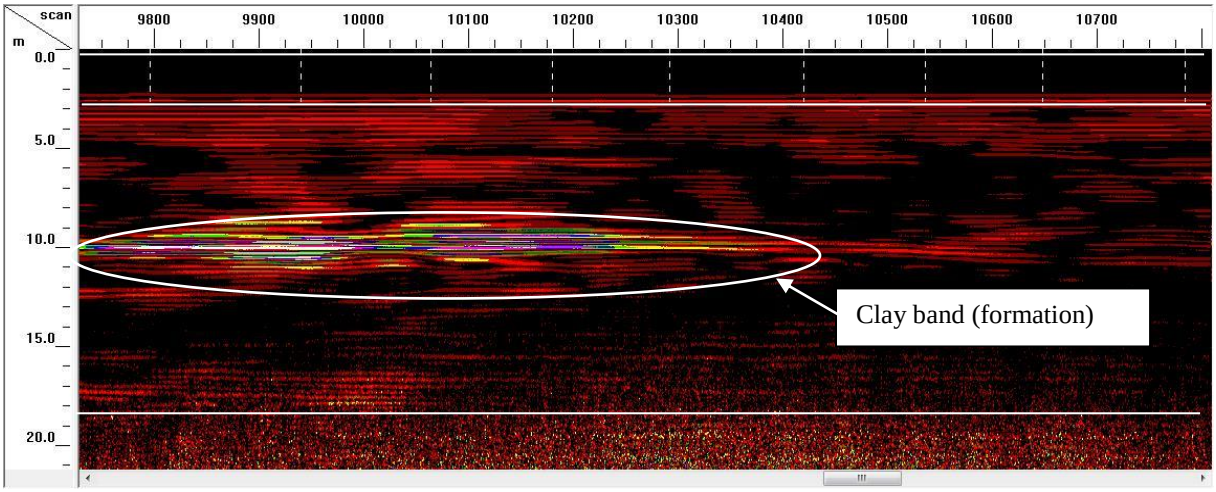


Figure 5.3j. Travertine rock mass bedding differences together with claystone layers, The disturbed zone thickness at 63-66 meters was measured 4 meters, (Line-1, distance between 63-71 m).

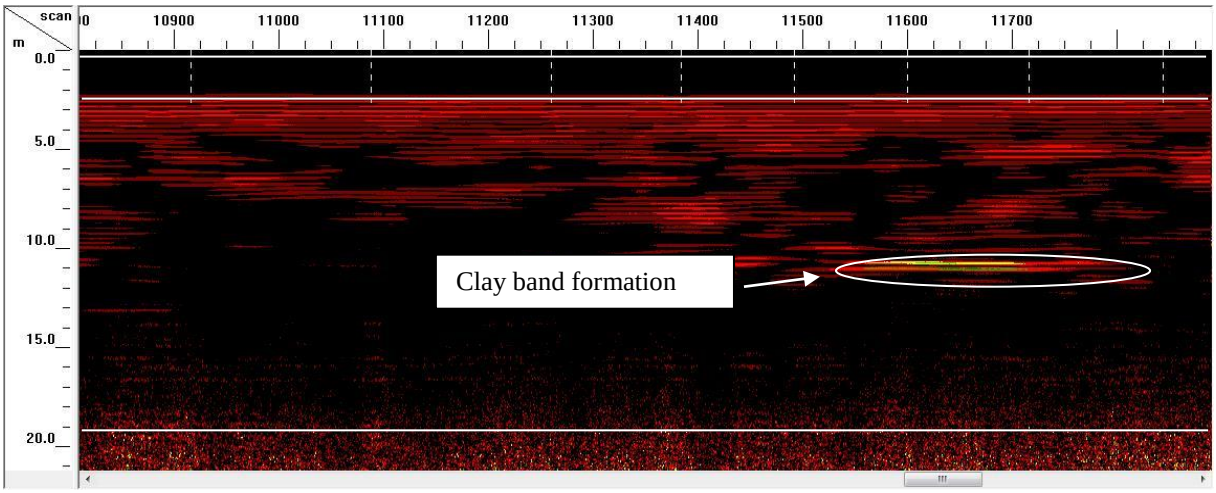


Figure 5.3k. Travertine rock mass bedding differences, the rock mass was determined more compact at this area, (Line-1, distance between 71-79 m).

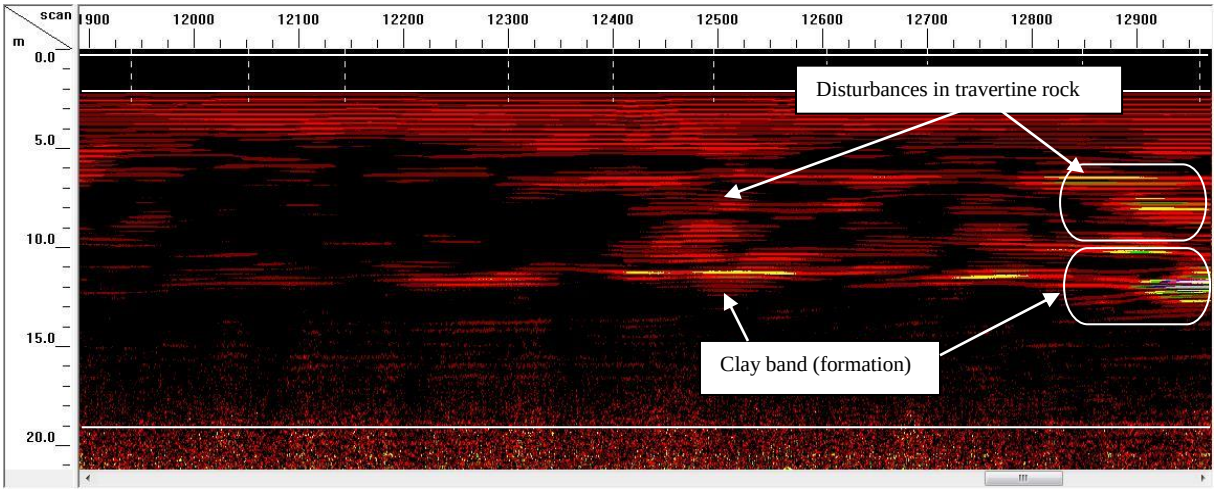


Figure 5.3l. Travertine rock mass bedding differences together with claystone layers, weakness zone, fractures, (Line-1, distance between 80-89 m).

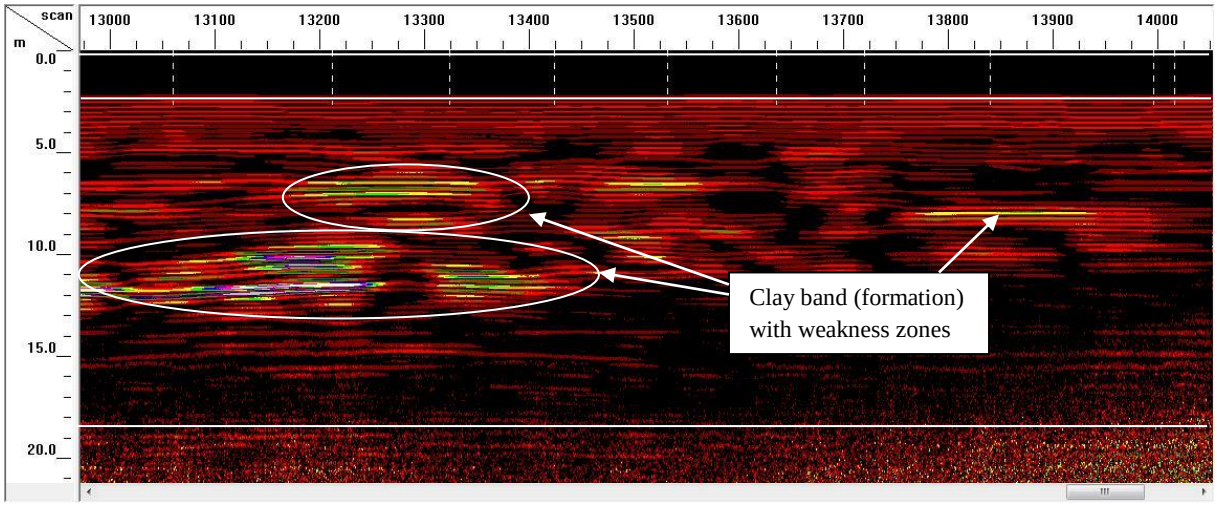


Figure 5.3m. Travertine rock mass bedding differences together with weakness zone disturbances, (Line-1, distance between 90-98 m).

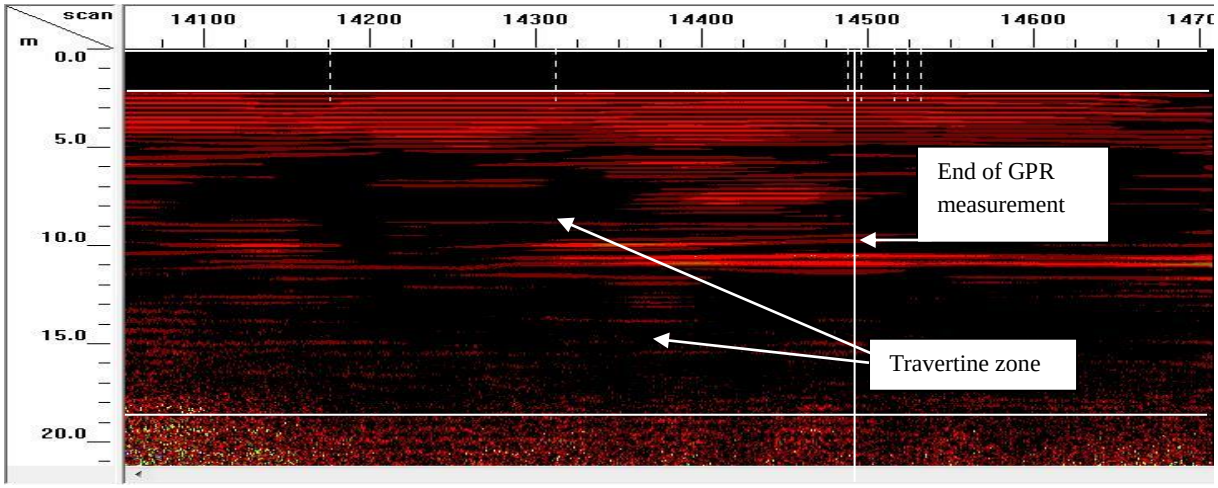


Figure 5.3n. Travertine rock mass bedding differences together with claystone layers, (Line-1, distance between 98-101 m).

b) Line-2 (L-2, SW-NE): This measuring line was elongated like Line-1 and the GPR readings were taken through Line-2 moving SW to NE direction. It is 5 meters away (NW direction) from Line-1. GPR information recognition depth was arranged for 21-22 meters and the measurement was performed accordingly. The data collection time took about 10 minutes and they were saved into the instrument's memory. After transferring the data into computer, Radan-7 software was facilitated to analyze the field data. The graphics given below cover the weakness zones and fracture planes which were determined from Line-1 readings. The other features of rock mass were checked through the GPR graphics (Figure 5.6) obtained from this measurements to visualize the travertine rock mass features under the surface.

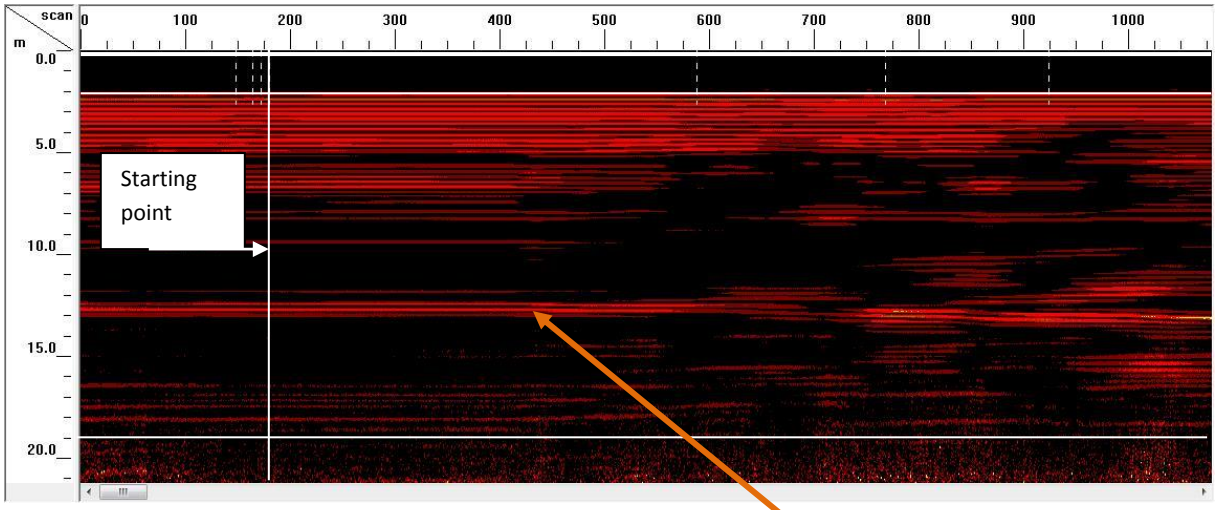


Figure 5.4a. Travertine rock mass bedding differences together with claystone layers, (Line-2, distance between 0-4 m).

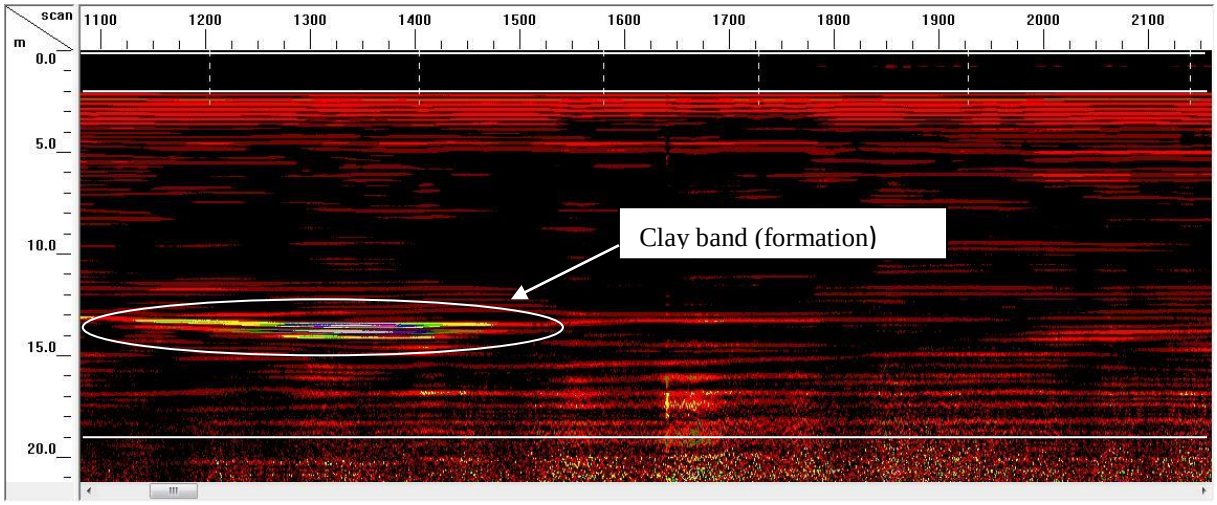


Figure 5.4b. Travertine rock mass bedding differences together with claystone layers, (Line-2, distance between 4-9 m).

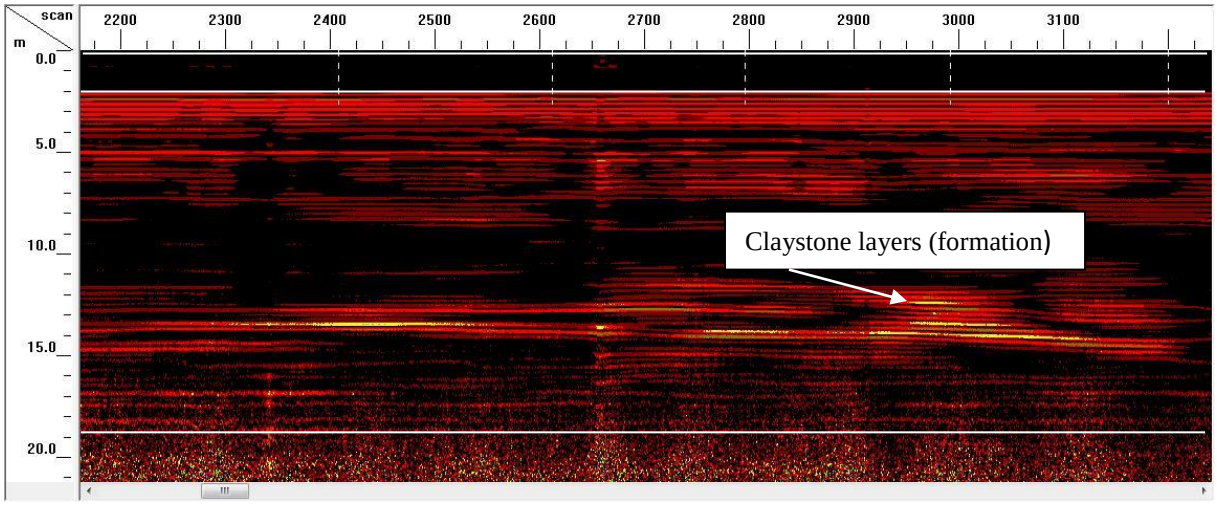


Figure 5.4c. Travertine rock mass bedding differences together with claystone layers, (Line-2, distance between 9-14 m).

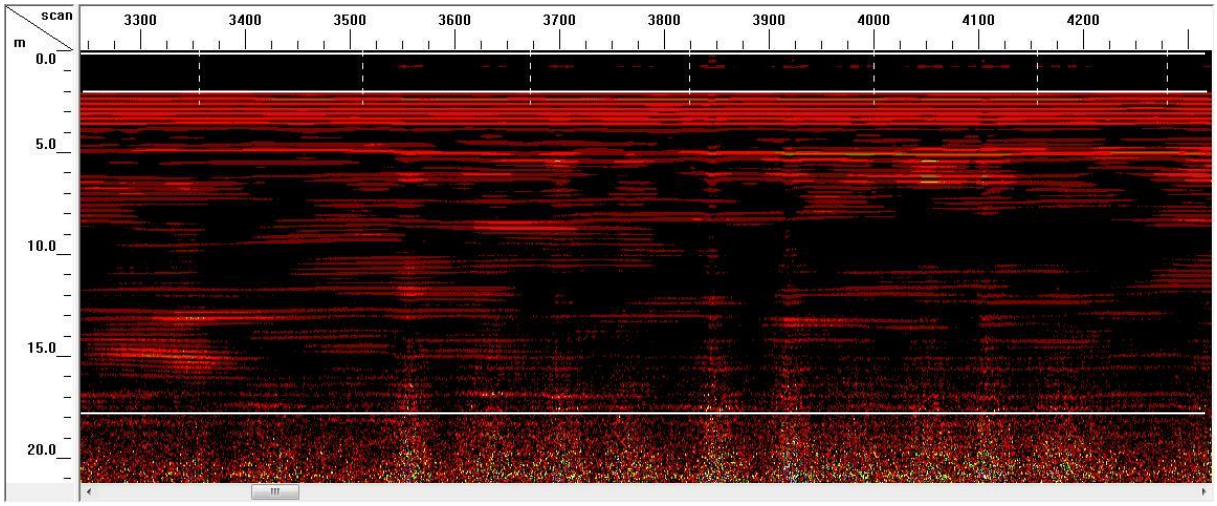


Figure 5.4d. Travertine rock mass bedding differences together with claystone layers, It is determined that relatively good quality travertine was located at depth intervals 2-14 meters, However the flowing texture in the travertine can be seen in these readings as well (Line-2, distance between 14-21 m).

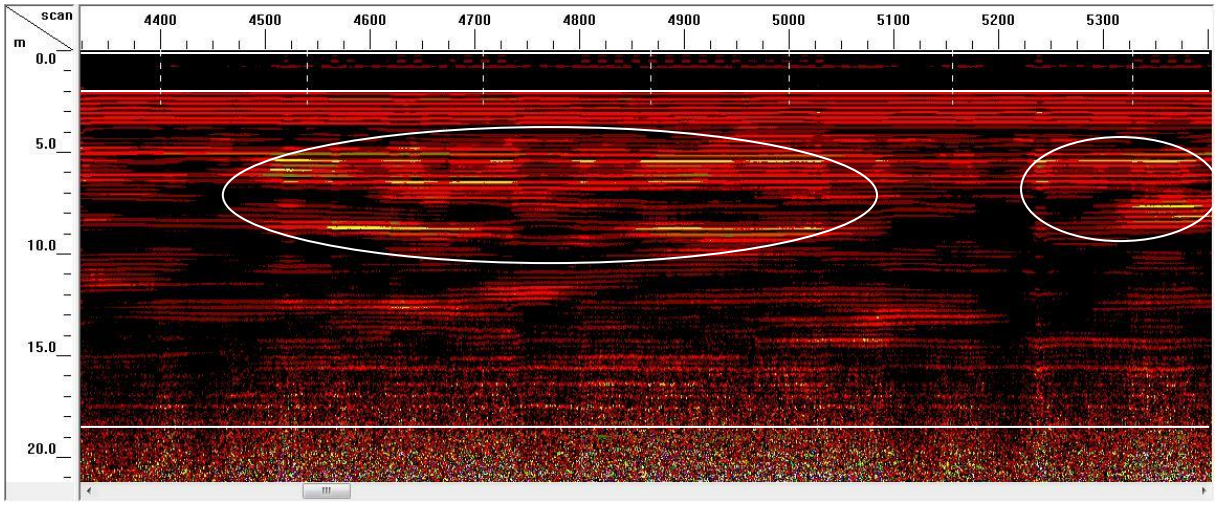


Figure 5.4e. Travertine rock mass with weakness zones (at 23-26 meters away from the Line-2 measurement starting point) are determined at this area, (Line-2, distance between 22--28 m).

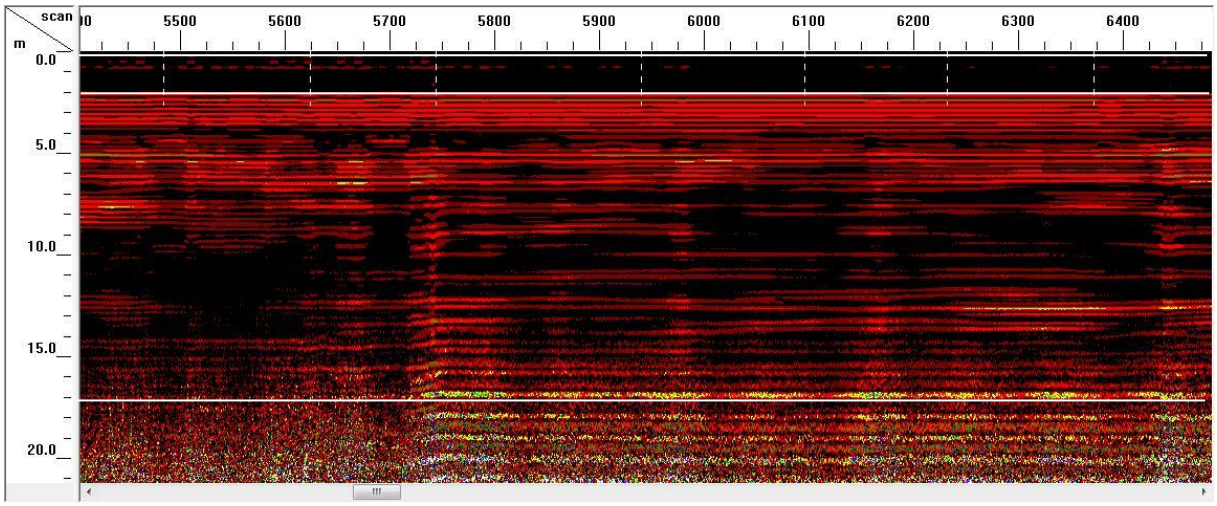


Figure 5.4f. Travertine rock mass bedding differences together with fracture planes, (Line-2, distance between 29-36 m).

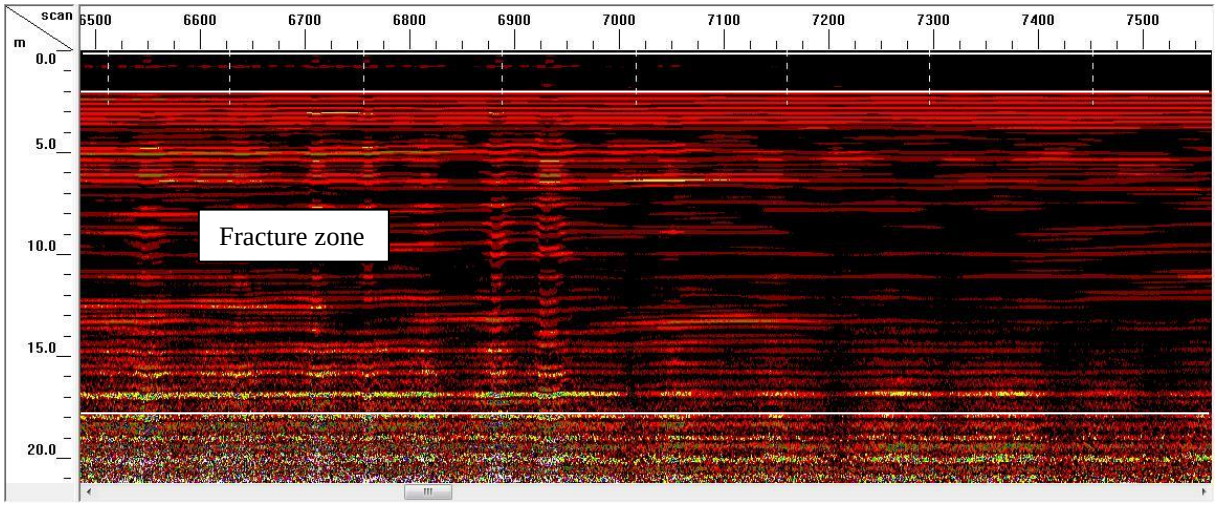


Figure 5.4g. Travertine rock mass bedding differences together with fracture zone at 36-39 meters away from Line-2 starting point, (Line-2, distance between 36-44 m).

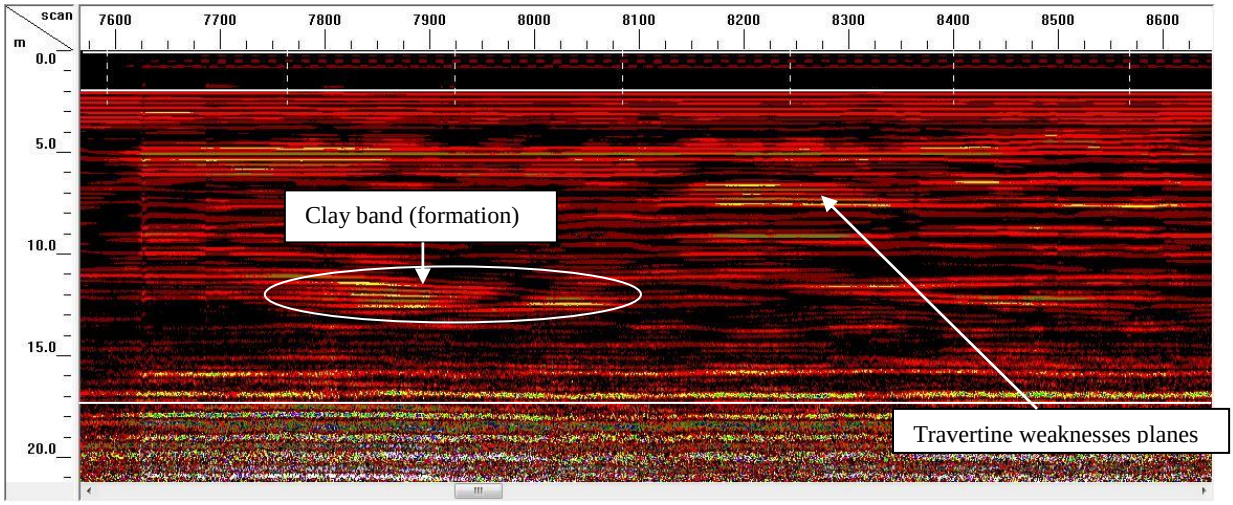


Figure 5.4h. Travertine rock mass bedding differences together with claystone layers and weakness layers in travertine rock mass, (Line-2, distance between 44-50 m).

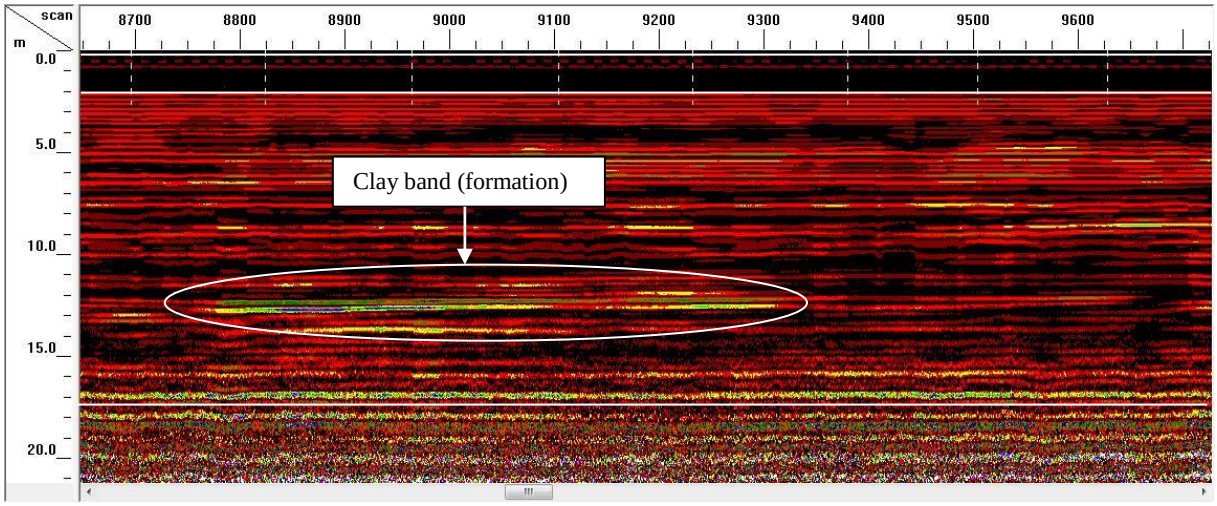


Figure 5.4i. Travertine rock mass bedding differences together with claystone layers and weakness layers in travertine rock mass. In this graphics, after the depth of 14 meters, travertine layers disappeared and the bedrock, limestone layers, (Line-2, distance between 51-59 m).

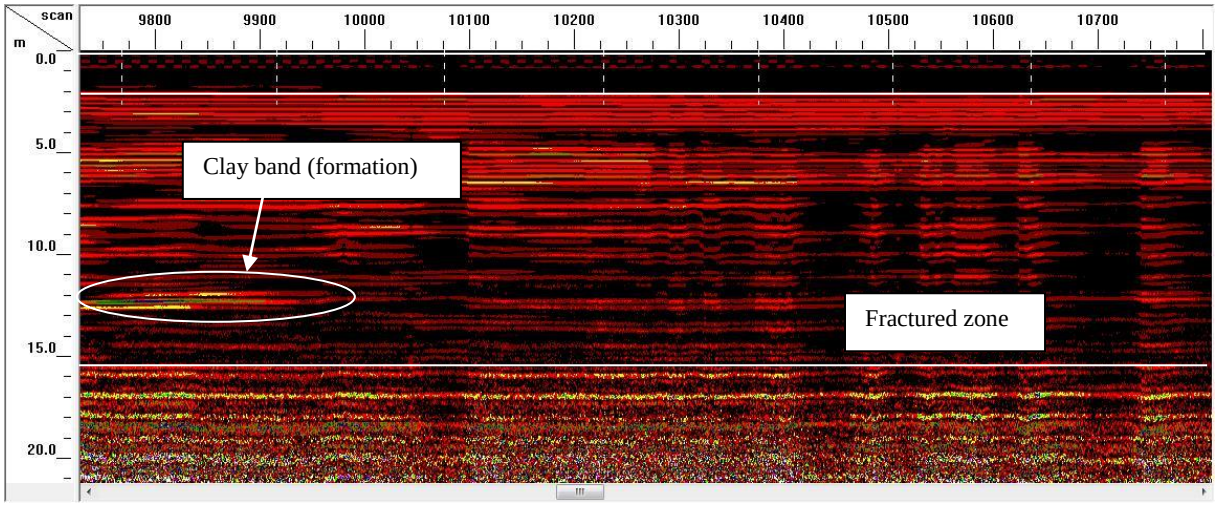


Figure 5.4j. Travertine rock mass bedding differences together with claystone layers and fractured zones, (Line-2, distance between 59-66 m).

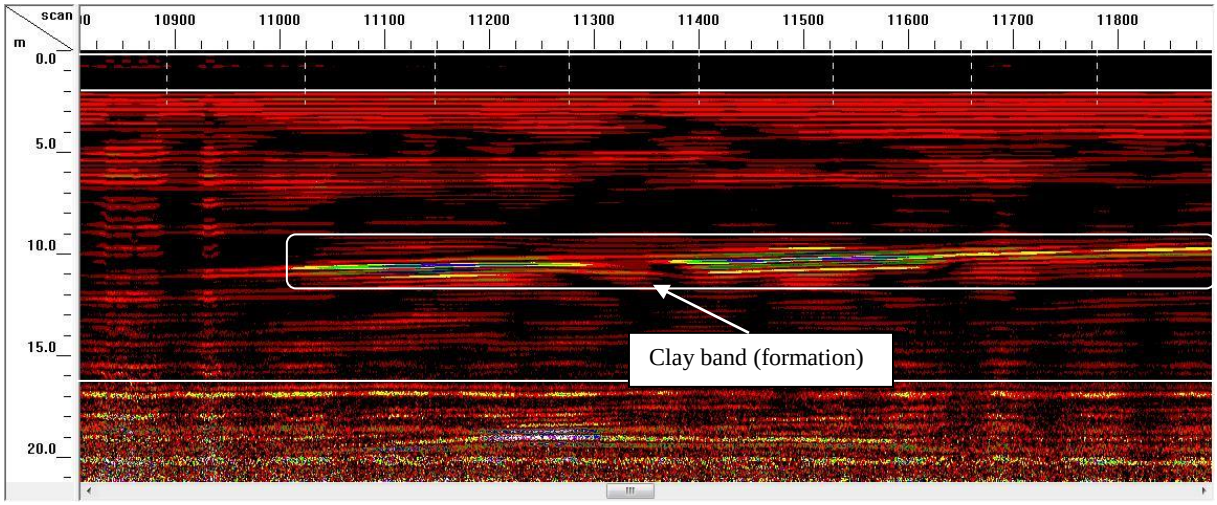


Figure 5.4k. Travertine rock mass bedding differences together with claystone layers and fractured (weakness) zones, (Line-2, distance between 67-75 m).

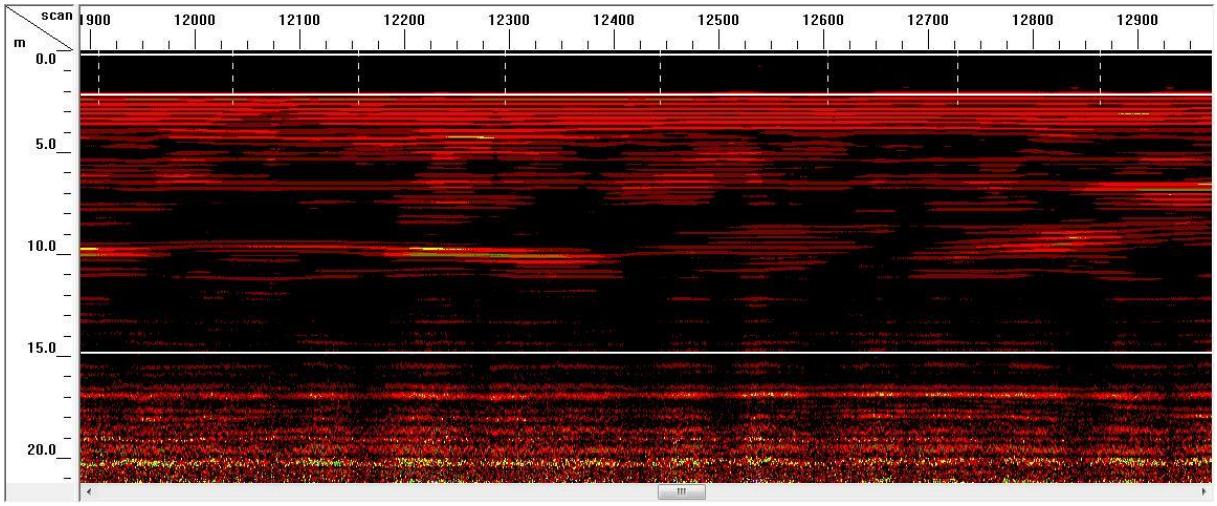


Figure 5.4l. Travertine rock mass bedding differences together with claystone layers, (Line-2, distance between 75-83 m).

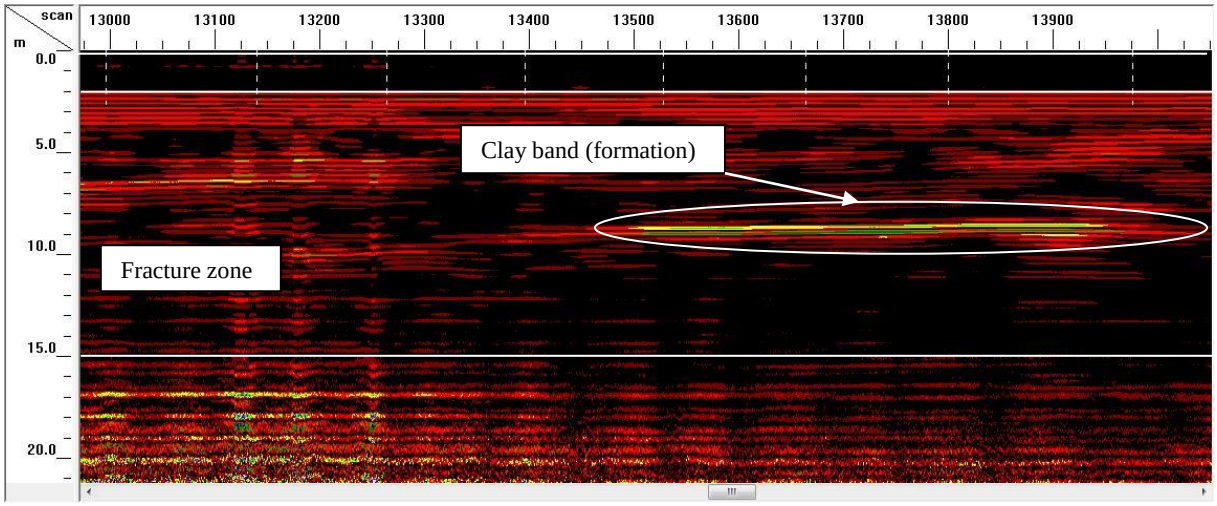


Figure 5.4m. Travertine rock mass bedding differences together with claystone layers and fracture zone, (Line-2, distance between 83-90 m).

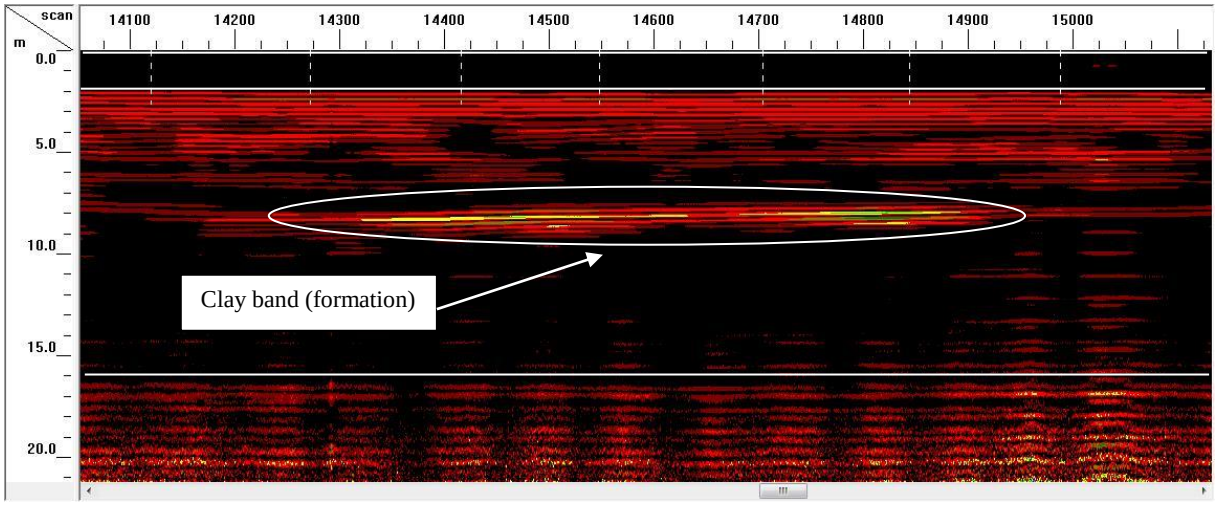


Figure 5.4n. Travertine rock mass bedding differences together with claystone layers. In this graphics first 2 meters of depth, weathered travertine can be seen. The depth between 2 and 16 meters were determined as travertine rock mass (relatively compact) including claystone intersection (2 meters thick). (Line-2, distance between 91-98 m).

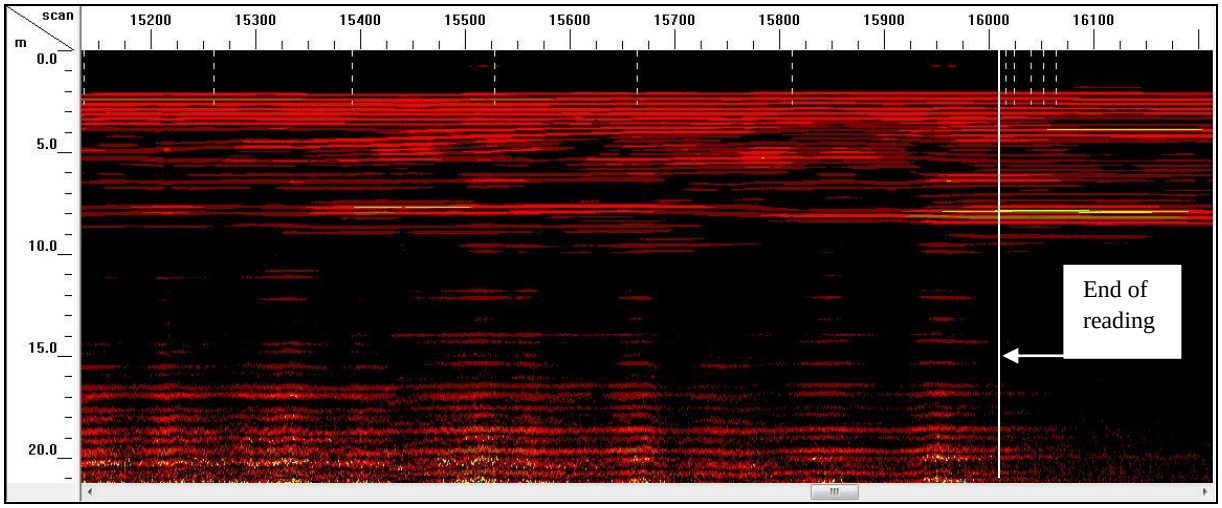


Figure 5.4o. Travertine rock mass bedding differences together with claystone layers. (Line-2, distance between 98-105 m).

c) **Line-3 (L-3, SW-NE):** This measuring line was elongated also like Line-1-2 and the GPR graphics were given below. The data for this graphics were taken through Line-3 moving SW to NE direction. It is 5 meters away (NW direction) from Line-2. GPR information depth was arranged for 21-23 meters and the measurement was performed accordingly. The data collection time took about 10 minutes and they were saved into the instrument's memory. After transferring the data into computer, Radan-7 software was used to analyze the field data. In this graphics the weakness zones and fractured zones were determined and plotted on the graphics as they were given at Figure 5.7. The other features of rock mass were checked in the graphics to understand the situation of travertine rock mass under the surface.

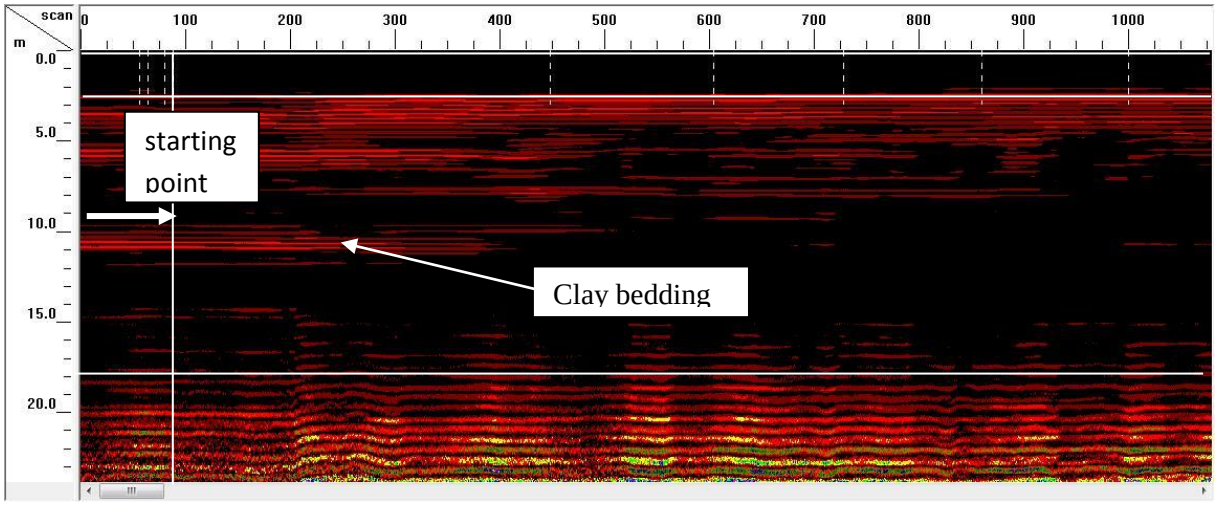


Figure 5.5a. Travertine rock mass with clay bedding, together with fractures and travertine foliation features, (Line-3, distance between, 0-5 m).

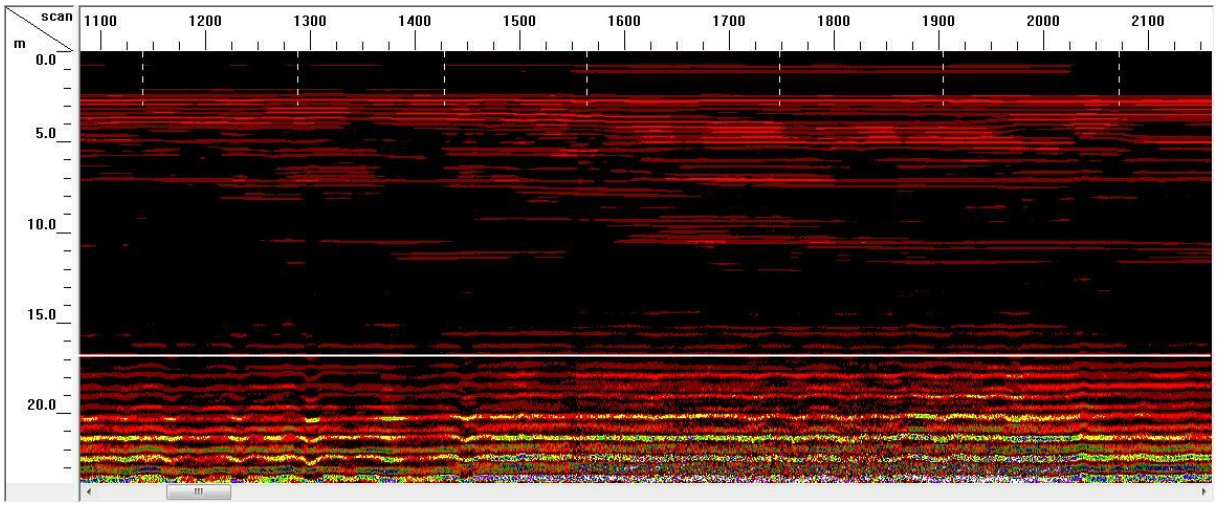


Figure 5.5b. Travertine rock mass under the line 3, together with weakness layers (foliations), (Line-3, distance between, 5-11 m).

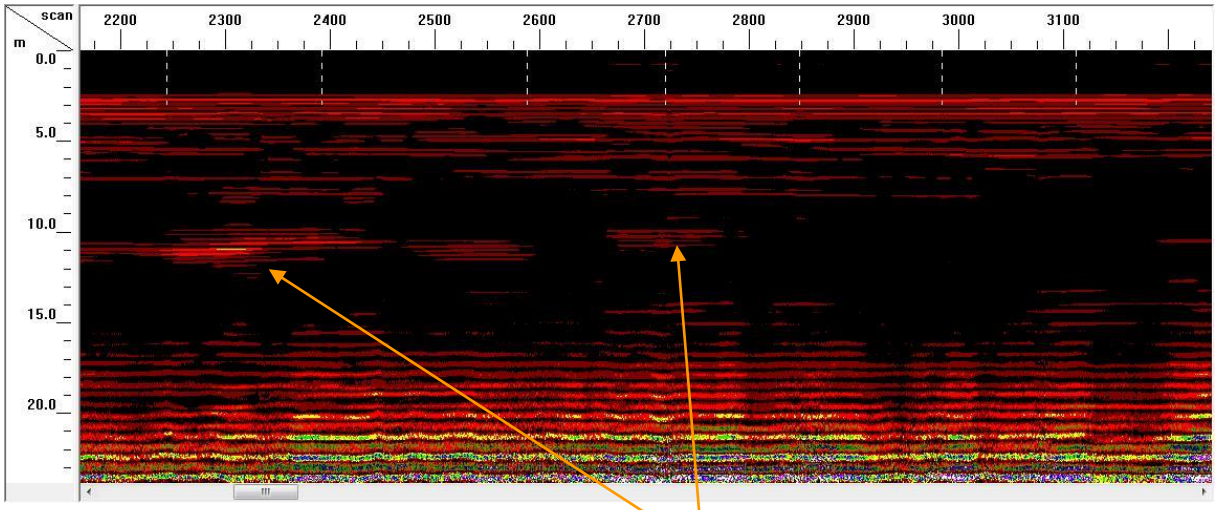


Figure 5.5c. Travertine rock mass beddings together with claystone layers, (Line-3, distance between, 11-17 m).

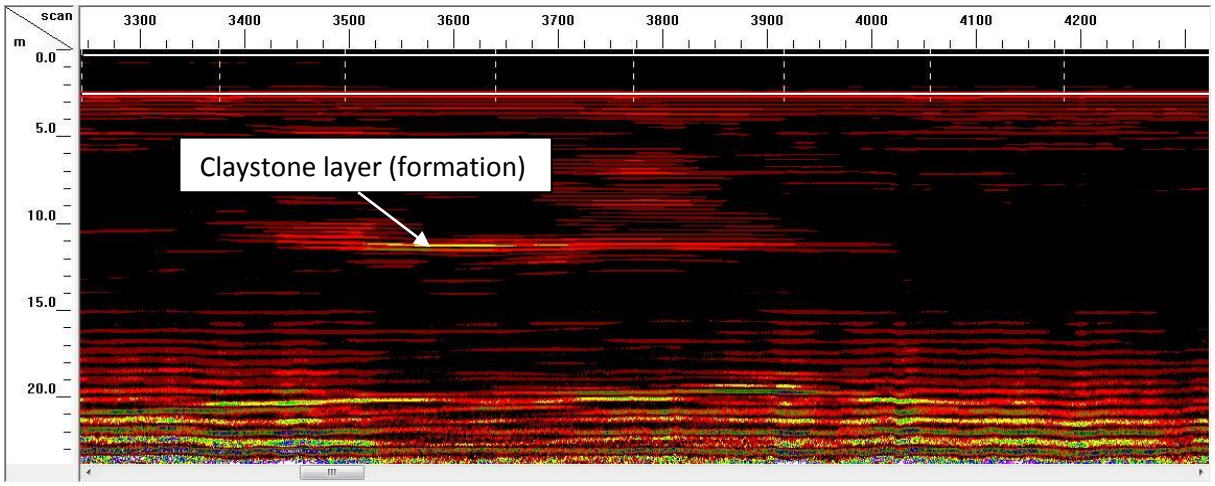


Figure 5.5d. Travertine rock mass beddings together with claystone layer, (Line-3, distance between, 17-24 m).

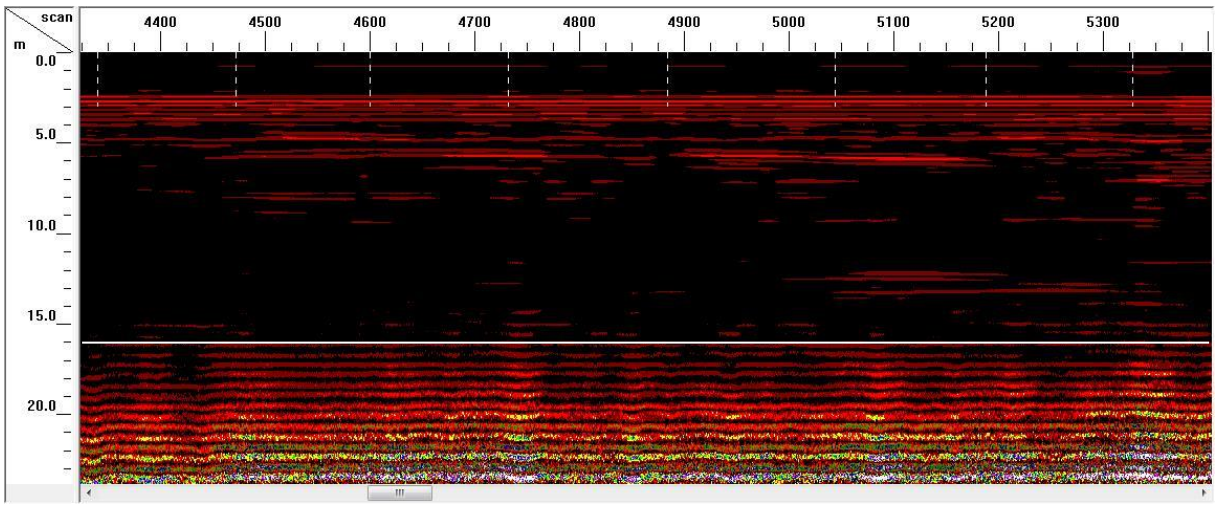


Figure 5.5e. Travertine rock mass beddings, in this graphic first 2 meters of depth includes weathered travertine. The depth between 2 and 16 meters were determined as relatively compact travertine rock mass (Line-3, distance between 24-31 m).

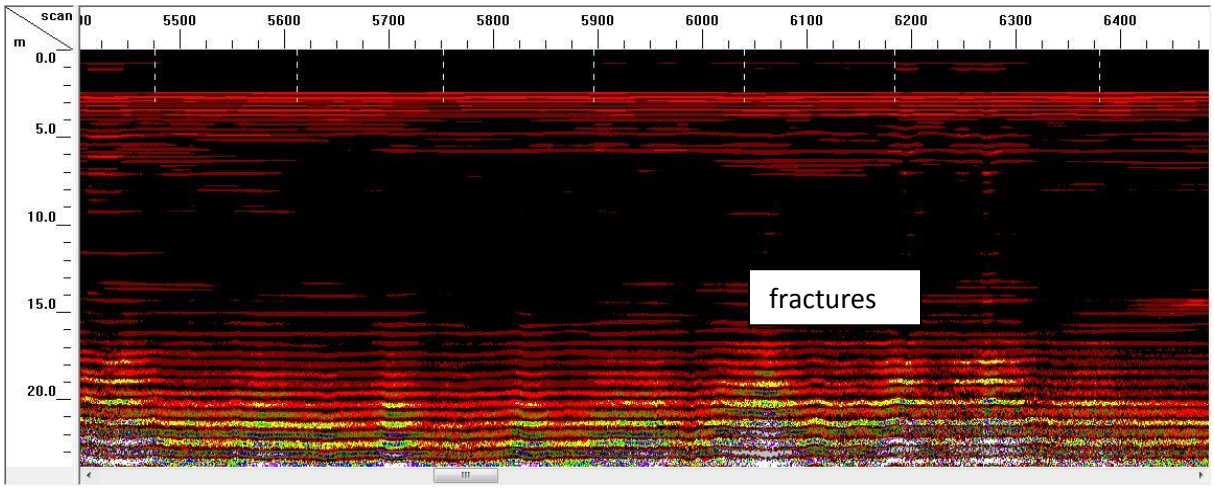


Figure 5.5f. Travertine rock mass beddings together with claystone layer, in this graphic first 2 meters of depth cover weathered travertine. The depth between 2 and 15 meters were determined as relatively compact travertine rock mass with less foliation. This graphic shows fractures as well, (Line-3, distance between 31-37 m).

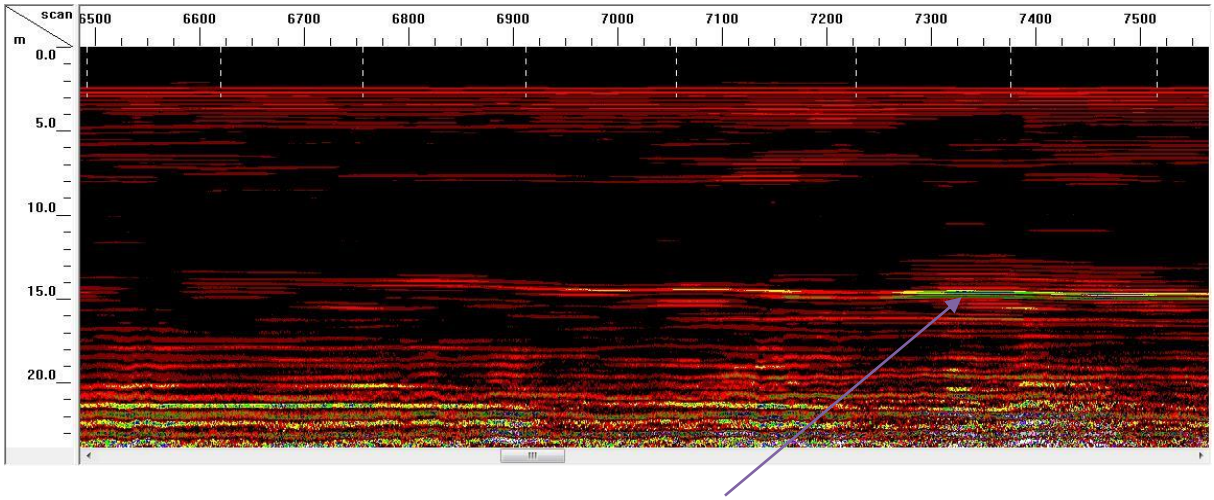


Figure 5.5g. Travertine rock mass beddings together with claystone layer, (Line-3, distance between 37-44 m).

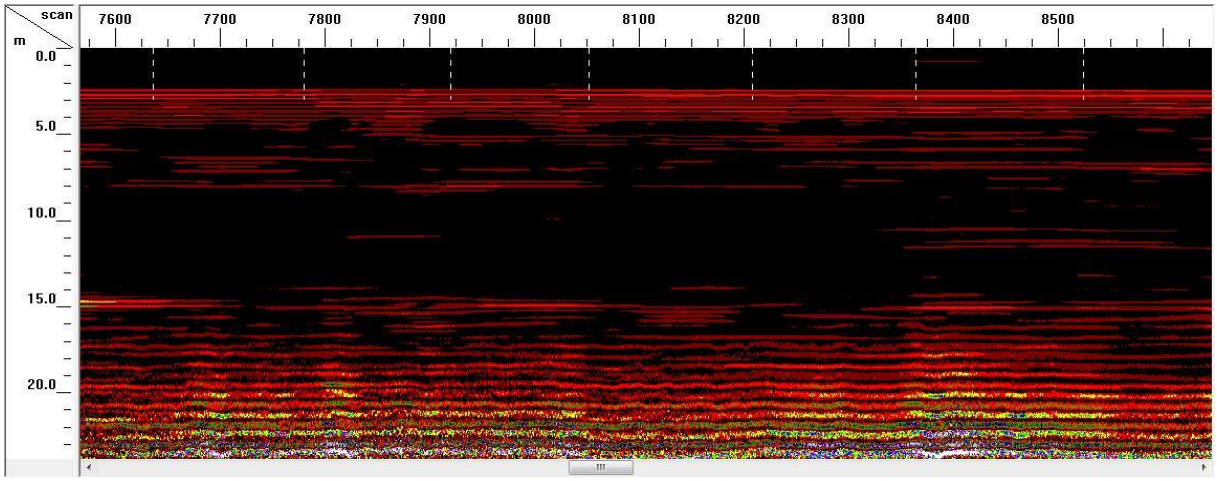


Figure 5.5h. Travertine rock mass, in this graphic first 2 meters of depth were seen as weathered rock mass. The depth between 2 and 14 meters here, the travertine rock mass has less weakness zone. (Line-3, distance between, 44-50 m).

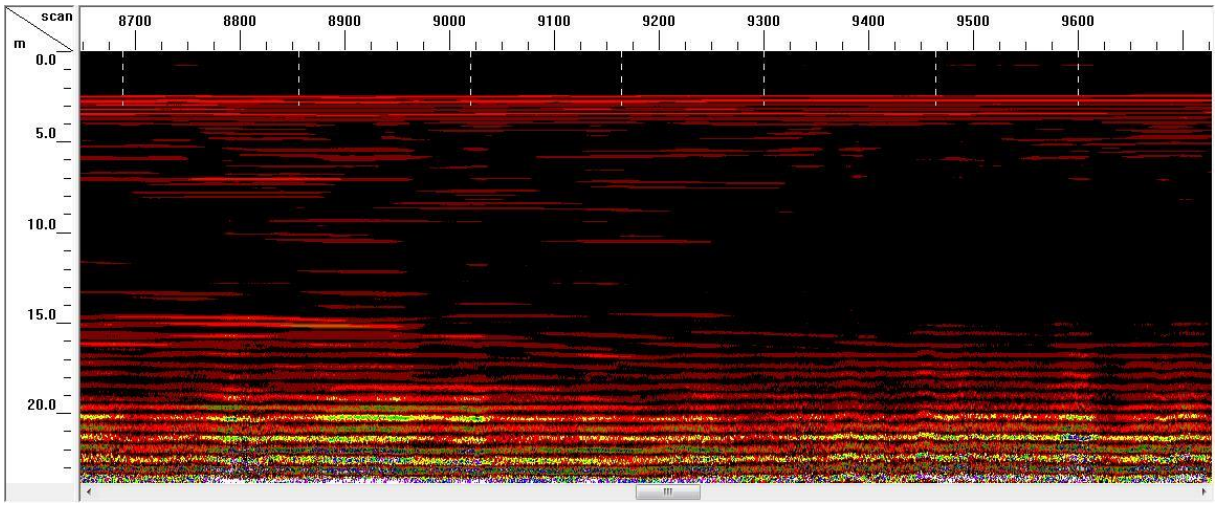


Figure 5.5i. Travertine rock mass beddings together with more foliated zone at deeper part (deeper than 15 meters). (Line-3, distance between, 50-56 m).

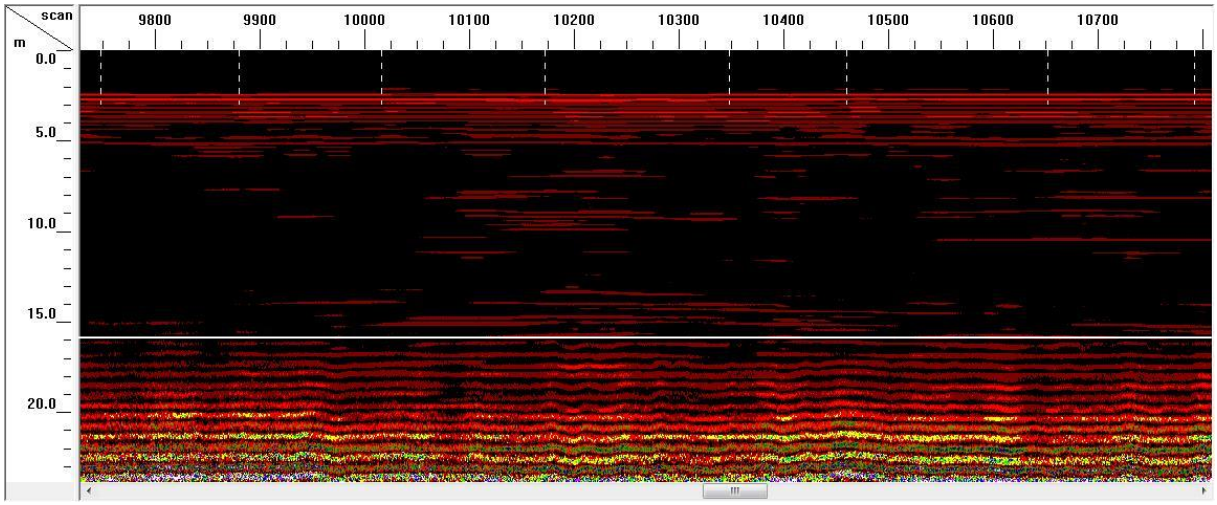


Figure 5.5j Travertine rock mass beddings together with claystone layer. The rock mass: 0-2 meter depth: weathered traverten, 2-16 meters depth: relatively massive travertine rock mass, >16 meters depth: bedding weakness obvious, (Line-3, distance between 56-63 m).

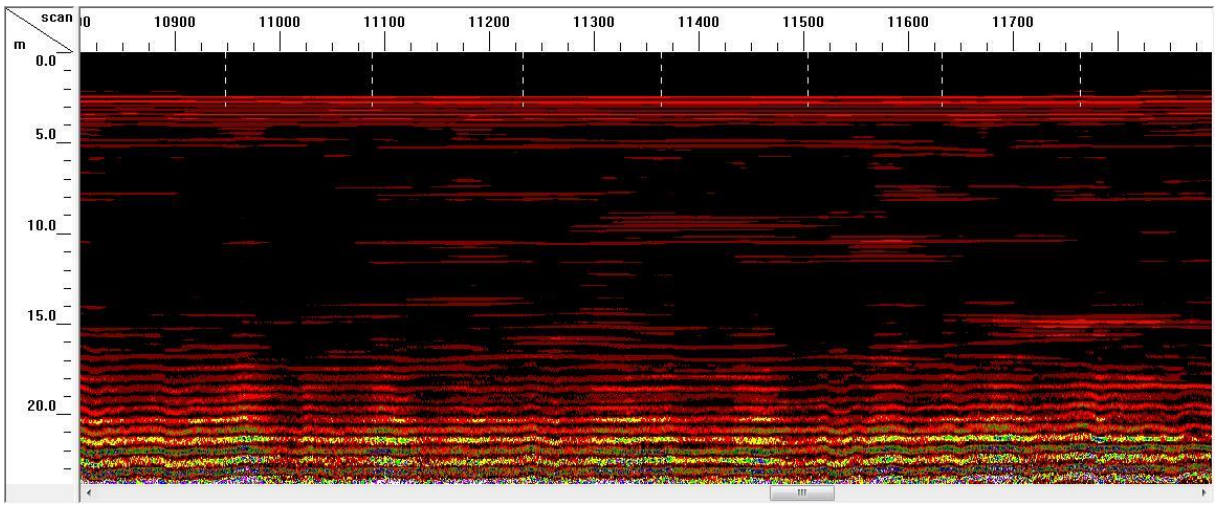


Figure 5.5k. Travertine rock mass bedding together with claystone layer. (Line-3, distance between, 63-70 m).

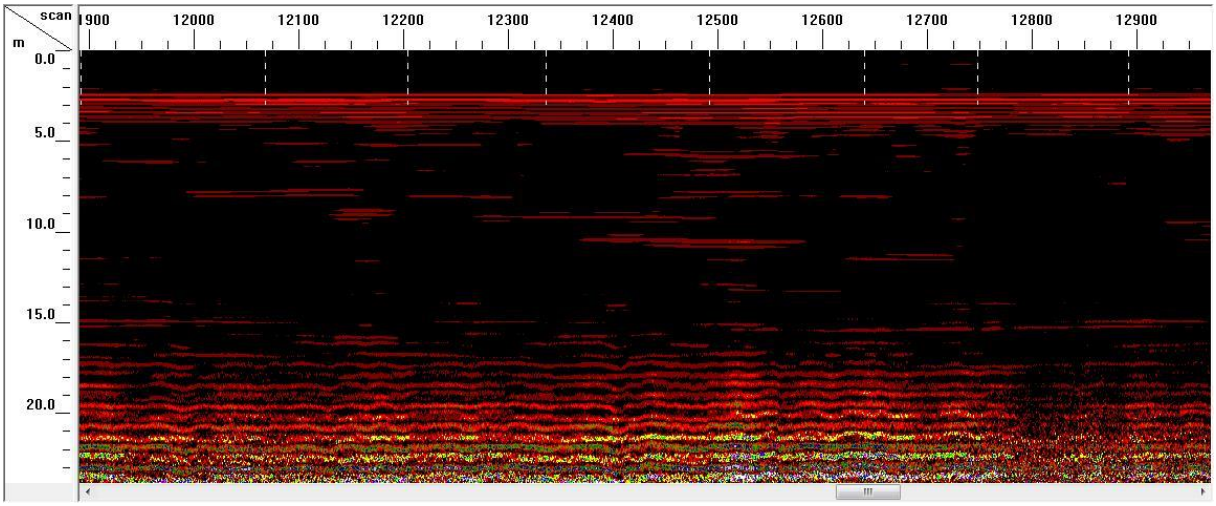


Figure 5.5l. Travertine rock mass features (Line-3, distance between, 70-77 m).

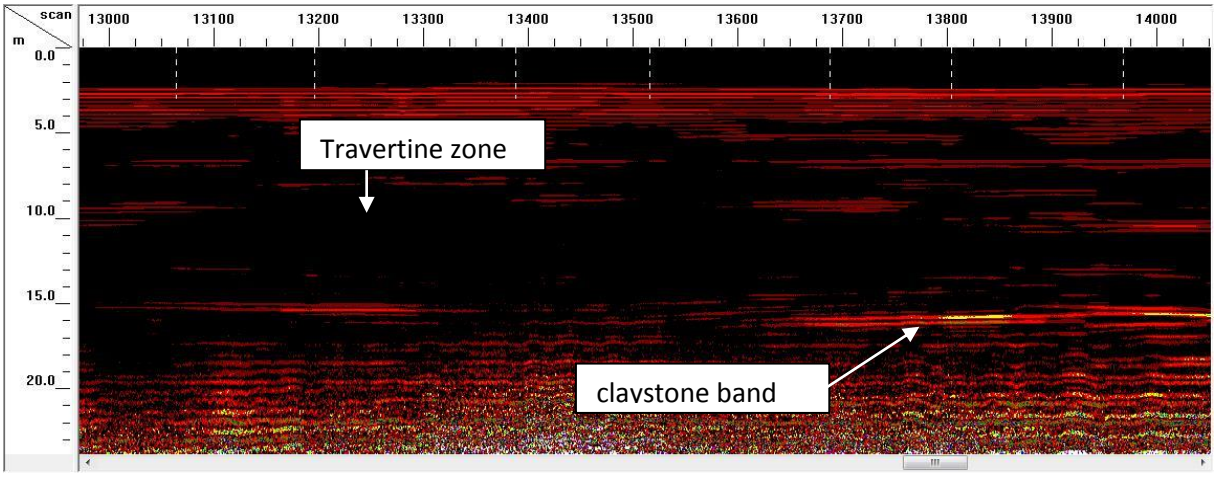


Figure 5.5m. Travertine rock mass bedding together with claystone, in this graphic at the depth between 2 and 15 meters there is relatively compact traverten rock mass, (Line-3, distance between, 77-83 m).

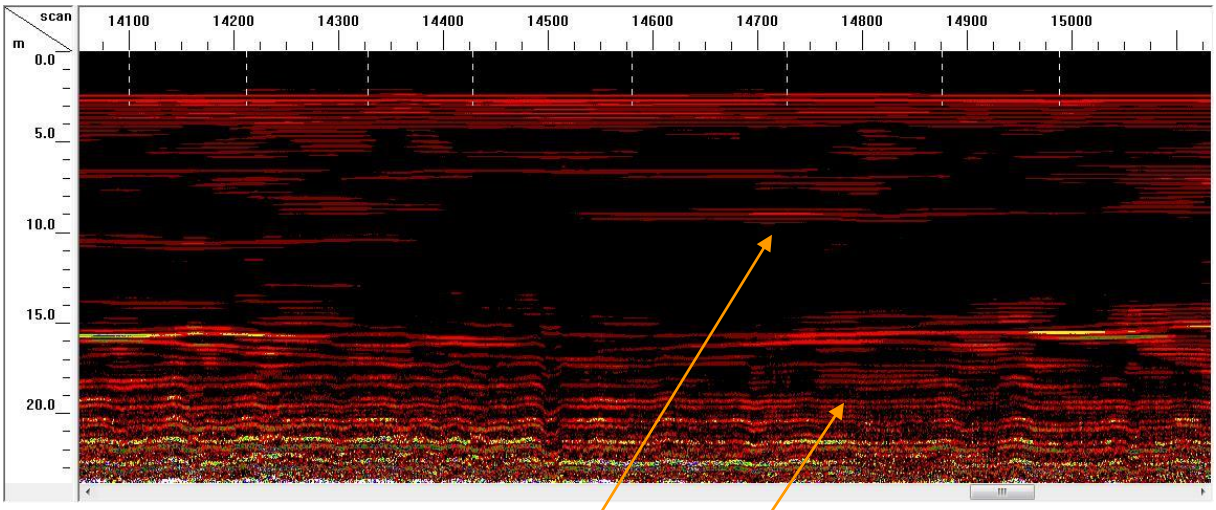


Figure 5.5n. Travertine rock mass together with claystone and base rock mass layers, (Line-3, distance between, 83-90 m).

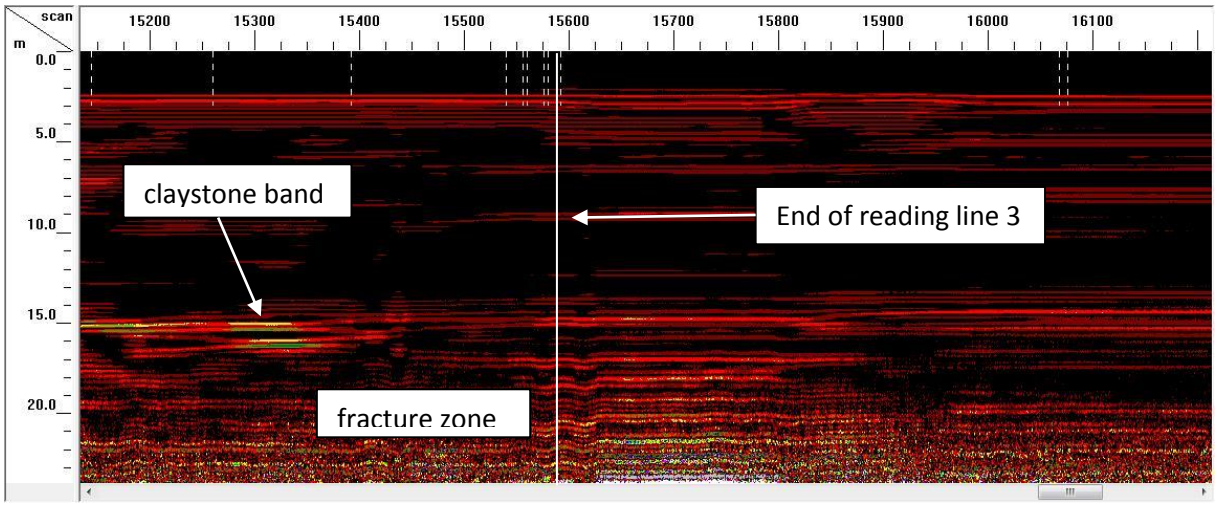


Figure 5.5o Travertine rock mass bedding together with claystone layers and fracture zones, (Line-3, distance between, 90-93 m).

d) Line-4 (L-4, SW-NE): This measuring line was elongated also like the other Lines and the GPR reading given below were taken through Line-4 moving SW to NE direction. It is 5 meters away (NW direction) from Line-3. The GPR antenna was arranged for 22-23 meters depth and the measurement was performed accordingly. The data collection time took about 10 minutes and they were saved into the instrument's memory. After transferring the data into computer, Radan-7 software was used to analyze the data and the results are given below for Line-4. In this graphics the weakness zones, claystone zone and fracture planes were presented as they were determined. The other features of rock mass were checked for these measurements to visualize the travertine rock mass under the measuring pit bench surface. The resultant GPR graphics obtained for this Line are given below;

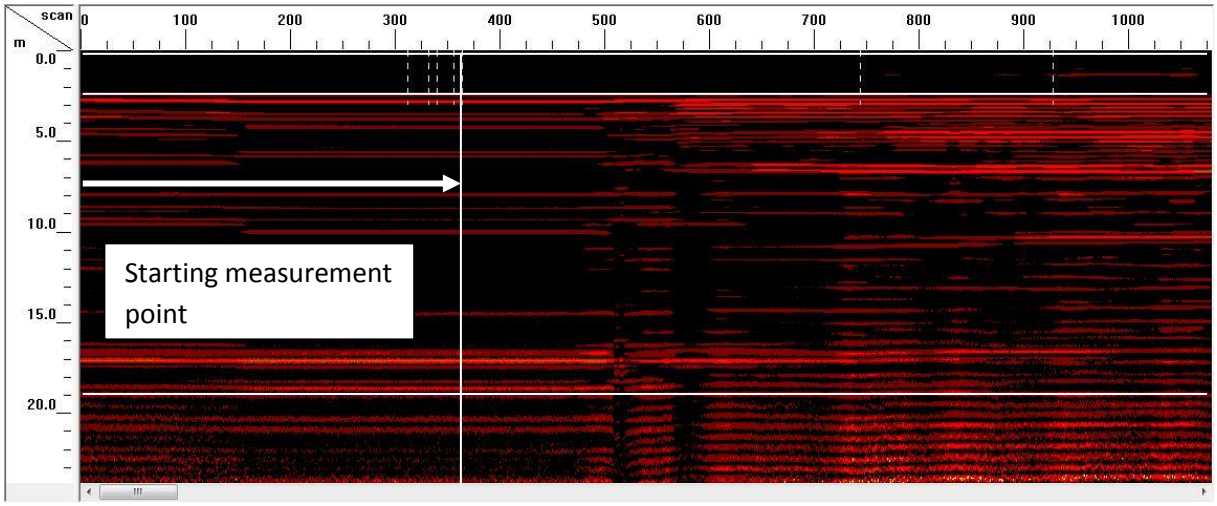


Figure 5.6a. Travertine rock mess features, (Line-4, distance between 0-2 m)

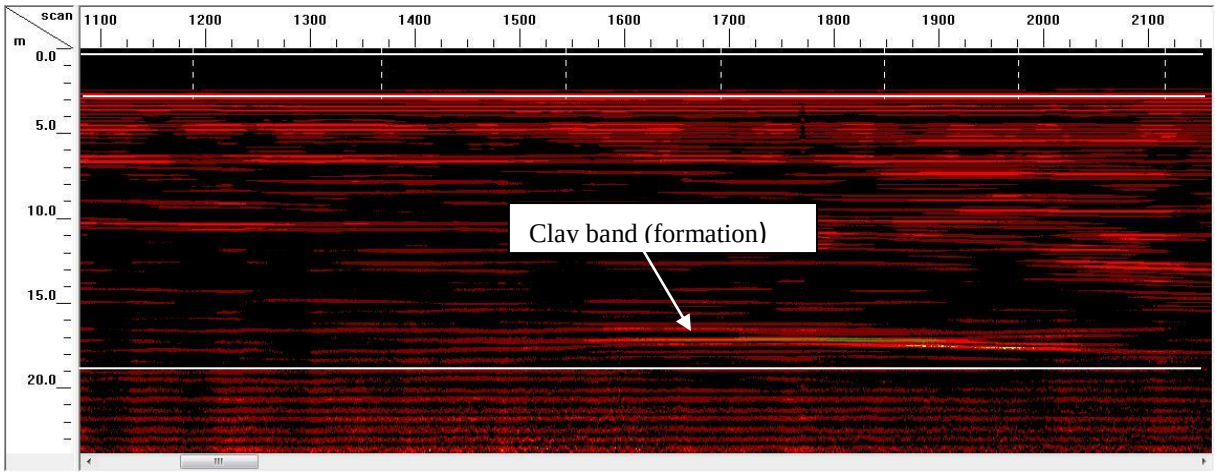


Figure 5.6b. Travertine rock mass bedding together with claystone layers and weakness zones (Line-4, distance between 2-8 m)

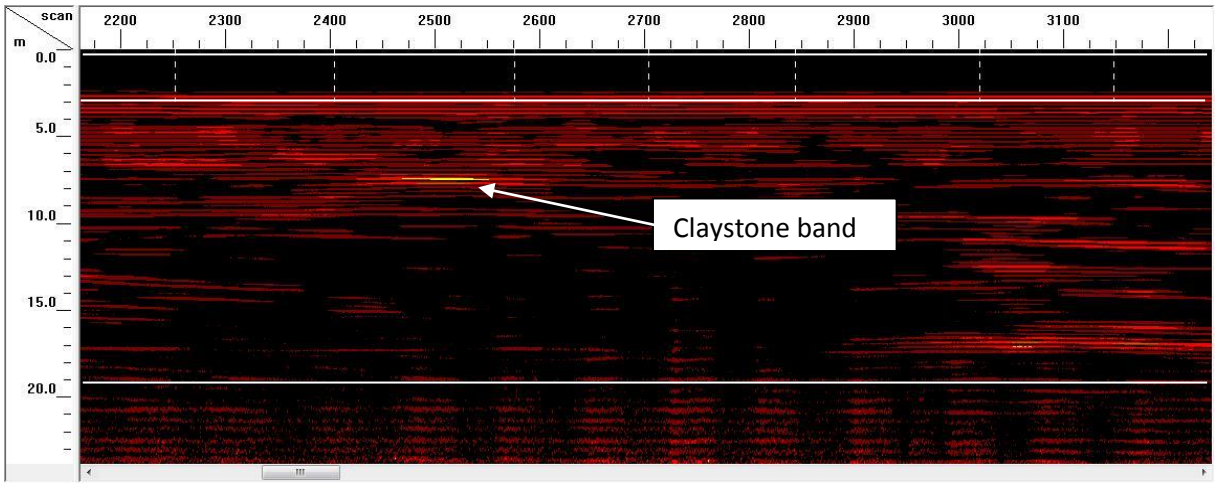


Figure 5.6c. Claystone layer and illustrated weakness location in it, (Line-4, distance between 8-14 m)

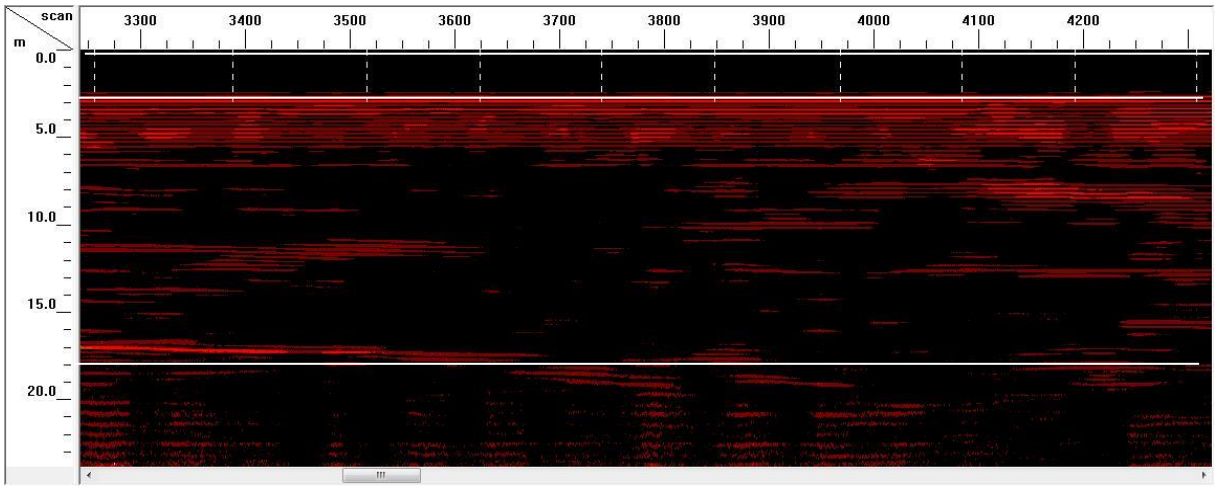


Figure 5.6d. Travertine rock mass bedding together with claystone layers, in the first 2 meters of depth there is weathered travertine. There is relatively less fractured travertine rock mass at the depth between 2 and 17 meters, (Line-4, distance between 14-23 m).

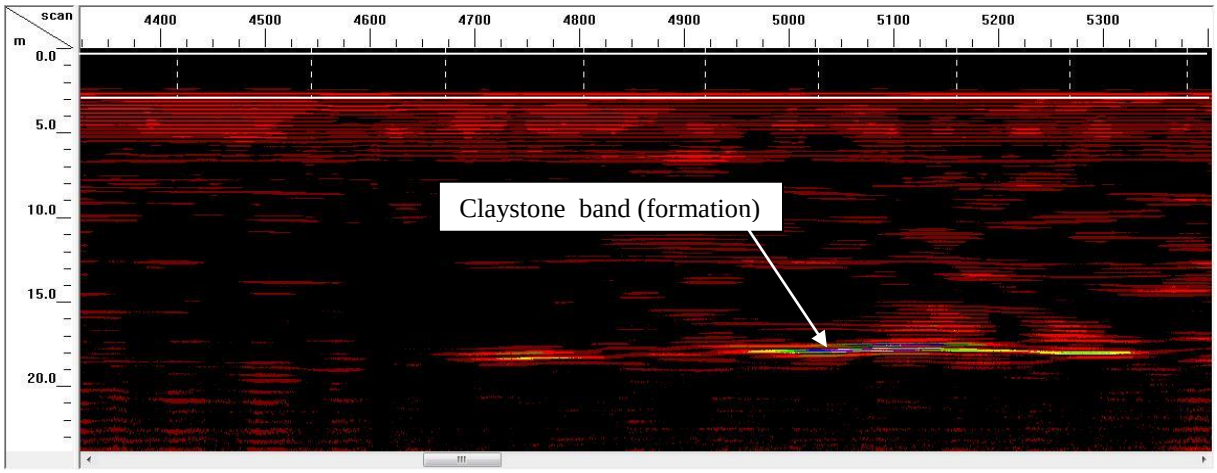


Figure 5.6e. Travertine rock mass features. The layers which were determined at the depth of 19 meters are notted as the base layers, (Line-4. distance between 23-31 m).

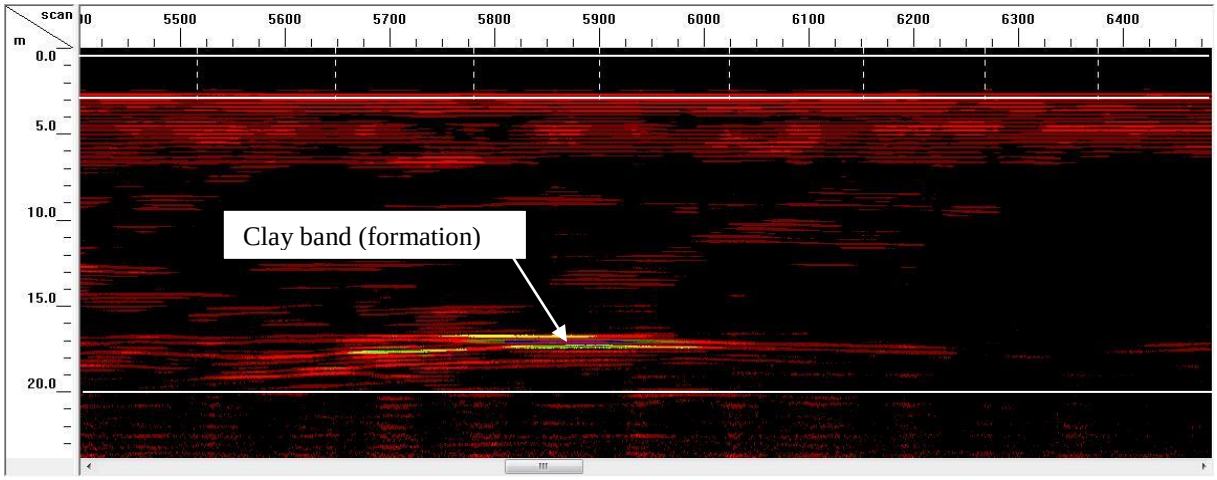


Figure 5.6f Travertine rock mass containing weakness zone at this part of measuring line. It is probably clay bands. (Line-4. distance between 31-38 m).

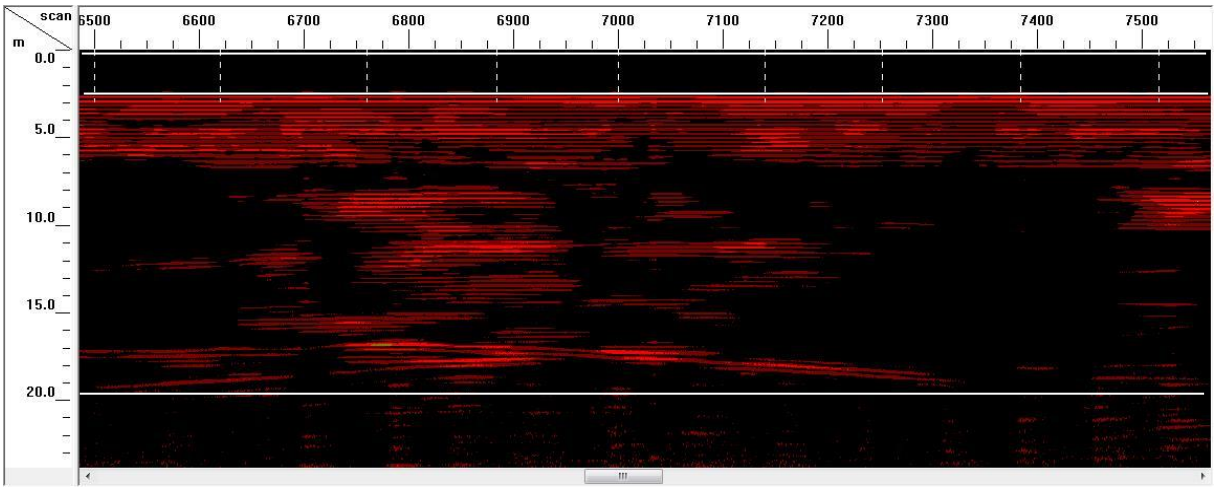


Figure 5.6j Travertine rock mass bedding together with foliations, travertine here was determined as more compact, (Line-4, distance between 37-45 m)

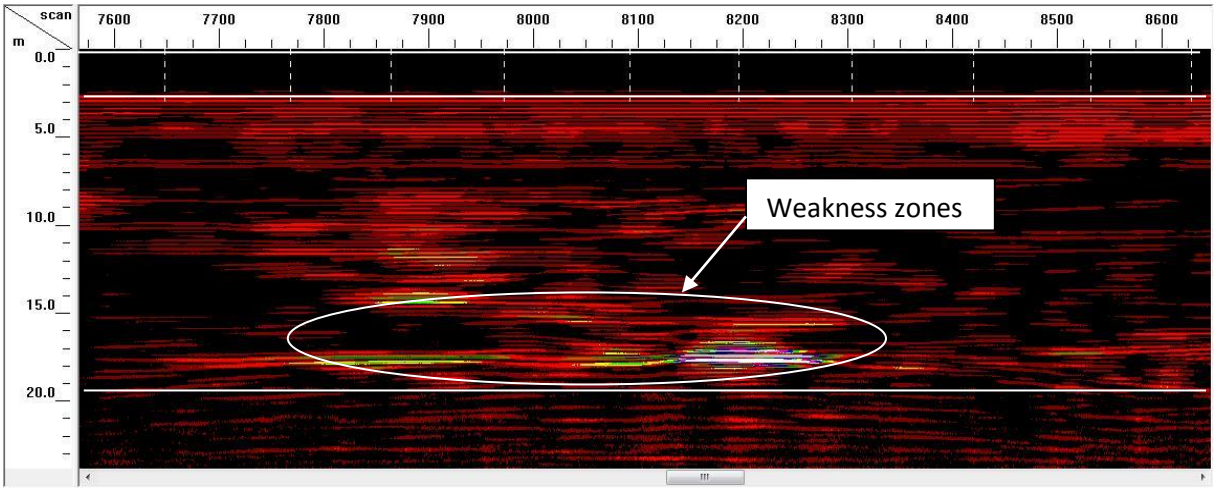


Figure 5.6k Travertine rock mass together with weakness zones, (Line-4, distance between 45-54 meters)

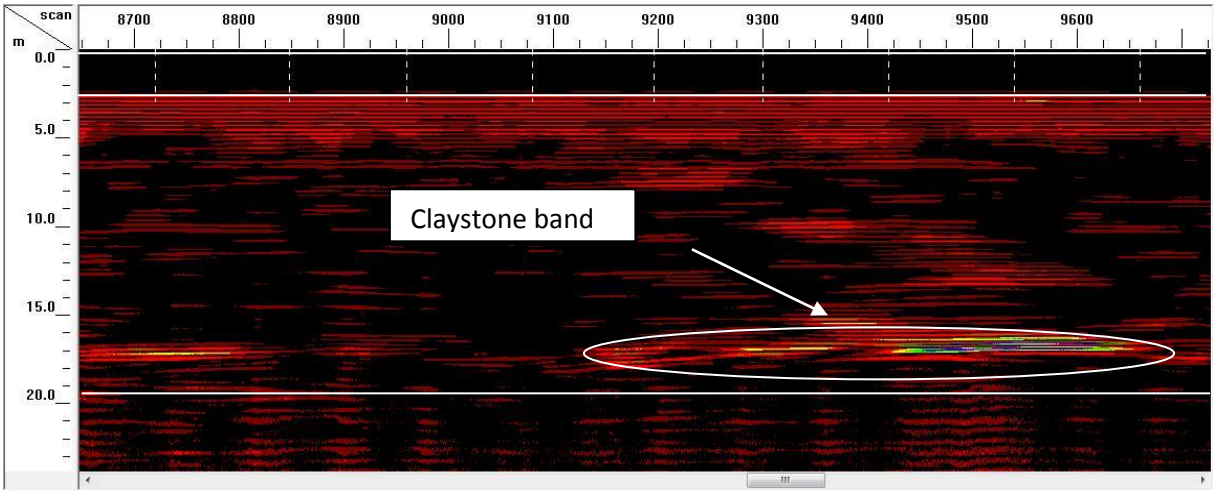


Figure 5.6l Travertine rock mass bedding together with claystone layer, first 2 meters of travertine were weathered. The depth between 2 and 19 meters cover relatively good travertine rock mass. (Line-4, distance between 54-62 m).

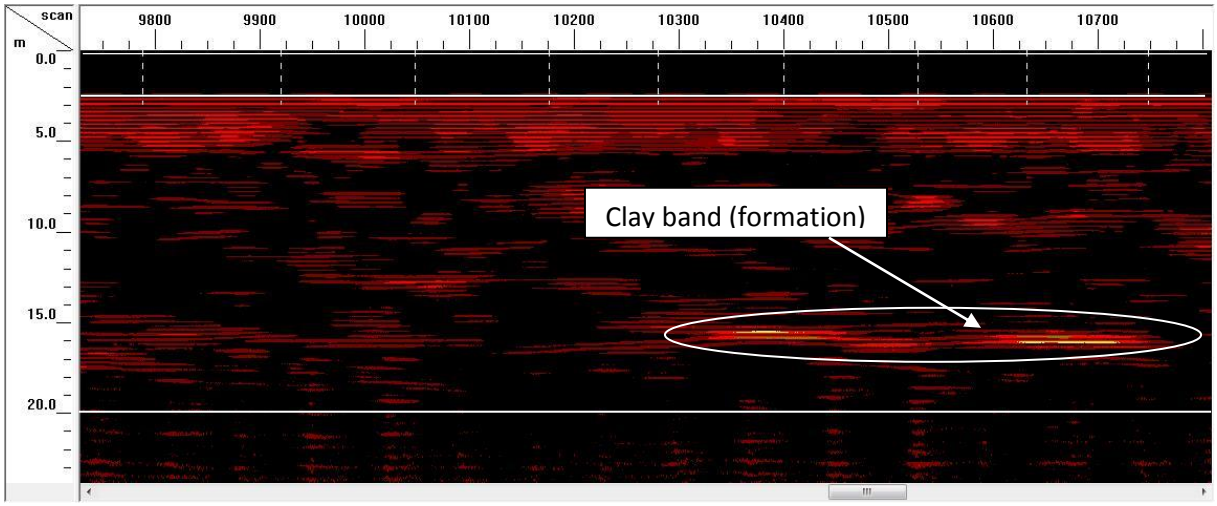


Figure 5.6m. Travertine rock mass bedding together with claystone layers, (Line-4, distance between 62-70 m)

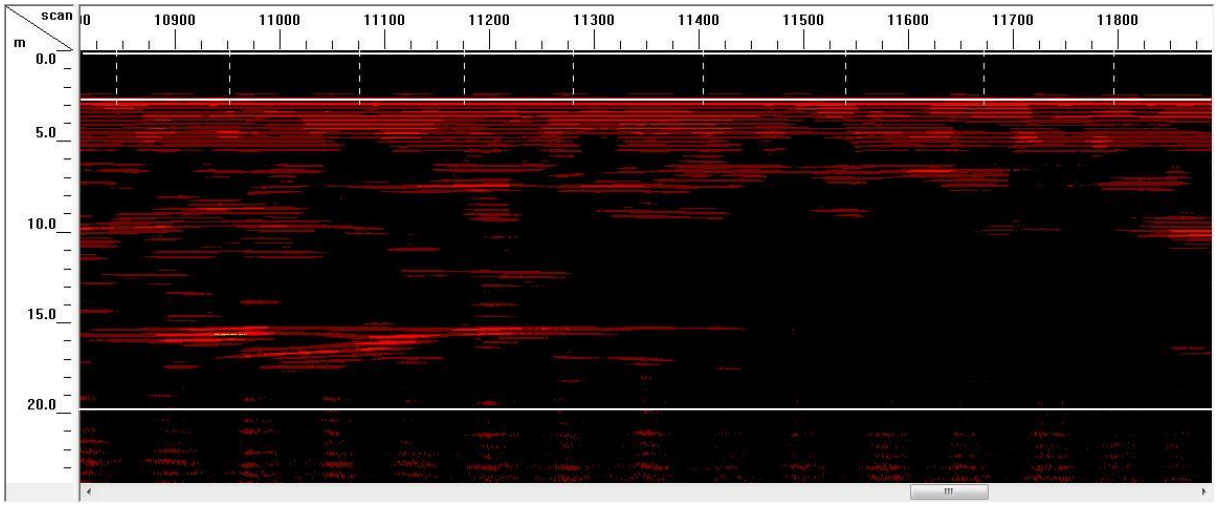


Figure 5.6n. Travertine rock mass features, (Line-4, distance between 70-78 m)

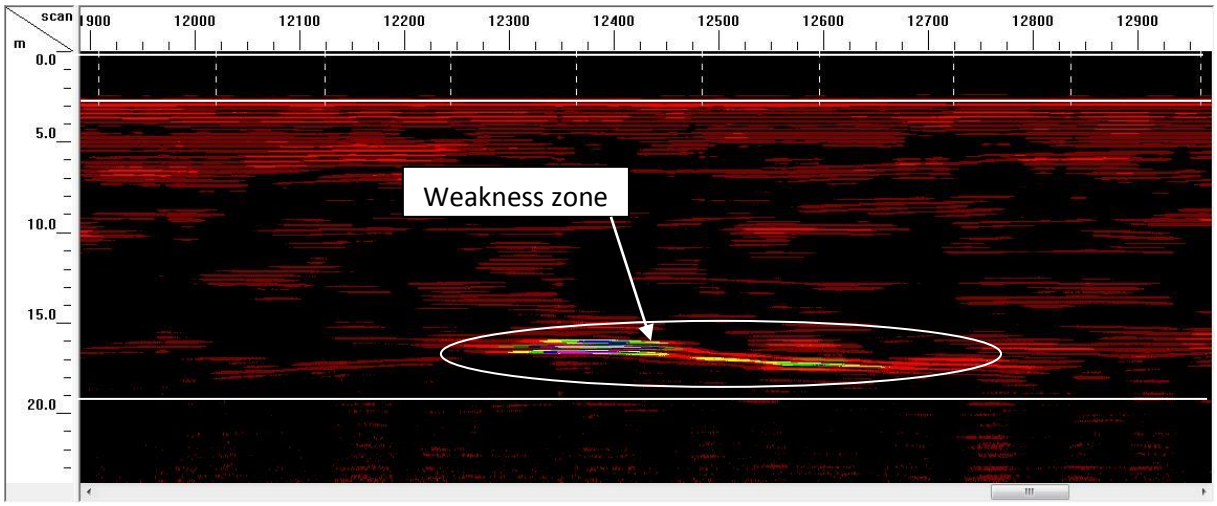


Figure 5.6o Travertine rock mass containing weakness zone at this location of the measurement, (Line-4, distance between 78-87 m)

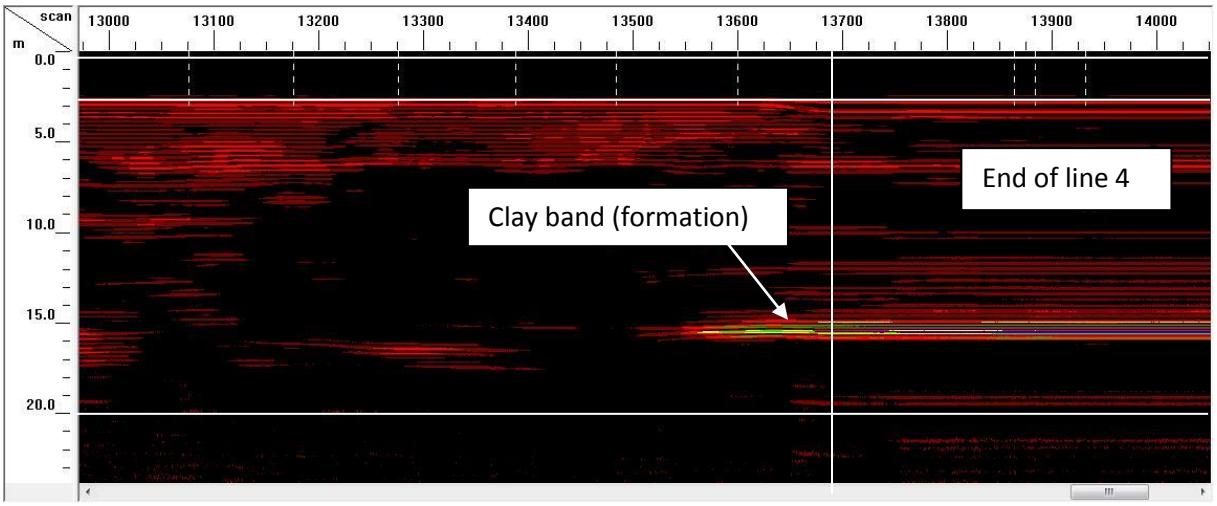


Figure 5.6p. Travertine rock mass bedding together with claystone layers, (Line-4, distance between 87- 93 m).

e) Line-5 (L-5, NE-SW): This line is last measuring line which was elongated from NE to SW direction. It was situated 10 meters away from the Line-4. GPR antennas were arranged to obtain rock mass features up to 7 meters depth. GPR readings were performed by moving the GSSI's GPR antennas from NE to SW. The data collected during the field test were saved to GPR equipment's internal memory. These data later were transferred to the computer to analyze but using RADAN-7 software. The GPR graphics supplied by Radan-7 then evaluated one by one by using different sunmodels in this program. The resultant graphics are then given below simultaneously;

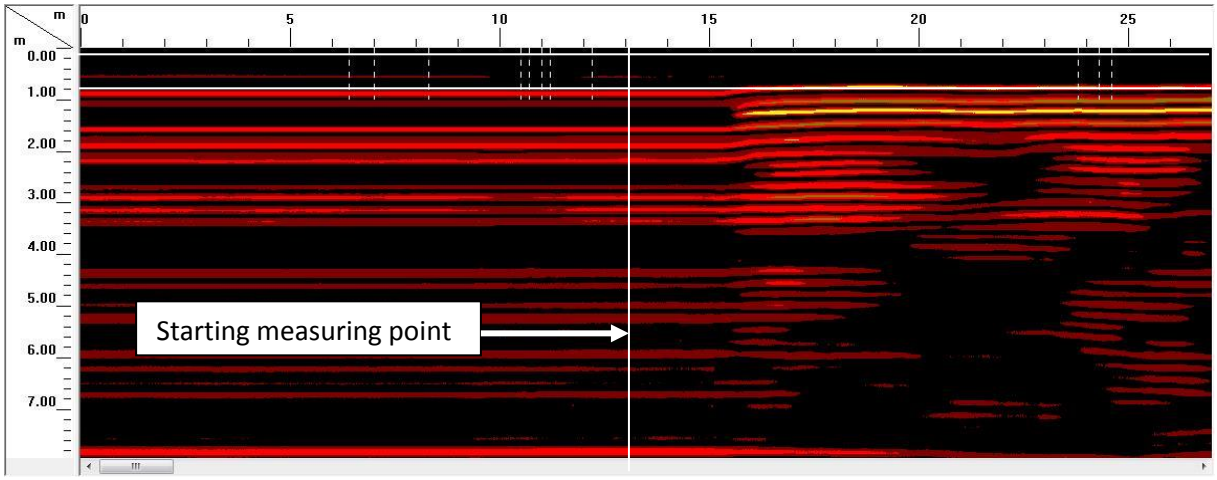


Figure 5.7a. Travertine rock mass bedding together with fracture top layers, (Line-5, distance between 0-1 m).

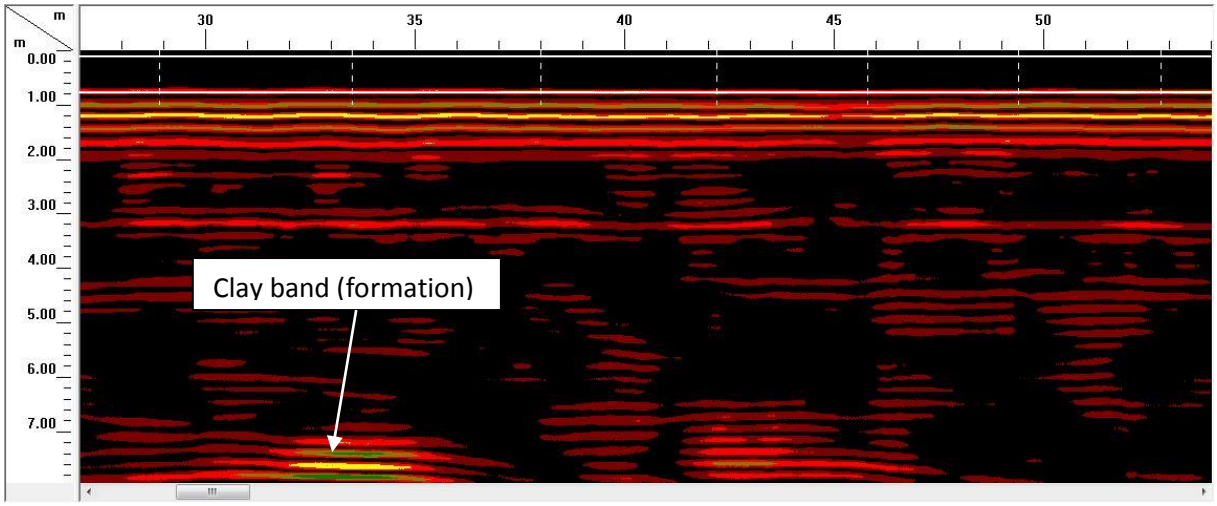


Figure 5.7b. Travertine rock mass bedding with claystone layer, (Line-5, distances between 1-7 m).

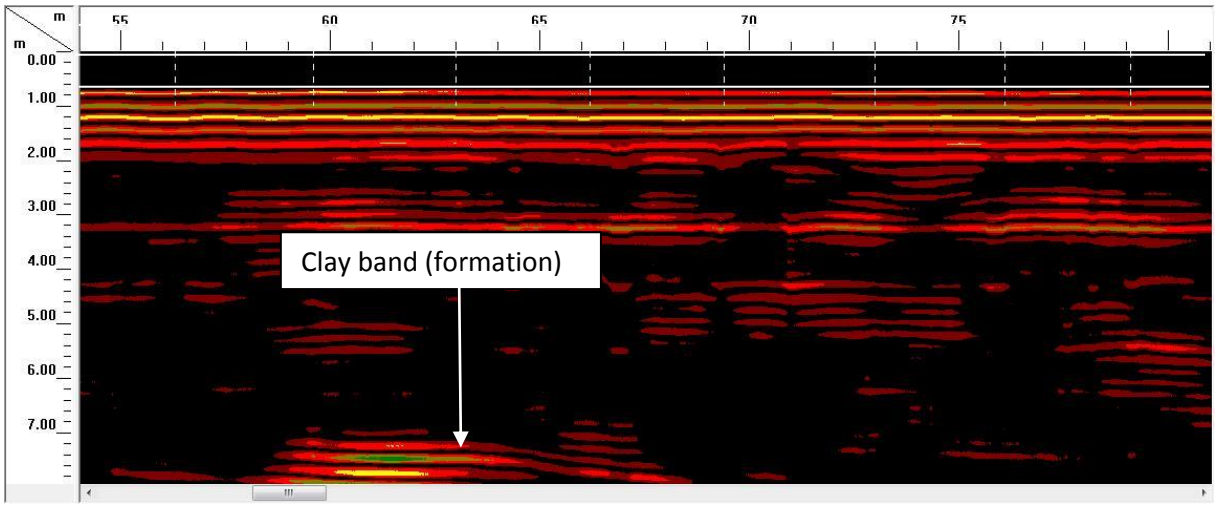


Figure 5.7c. Travertine rock mass was determined here with obvious clayband weakness zones, (Line-5, distance between 7-14 m).

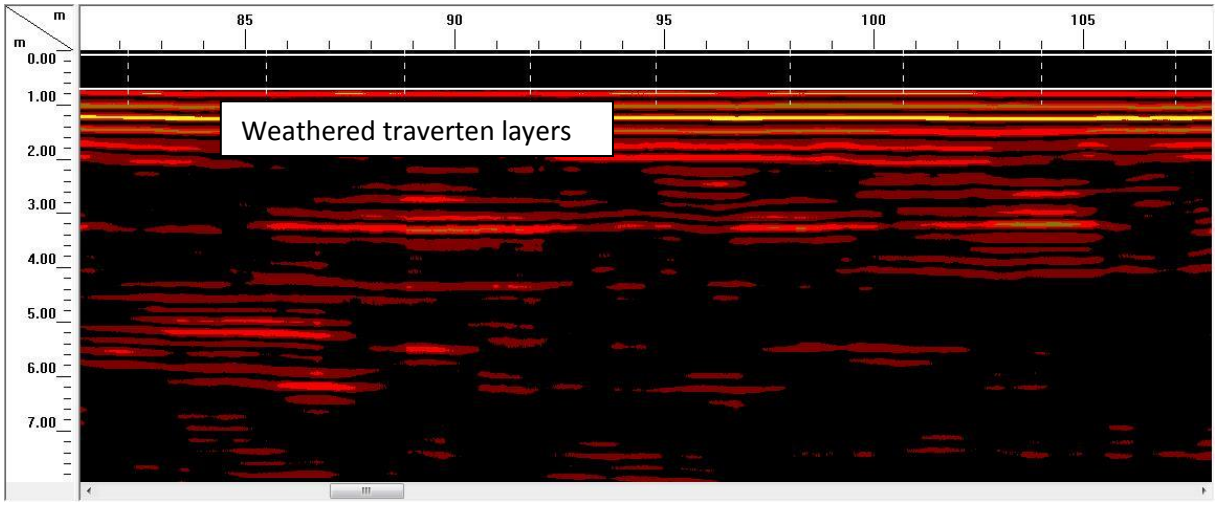


Figure 5.7d. Travertine rock mass beddings, (Line-5, distance between 14- 22 m).

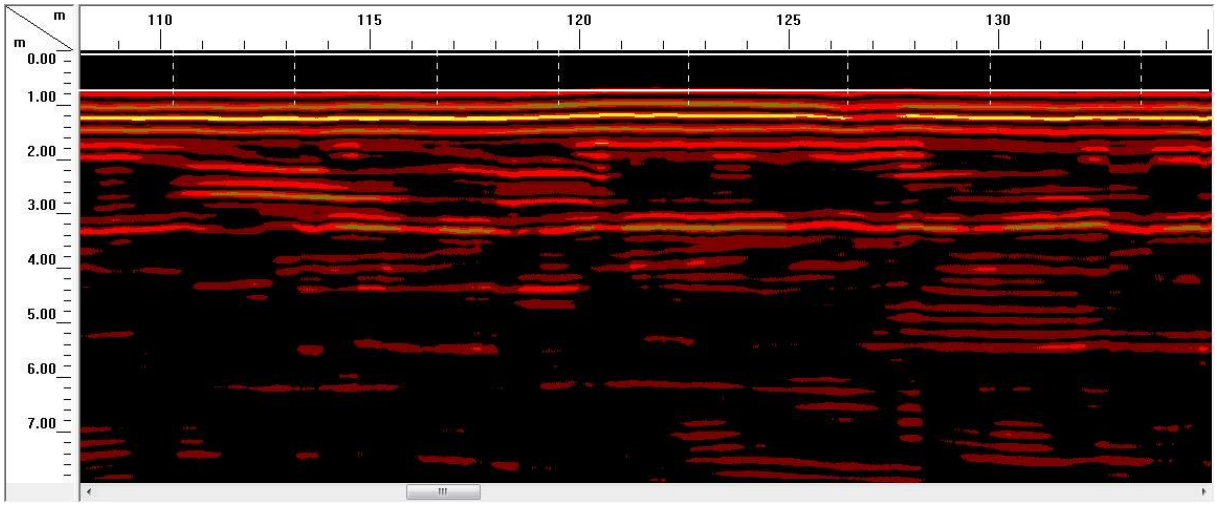


Figure 5.7e. Travertine rock mass features, (Line-5, distance between 22-29 m).

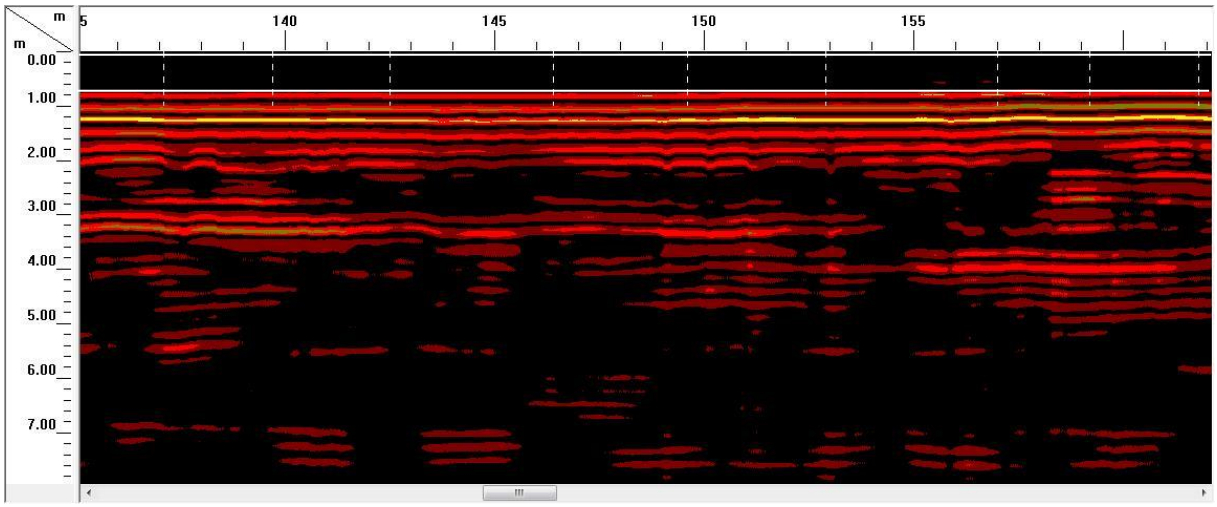


Figure 5.7f. Travertine rock mass foliations, (Line-5, distance between 29-36 m).

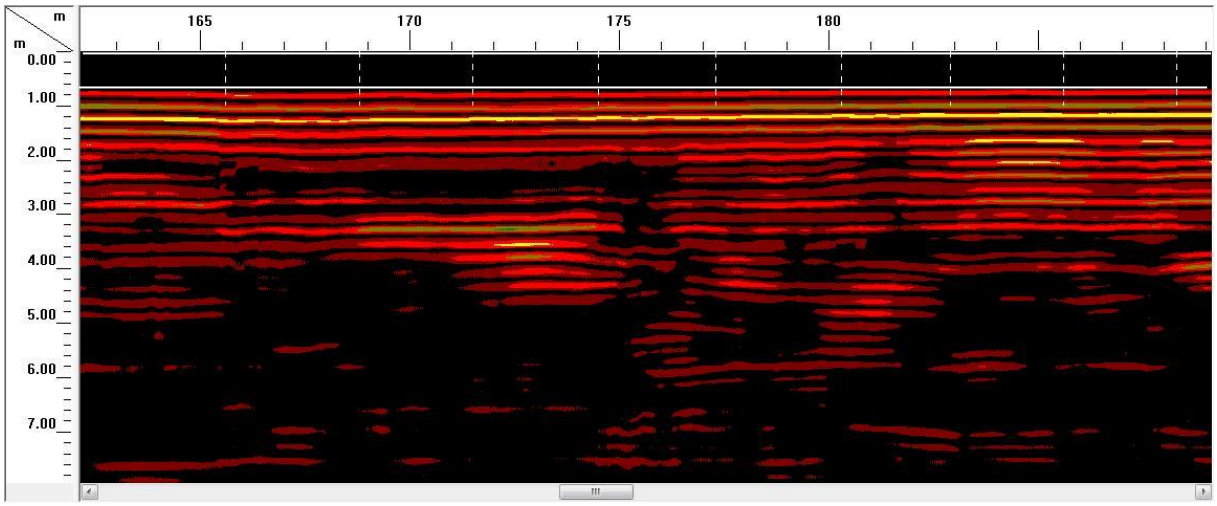


Figure 5.7g. Travertine rock mass beddings, (Line-5, distance between, 36-44 m).

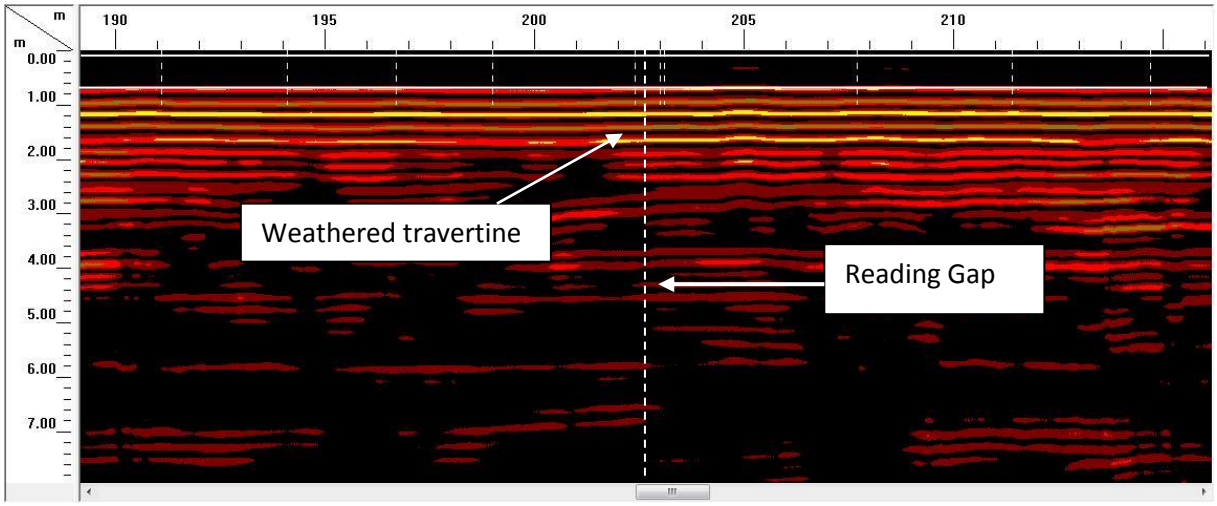


Figure 5.7h. Travertine rock mass features, (Line -5, distance between 44-51 m).

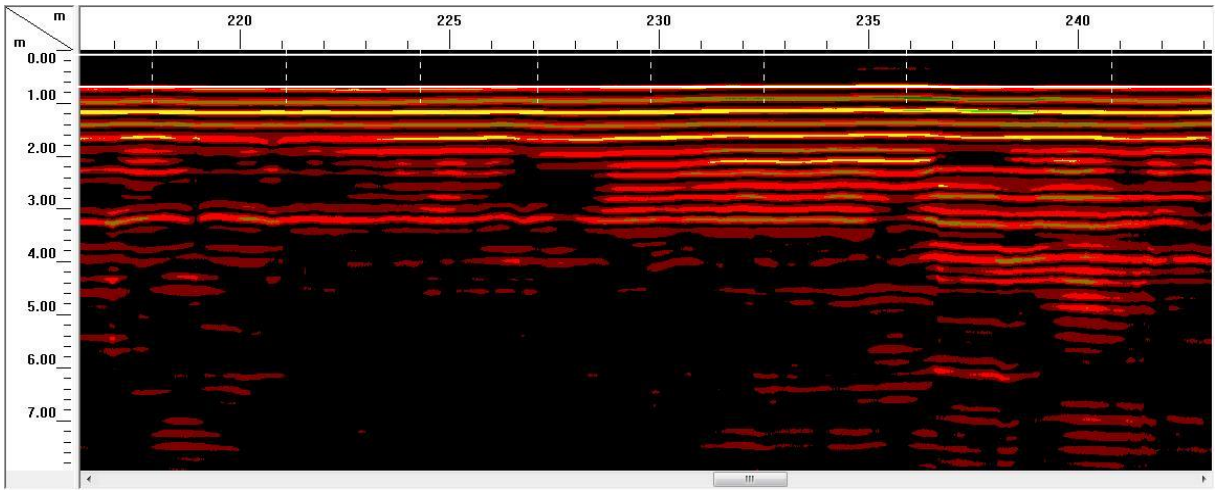


Figure 5.7i. In this part of GPR graphic, travertine rock mass weathering was determined more clearly, (Line-5, distance between (51-58 m).

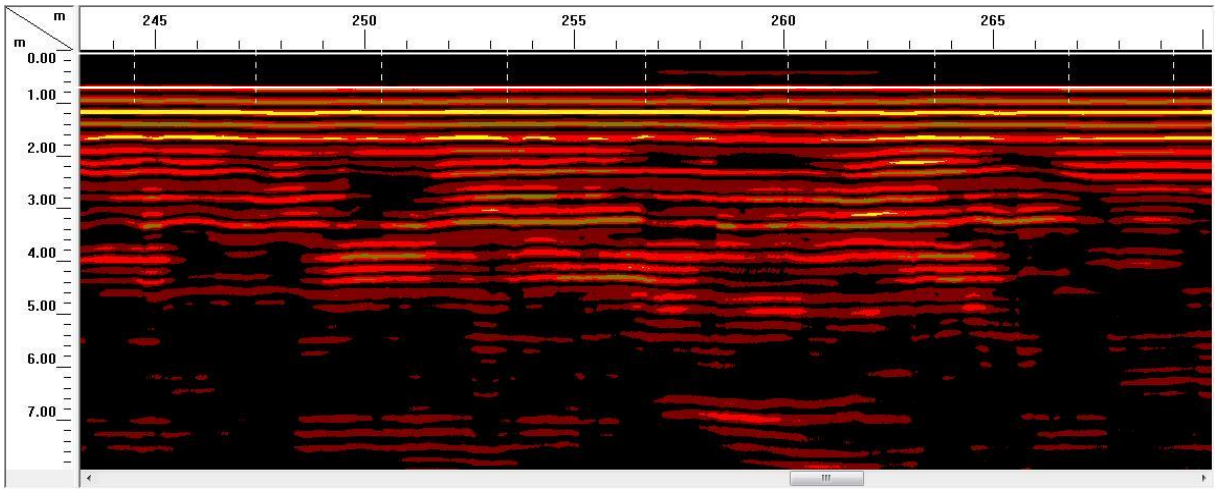


Figure 5.7j Weathered travertine rock mass features, (Line-5, distance between 58-65 m).

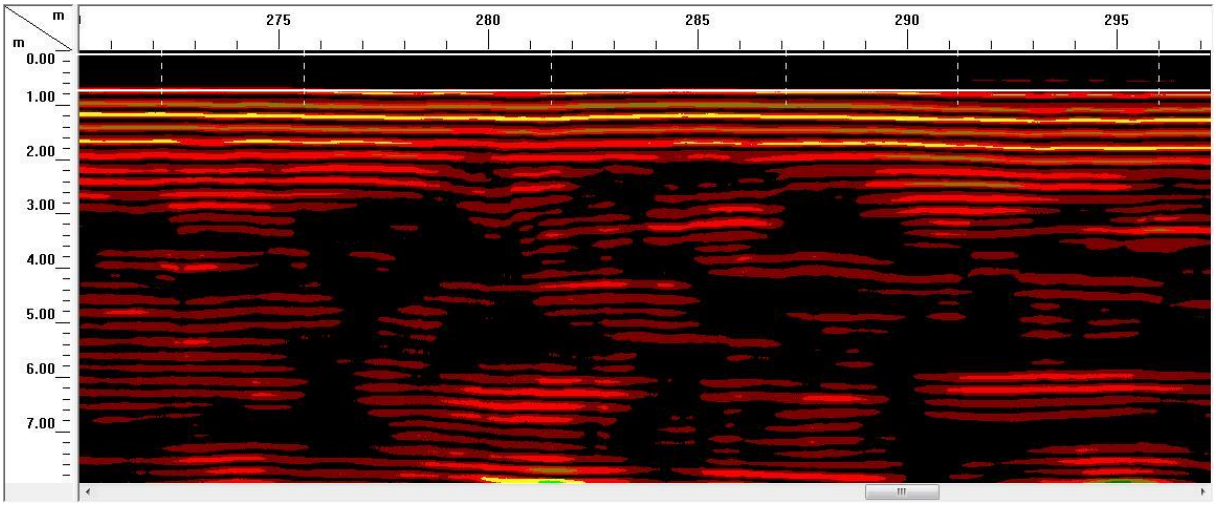


Figure 5.7k. Travertine rock mass beddings, (Line-5, distance between 65-70 m).

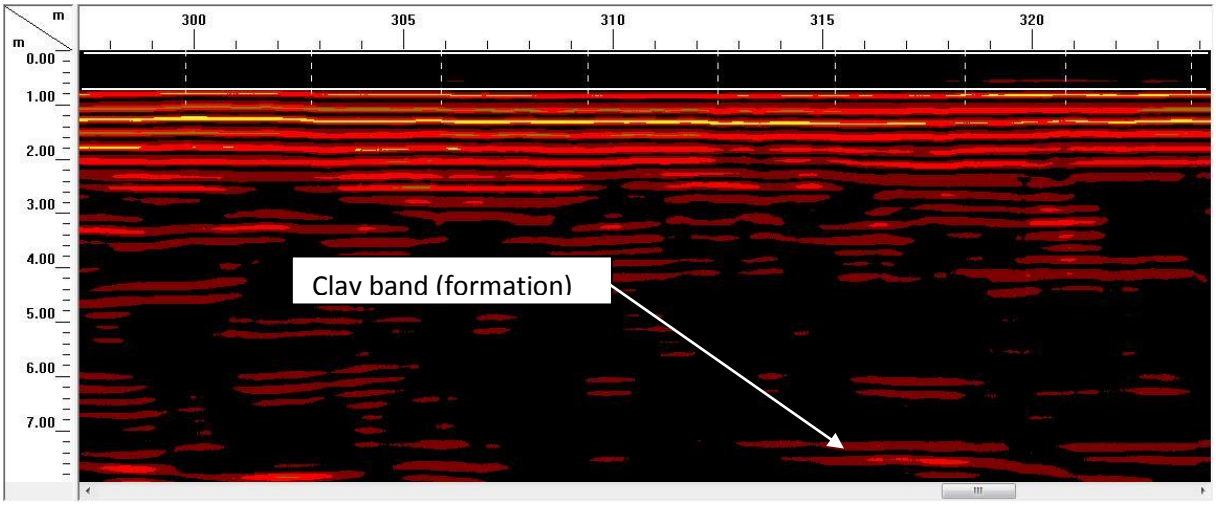


Figure 5.7l. Travertine rock mass bedding together with claystone layers, this graphic shows relatively more compact travertine rock mass, (Line-5, distance between 70-78 m).

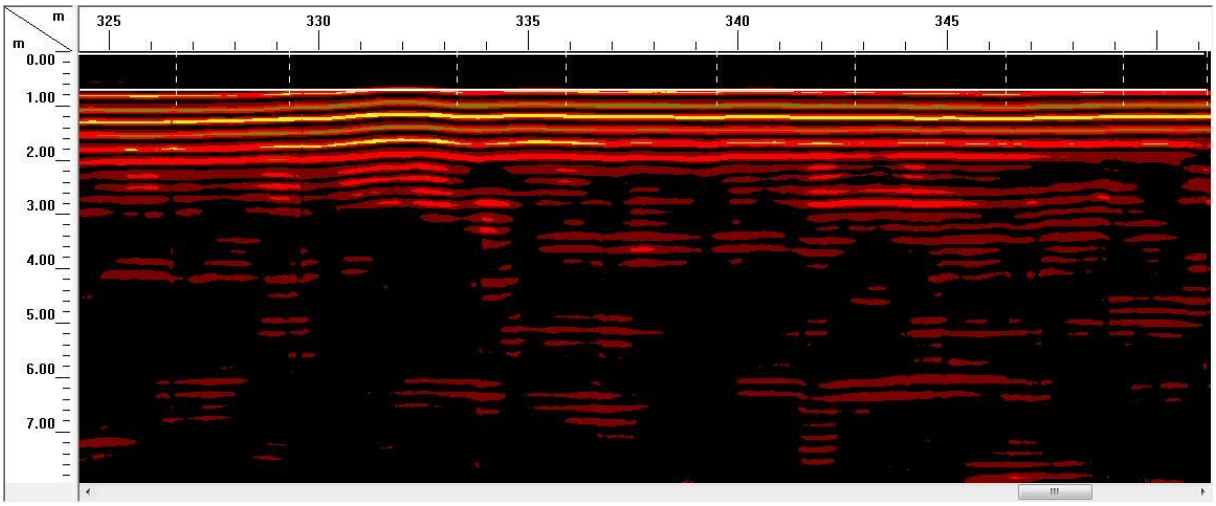


Figure 5.7m. Travertine rock mass bedding together with toplayers of weathered traverten rock mass, (Line-5, distance between, 78-86 m).

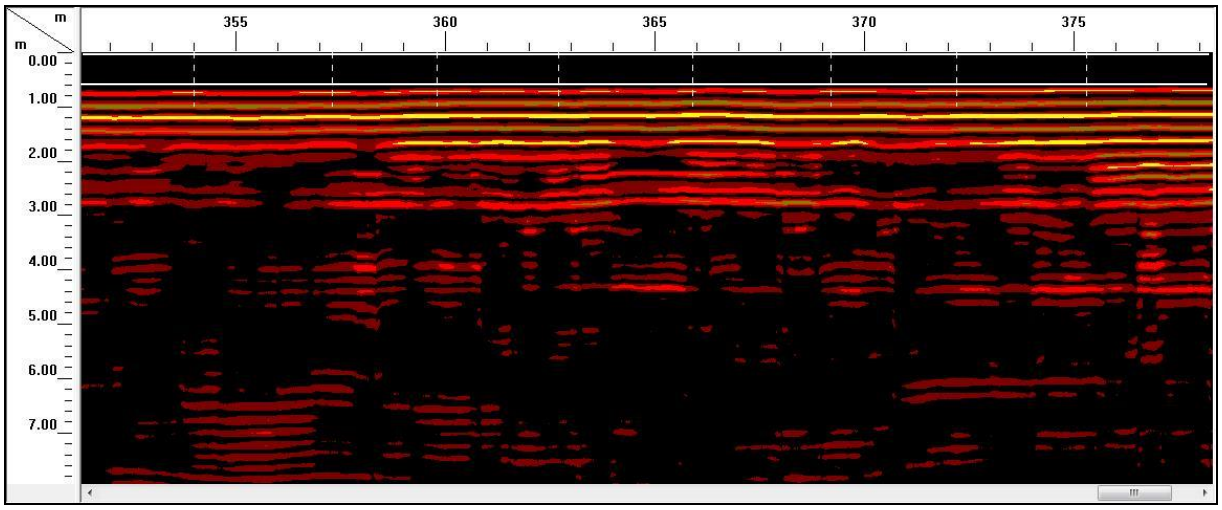


Figure 5.7n. Travertine rock mass bedding features, (Line-5, distance between, 86-93 m).

5.1. Three Dimensional (3D) Fracture Extension in the Searched Travertine Mine

Three–dimensional (3D) ground–penetrating radar measurements (GPR) represent an efficient high resolution geophysical surveying method allowing to explore mining sites in a non–destructive manner. In order to analyze effectively large 3 dimensional GPR data sets, modern visualization techniques have been combined with GPR data interpretation techniques. However, in this study, we focus on the application of data attributes (namely energy, coherency and similarity), originally developed for mining and petroleum reservoirs related problem addressed by reflection seismology to emphasize temporal and spatial variations within GPR data cubes. Based on the measurements in the searched travertine mine case, potential differences due to rock mass feature variations were pointed out for further rock mechanic related researches.

The study area were analyzed by GPR including the application of GPR, collection of radar data, recording data on the base of the passage ways features, resolution of radar profiles (Radan-7 graphics) and 3 dimensional presentation of the searched travertine bench. The resultant features obtained from GPR graphics like cracks, fractures, travertine bedding differences, clay or other rock bedding in travertine rock mass were pointed on 3 dimensional research area model to understand the features extensions in the whole measuring area.

The field measurements results along the 5 lines show the following main rock features. Line-1 for example has length of 105 meters and the GPR tests were used to

produce the graphics which show; existing very important fracture location at 15, 60, and 88 meters away from the Line-1 starting point shown in Figure 5.5. Fracture features at these locations continued from 2 to 7 meters depth. There are another cracks located at 6 and 17 meters from starting point and they were observed at 2 to 19 meters depth. The profiles resolutions show three kinds of colors to differentiate different layers, like yellow, black and blue. Yellow color mostly horizontal lines in the graphics are thought to represent weakness layers and claystone bands in travertine rock mass. These layers are said to be lower quality in travertine or mostly they represent weathered claystone beddings in travertine rock mass. The black color shows in the graphics where the quality of travertine rock mass has higher quality. The black colored areas in the graphics are seen to be diffused to different layers, specially between 2-20 meters of the subsurface studying area. The blue color layers determined in the test area show mainly clay band or claystone beddings. This color is observed to be situated mostly in obtained graphics between 6-10 meters depth which is named as claystone bedding extension in this research.

Field GPR measurements and related rock section graphics obtained for Line-2 demonstrates that; a fracture located 25 meters away from the Line-2 starting point has a continuity starting from 1 meter depth to 7 meters depth (Figure 5.6). Next fractures were determined at 67 and 103 meters location and they are continuing 16 meters depth to further down. This line (Line-2) measurement show fewer amounts of fracture and claystone layers. Because it is located 10 meters away from actual mine bench face which is also 25-50 meters away from the hill side South slope where the travertine mine situated. The graphics obtained from Line-2 represent travertine inner bedding features which evaluated like a flowing patterns in the travertine rock masss. In this respect the quality of the travertine under the Line-2 is advised to be tested by obtaining shallow depth (around 25 meters) drilling carrots. The GPR graphics represent also that the travertine rock mass has massive in some part of the graphics. SO their economical outcomes should be evaluated as well by drilling.

Line-3 measurements show that there are very few major fracture zone under it. GPR graphics presents the claystone bedding features at the depth of 7-10 meters depth. Some part of the graphics present that the weakness zone like claystone beddings are diffused in to travertine rock mass which were pointed accordingly on the related graphics shown above (Figure 5.7).

Fourth line (Line-4) radar readings (GPR) presented graphics that the travertine rock mass here are more massive with respect to the rock mass under Line-1. It is expected that the Line-4 area (Figure 5.8) might have more massive travertine rock mass. The claystone bedding was observed under this line at depth of 7-9 meters as well. It is also observed that there might be fracture at 6 meters away from the starting point of Line-4 and continuing up to 7 meters depth.

Line-5 GPR measurements (Figure 5.9) present almost no major fracture pattern. The rock mass under Line-5 are determined mostly massive type of travertine with it is own flowing rock mass pattern. The claystone layers are also determined in this line measurement. So it is became obvious that the claystone layers (can be named as clay band with 1-2 meter thickness) are situated all over the test area. Travertine near the surface, near the mentioned claystone intersection (at the depth of 7-9 meters) is expected to be less in quality. Figure 5.10 demonstrates the fracture determined from the GPR readings.

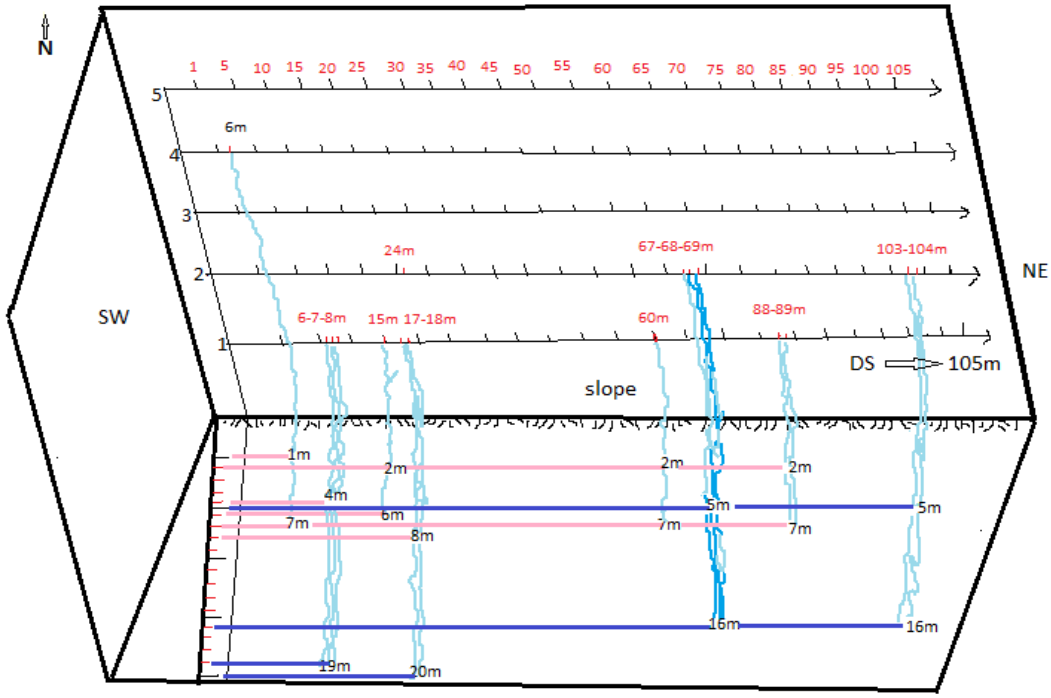


Figure 5.8. Three dimensional model of measured travertine rock mass at the mine. The fracture orientations are presented here according to the GPR graphics obtained from the field tests along the presented measuring lines. Red recordings represent the distance from the line starting point. Blocks front face represents the depth and illustrates the depth continuity of the determined fractures.

6. CONCLUSIONS

Ground penetration radar (GPR) has been developed into a sophisticated technique that can provide detailed images of the near surface. Most of the research on GPR has been conducted for engineering and environmental applications. However, all of the development in these areas has applications for archeological site characterization and shallow depth engineering applications. GPR has two advantages over most other non-invasive geophysical techniques. Firstly, GPR provides a three dimensional pseudo-image that can easily be converted to depths that are accurate down to a few centimeters. Secondly, GPR responds to both metallic and non-metallic objects. GPR is an excellent tool for mapping nearly any inhomogeneity in the subsurface where there is characterized by a small difference in density, or porosity.

One of the most reliable GPR equipment was used in this research study and it was GSSI's SIR-3000 ground penetration radar system. This equipment consist of several parts to from modern GPR tool with all of the trappings needed to make it very effective in a many diverse applications. The instrumentation in this area of measuring techniques advances rapidly. Electro-magnetic energy differentiation in the air (radar signals) is used to detect metallic objects (like plane, helicopters etc.) in it for commercial and army base purposes. However the same radar signal directed to the ground can also present some features according to its energy level. By increasing the energy radar signal produce deeper view to detect major features in the rock masses. When this features of radar signals equipped with related safety regulations and computer screen visualization, the rock mass depth can be seen on the computer evaluation graphics (Radan-7 graphics) as shown in figures above. Beside of the cost of GPR equipment cost, if the miners require shallow depth visualization before a drilling operation, this equipment is one of the most fruitful equipment. Its results are not limited with the angle of the field, because it has different types suitable for; city roads, countryside (rocky fields) and in-building measurements.

This thesis study includes practical field works by using GSSI's SIR-3000 ground penetration radar applications in a travertine mine, 5 kilometers away from Selcuk University main campus in Konya. The research followed here covers the discussion about general parameters of GPR, methodology, principle measurement, electromagnetic wave, antennas system, field measurement and data analyzing. The

GPS equipment handled in this research, GSSI's SIR300 has ability to handle large data volumes in its memory and it has capability hand out this data set through cost effective and quick manner to into computers. Then the data set can be handled by related software for example Radan-7 to produce GPR graphics (ground section graphics) to visual underground for further evaluation. The data set can be by different software programs to obtain more understandable picture to decide what is located in underground measured with GPR. During this thesis research, different parameters of GPR are handled to visualize the travertine rock mass in the selected mine. Then GPR field tests were decided to handled to obtain 7 and 21 meters depth view trough respective radar signal features. After analyzing the line readings, 3 dimensional model blocks was prepared to understand the major fracture pattern at a small area of the mine. It is concluded that the GPR is convenient and reliable method to decide where were the major rock fractures; and where were the main feature differences in a selected travertine mine. GPR application on shallow travertine mine is then concluded as a practical application and it can be used for different rock mass feature capture also.

REFERENCES

Annan, A.P. (1973) Radio Interferometry Depth Sounding: Part I – Theoretical Discussion, Geophysics, V38, N3, pp.557-580.

Annan, A.P., Waller, W,M., Strangway, D,W., Rossiter, J,R., Redman, J,D and Watts, R.D., 1975 The electromagnetic response of a low- loss, 2- layer, dielectric earth for horizontal electric dipole excitation Geophysics, V40, N2.

Annan, A.P. and Davis, J.L. (1976) Impulse Radar Soundings in Permafrost. Radio Science, V11, pp383-394.

Annan, A.P. and Davis, J.L. (1977) Impulse radar applied to ice thickness measurements and freshwater bathymetry. Geological Survey of Canada, Report of activities, Paper 77-1B, pp117-124.

Annan, A.P. and Davis, J.L. (1978) Methodology for Radar Transillumination Experiments. Report of Activities. Geological Survey of Canada, Paper, 78-1B, pp107-110.

Annan, A.P. and Davis, J.L. (1989) Ground penetrating radar for high resolution mapping of soil and rock stratigraphy. Geophysical prospecting, V37, pp531-551.

Annan A.P. and Cosway, S.W. (1991) Ground Penetrating Radar Survey Design. 53rd Annual Meeting of the European Association of Exploration Geophysicists. Florence, 1991.

Annan, A.P. and Cosway, S.W. (1992) Ground Penetrating Radar Survey Design. Proceedings of the Symposium on the Application of Geophysics to Engineering and Environmental Problems, SAGEEP'92, April 26-29, 1992, Oakbrook, IL, US, pp329-351.

Annan, A.P., Redman, J.D., Pilon, J.A., Gilson, E.W., and Johnston, G.B. (1997) Crosshole GPR for Engineering and Environmental Applications. Proceedings of the High Resolution Geophysics Workshop, University of Arizona, Tuscon, AZ,

Antunes Aranha, P.R., Ribeiro Rocha, C.H. and Garcia Sobreira, A.F. (2002) The use of GPR for characterizing underground weathered profiles in the sub-humid tropics. Journal of Applied Geophysics, V49, pp195–210.

Arcone, S.A., Paige, R.P. and Liu, L. (2003) Propagation of a Ground-Penetrating Radar (GPR) Pulse in a Thin-Surface Waveguide, Geophysics, V68, N6, pp1922-1933.

Balanis, C. (1989) Advanced engineering electromagnetics: John Wiley &Sons, Inc.

Bedal, Leigh -Ann (2000) Paradise Found: Petra's Urban Oasis. Expedition, V42, N2, pp23-36.

Bekic, G. (1964) Results - Find and compare a variety of articles since 1964 to 2014 on environmental expert on the world's largest environmental industry www.environmental-expert.com/articles/calendar-older.

Beres, M., and F.P. Haeni (1991) Application of ground penetrating radar methods in hydrogeologic studies. Ground Water, V29, N3, pp375-386.

Bristow, C.S. and Jolt, H.M. (2003) Ground penetrating radar in sediments: Special Publications, (Eds), N211, London, Geological Society, pp9-27.

Cai, J., McMechan, G.A. and Fisher, M.A. (1996) Application of ground-penetrating radar to investigation of near-surface fault properties in the San Francisco Bay region. Bulletin of the Seismological Society of America, V86, pp1459-1470.

Cardimona, S. (2002) Subsurface investigation using ground penetration radar. Proceeding of 2nd Annual Conference on the Application of Geophysical and NDT Methodologies to Transportation Facilities and Infrastructure.

Christie, M., Tsoflias, G.P., Stockli, D.F., and Black, R., (2008) Assessing fault displacement and off-fault deformation in an extensional tectonic setting using 3-D Ground-Penetrating Radar imaging, Journal of Applied Geophysics, doi:10.1016/j.jappgeo.2008.10.013.

Conyers Lawrence B. & Dean Goodman 1997. Ground-penetrating Radar: An Introduction for Archaeologists. Walnut Creek, (CA): AltaMira..

Conyers, L. B., and Goodman, D, (1997) Ground-Penetrating Radar: An Introduction for Archaeologists. AltaMira Press.

Conyers, L.B., and C. Cameron (1998) Ground-Penetrating Radar Techniques and Three-Dimensional Computer Mapping in the American Southwest. Journal of Field Archaeology, V25, N4, pp417–430.

Conyers, L.B., and Lucius, J.E. (1996) Velocity Analysis in Archaeological Ground-Penetrating Radar Studies. Archaeological Prospection, V3, N1, pp25–38.

Cook, J.C. (1973) Radar Exploration Through Rock in Advance of Mining. Trans.Society Mining Engineers, AIME, V254, pp140-146.

Coon, J.B., Fowler, J.C. and Schafers, C.J. (1981) Experimental Uses of Short PulseRadar in Coal Seams. Geophysics, V46, N8, pp1163-1168.

Daniels, D.J. (2004). Ground Penetrating Radar (Ed.), Knoval Institution of Engineering and Technology, 2cd edition, pp1–4.

Daniels, D.J. (2004) Ground Penetrating Radar, The Institution of Electrical Engineers, UK, Second edition,.

Davis, J.L. and Annan, A.P. (1986) Borehole Radar Sounding in CR-6, CR-7 and CR-8 at Chalk River, Ontario. Technical Record TR-401, Atomic Energy of Canada Ltd.

Doolittle, J.A. and Collins, M.E. (1995) Use of soil information to determine application of ground-penetrating radar. Journal of Applied Geophysics, V33, pp101-108.

Durig, U., Pohl, D. W. and Rohner, F. (1986) Near-Field Optical-Scanning Microscopy, J. Applied Physics, V59, N10, pp3318-3327.

Engheta, N, Papas, C,H. and Elachi, C. (1982) Rhadiation patterns of interfacial dipole antennas Radio Science, V17, pp1557-1566.

Eren, Y. (1993a) Eldes-Derbent-Tepeköy-Söğütözü (Konya) Arasının Jeolojisi. PhD Thesis, Selcuk University, Applied Science Institute, Konya p224.

Eren, Y. (1993b). Stratigraphy of autochthonous and cover units of the Bozdağlar massif, NW, Konya. Geological Bulletin of Turkey. V36, pp7–23.

Eren, Y., Kurt, H., Rosselet, F., Stampfli, G.M., (2004). Paleozoic deformation and magmatism in the northern area of the Anatolide block (Konya), witness of the Palaeotethys active margin. Eclogae Geologicae Helvetiae, V97, pp293–306.

Fisher, E., McMechan, G.A., and Annan, A.P. (1992) Acquisition and Processing of Wide-Aperture Ground Penetrating Radar Data: Geophysics, V57, pp495-504.

Freeland, R.S. Yoder, R.E. and Ammons, J.T. (1998) Mapping shallow underground features that influence site-specific agricultural production. Journal of AppliedGeophysics, V40, pp19–27.

Gerhards, H. (2008) Ground Penetrating Radar as a Quantitative Tool with Applications in Soil Hydrology. PhD Thesis, Heidelberg University.

Gerald, O. and Buchegger, T. (2006) Erwin Schimb¨ack, Reimar Pfeil, Andreas Stelzer, and Robert Weigel, (2006) Adaptive ground clutter removal algorithm for ground penetrating radar applications in harsh environments, Sensing and Imaging: An International Journal, V7, N3, pp71–89.

Göncüoglu, M.C., Direk, K., Kozlu, H., (1997) Pre-alpine and alpine terranes in Turkey: explanatory notes to the terrane map of Turkey. Annales Géologique de Pays Héllenique V37, pp1–3.

Grant and Schultz (1994) Erosion of ejecta at Meteor Crater: Constraints from ground penetrating radar. Proceedings Fifth International Conference on Ground-Penetrating Radar. Waterloo Centre for Groundwater Research and the Canadian Geotechnical Society, pp789-803. June 12–14, 1994, Kitchner, Ontario, Canada.

Griffin, S., Pippett, T. (2002). Geophysical and Remote sensing Methods for Regolith Exploration, CRLEME Open File Report, N144, pp80-89.

GSSI (2009) StructureScan Mini: All-in-one handheld GPR system. Webpage: www.geophysical.com

GSSI (2011) RADAN-7, User's Manual, Geophysical Survey Systems Inc. (GSSI), MN43-199, p127, Webpage: www.geophysical.com.

Harry M.J. (2009) Ground Penetration Radar Theory and Application, V1, Elsevier, First edition.

Hülsmeyer, C. (1904) Verfahren, um entfernte metallische Gegenst • ande mittels elektrischer Wellen einem Beobachter zu melden(patent DE 165 546),

Ishida, T., Makino, T., and Wang, C. (2000) Dielectric-Relaxation Spectroscopy of Kaolinite, Montmorillonite, Allophane, and Imogolite Under Moist Conditions, Clays and Clay Minerals, V48, N1, pp75-84.

Jackson, M.L. (1959) Frequency distribution of clay minerals in major great soil groups as related to the factors of soil formation. Clays and Clay Minerals, V6, pp133-143.

Kelso, C. M., Flammer, P. D., DeSanto, J. A., and Collins, R. T. (2001) Integral Equations Applied to Wave Propagation in Two Dimensions: Modeling the Tip of a Near-Field Scanning Optical Microscope, J. Opt. Soc. Am. A, p. 1993-2001.

Kurt, H. (1994) Petrography and Geochemistry of Kadınhanı (Konya) Area, Central Turkey. PhD, Glasgow University, U. K. p191.

Kadioglu, S., Aldas, G.U., Karpuz, C., Düzgün, Ş.B. and Kadioglu, Y.K. (2005) Taş ocağı seçiminde mühendislik disiplininin önemi: Gölbaşı andezitlerinde bir uygulama, (in Turkish), Madencilik, 2005, V44, N3, pp.25-33, Chambers of Mining Engineering, Ankara, Turkey, ISSN: 0024-9416.

Kadioglu, S. & Kadioglu, Y.K. (2006) Determination of thicknesses and discontinuities in a marble area by ground penetrating radar (GPR) method, J. Fac.Eng.Arch. Selcuk Univ., V21, N1-2, 2006

Lawrence and Goodman (1997) Ground-Penetrating Radar: An Introduction for Archaeologists. AltaMira, WalnutCreek, California.

Löwy, H, (1910) Eine 1910 elektrodynamische Methode zur Erforschung desErdinneren. Physikalische Zeitschrift, V11, pp697-705.

McNeill, (1980) Electrical conductivity of soils and rock. Technical Note TN-5. Geonics Limited, Mississauga, Ontario.

Saarenketo, T. (1998) Electrical properties of water in clay and silty soils. *Journal of Applied Geophysics* V40, pp73-88.

Meyers, R., Smith,D.G., Jol, H.M. and Peterson, C.R. (1996) Evidence for eight great earthquake-subsidence events detected with ground-penetrating radar, Willapa barrier, Washington: Geology, V24, pp99-102.

Mishchenko M. I., Travis L. D., Lacis A. A. (2002) Scattering, Absotption, and Emission of Light by Small Particles. Cambridge Univ. Press, Cambridge (http://www.giss.nasa.gov/~crmim/books.html)

Morey, R.M. (1974) Continuous Subsurface Profiling by Impulse Radar. Proceedings of Engineering Foundations Conference on Subsurface Explorations for Underground Excavations and Heavy Construction, Henniker, New Hampshire, pp213-232.

Okay, A.I., and Tüysüz, O. (2003) Tethyan sutures of northern Turkey. In: Durand, B. Jolivet, L., Jolivet, L., Horváth, Séranne, M., 1999. (Eds.), The Mediterranean Basins:Tertiary extension within the Alpine orogeny Geological Society, London, Special Publication. V156, pp475–516.

Nancollas, (1979).The Growth of Gypsum Crystals on Barite and Calcite", J.S. Gill and G.H. Nancollas, Desalination, 29, 247.

Okay and Tüysüz, (2003) Okay, A.I., and Tüysüz, O., 2003. Tethyan sutures of northern Turkey. In: Durand, B., Jolivet, L., Jolivet, L., Horváth, Séranne, M., 1999. (Eds.), The Mediterranean Basins:Tertiary extension within the Alpine orogeny Geological Society, London, Special Publication V156, pp475–516.

Olhoeft, G.R. (1984) Clay-organic reaction measured with complex resistity, in Expanded abstracts, 54th Annual International Meeting and Exposition of the Society of Exploration Geophysicists,

Olhoeft, G.R. (1985) Electrical Properties of Rocks and Minerals, Short Course Notes, http://mars.mines.edu/pub/85ShortCourseNotes.pdf, p218.

Olhoeft, G.R. (1987) Electrical properties from 10^{-3} to 10^{+9} H- Physics and Chemistry. proceedingsof the 2nd International Symposium on the Physicsand Chemistry of Porous Media, American Inst. of Physics Conf. Proceedings, V154, pp. 281-298.

Olhoeft, G.R. (1988) Interpretation of Hole-to-Hole Radar Measurements: In Proceedings of the Third Technical Symposium on Tunnel Detection, January 12-15, 1988, Golden, CO, pp616-629.

Olhoeft, G.R. (2000) Maximizing the information return from ground penetrating radar: J. Applied Geophys., V43, pp175-187.

Olsson, O., Falk, L., Forslund, O., Lundmar, L., and Sandberg,, E. (1990) Crosshole Investigations—results from Borehole Radar Investigations. Stripa Project TR 87-11. Swedish Nuclear Fuel and Waste Management Co., Stockholm.

Owen, T.R. (1981) Cavity Detection Using VHF Hole to Hole Electromagnetic Techniques. Proceedings of the Second Tunnel Detection Symposium, Colorado School of Mines, Golden CO, July 21-23, 1981, U.S. Army MERADOM, Ft. Belvoir, VA, pp126-141.

Özcan, A., Göncüoğlu, M.C., Turhan, N., Uysal, S., Şentürk, K., Işık, A. (1988) Late Palaeozoic evolution of the Kütahaya-Bolkardağ Belt. METU Journal of Pure and Applied Science,V21, pp211–220.

Paterson, D.G. (2000) Mapping rehabilitated coal mine soils in south Africa using GPR, 8th International Conference on Ground Penetrating Radar. (eds: Noon, D.A. Stickley, G.F.).

Peart R.J. and Raines, M, G, (1994) Application of ground penetrating radar with BGS Core programme the results nora.nerc.ac.uk/11336/1/IR04021.

Robertsson, J.O.A. and Holliger, K. (1998) Finite-difference modelling of electro-magnetic wave propagation in dispersive and attenuating media, Geophysics, V63, pp856-867.

Robinson, D., Jones, S., Wraith, J., Or, D. and Friedman, S. (2003) A review in dielectric and electrical conductivity measurements in soils using time domain reectometry, Vadose Zone J. V2, pp444-475.

Sihvola, A. (1999) Electromagnetic Mixing Formulas and Applications, IEE, London, p284.

Smith G.S. (1984) Directive properties of antennas for transmission into a material half-space IEEE Trans, Antennas propagate, Vol, AP -32, pp322-246.

Smith, D.G., and Jolt, H.M. (1995) Ground penetrating radar: Antennae frequencies and maximum probable depths of penetration in Quaternary sediments: Journal of Applied Geophysics, V33, pp93-100.

Soil Survey Staff (1999) Soil Survey Manual. US Department of Agriculture - Soil Conservation Service, Handbook N18, US Government Printing Office. Washington, DC.

Soil Survey Staff, (1999) Soil Taxonomy, A Basic System of Soil Classification for Making and Interpreting Soil Surveys 2nd Edition. US Department of Agriculture - Natural Resources Conservation Service, Agriculture Handbook No. 436, US Government Printing Office, Washington, DC.

Seren A. & Demirkol Acikgoz, A. (2012) Imaging fractures in a massive limestone with ground penetrating radar, Haymana, Turkey", Scientific Research and Essays, V7, N40, pp.3368-3381, DOI: 10.5897/SRE11.1877

Ulaby, F. T., Moore R. K., and Fung, A. K., 1982, Microwave Remote Sensing, Active and Passive, Volume II, Radar Remote Sensing and Surface Scattering and Emission Theory, Addison-Wesley Publishing, London, pp456-1064.

Ulriksen, C.P.F. (1982) Application of Impulse Radar to Civil Engineering. Unpublishe Ph.D. Thesis, Dept. of Engr. Geolo., U. of Technology, Lund, Sweden. Ulriksen, C.P.F., 1982, Application of Impulse Radar to Civil Engineering. Unpublished Ph.D. Thesis, Dept. of Engr. Geolo., U. of Technology, Lund, Sweden.

Ward, S.H., and Hohmann, G.W. (1987) Electromagnetic Theory for Geophysical Applications, *in* Electromagnetic Methods in Applied Geophysics, M. N. Nabighian, ed., Investigations in Geophysics, N3., Soc. Exploration Geophysics, Tulsa, OK, pp131-311.

Wollny, K, and Sass, O, (2001) Investigations regrdding alpine talus slopes using ground penentrating rada (GPR) in the bavarian Alps, Germany Earth Surface Processes and Landforms, V26, N10, pp1071-1086.

Wtorek, J. (2003) Electrical and Magnetic Properties of Soil, EUDEM2, Technology Survey, IST-2000-29220, http://www.eudem.info/.

Yelf, R.J. (2007) Application of Ground Penetrating Radar to Civil and Geotechnical Engineering Georadar Research Pty Ltd, 412 Eastbank Road, Coramba, Coffs Harbour, NSW 2450, Australia.

Zoubir, A.M:, Ian James Chant, Christopher L. Brown, Braham Barkat, and Canicious Abeynayake, "Signal processing techniques for landmine detection using impulse ground penetrating radar," *IEEE Sensor Journal*, V2, N1,pp. pp41–51, February 2002.